“Use of reflected GNSS SNR data to retrieve either soil moisture or vegetation height over a wheat crop”
by Sibo Zhang et al.

Cover letter to the editor

28 August 2017

Dear Dr. Alberto Guadagnini,

In response to your comment ("*I do think that the Authors have taken advantage of the constructive comments emerged during the review process and the manuscript has considerably improved. I see no particular reasons to further delay acceptance. I do recommend a thorough check of the use of the English language by the Authors, though, which is some cases appears to be awkward*"), we checked the English and the revised text can be found enclosed.

Yours sincerely,

Jean-Christophe Calvet, Sibo Zhang.

Use of reflected GNSS SNR data to retrieve either soil moisture or vegetation height over a wheat crop

Sibo Zhang[1,2], Nicolas Roussel[3], Karen Boniface[2,3,4,6], Minh Cuong Ha[3], Frédéric Frappart[3,5], José Darrozes[3], Frédéric Baup[4], and Jean-Christophe Calvet[1]

[1]CNRM – UMR3589 (Météo-France, CNRS), Toulouse, France

[2]Fondation STAE, Toulouse, France

[3]GET (UMR5563 CNRS/Université Paul Sabatier, UR254 IRD), Toulouse, France

[4]CESBIO, Université de Toulouse, CNES/CNRS/IRD/UPS, Toulouse, France

[5]LEGOS – UMR566 (CNES, CNRS, IRD, UPS), Toulouse, France

[6]now at Joint Research Centre / European Commission, Ispra, Italy

Correspondence to: Jean-Christophe Calvet (jean-christophe.calvet@meteo.fr)

Abstract. This work aims to estimate soil moisture and vegetation height from Global Navigation Satellite System (GNSS) Signal to Noise Ratio (SNR) data using direct and reflected signals by the land surface surrounding a ground-based antenna. Observations are collected over a rainfed wheat field in southwestern France. Surface soil moisture is retrieved based on SNR phases estimated by the Least Square Estimation method, assuming the relative antenna height is constant. It is found that vegetation growth breaks up the constant relative antenna height assumption. A vegetation height retrieval algorithm is proposed using the SNR dominant period (the peak period in the average power spectrum derived from a wavelet analysis of SNR). Soil moisture and vegetation height are retrieved at different time periods (before and after vegetation significant growth in March, respectively). The retrievals are compared with two independent reference datasets: *in situ* observations of soil moisture and vegetation height, and numerical simulations of soil moisture, vegetation height and above-ground dry biomass from the ISBA (Interactions between Soil, Biosphere and Atmosphere) land surface model. Results show that changes in soil moisture mainly affect the multipath phase of the SNR data (assuming the relative antenna height is constant) with little change in the dominant period of the SNR data, whereas changes in vegetation height are more likely to modulate the SNR dominant period. Surface volumetric soil moisture can be estimated (R^2 = 0.74, RMSE = 0.009 m^3m^{-3}) when the wheat is smaller than one wavelength (~ 19 cm). The quality of the estimates markedly decreases when the vegetation height increases. This is because the reflected GNSS signal is less affected by the soil. When vegetation replaces soil as the dominant reflecting surface, a wavelet analysis provides an accurate estimation of the wheat crop height (R^2 = 0.98, RMSE = 6.2 cm). The latter correlates with modeled above-ground dry biomass of the wheat from stem elongation to ripening. It is found that the vegetation height retrievals are sensitive to changes in plant height of at least one wavelength. A simple smoothing of the retrieved plant height allows an excellent matching to *in situ* observations, and to modeled above-ground dry biomass.

1 Introduction

In situ observations of soil moisture and vegetation variables are key to validate land surface models and satellite-derived products. Recent international initiatives, such as the International Soil Moisture Network (Dorigo et al., 2013) or the Committee on Earth Observation Satellites (CEOS) Land Product Validation group (Morisette et al., 2006) have improved the access to such observations. However, they remain very sparse and there is a need to develop new automatic techniques to monitor land surface variables at a local scale. Global Navigation Satellite System (GNSS) reflectometry could be a solution. A number of studies demonstrated that GNSS multipath signals can be used to retrieve various geophysical parameters of the surface surrounding a GNSS receiving antenna (Motte et al., 2016). Over land, variables such as soil moisture, snow depth and vegetation status can be observed (Larson et al., 2008; Small et al., 2010; Larson and Nievinski, 2013; Wan et al., 2015; Boniface et al., 2015; Larson, 2016; Roussel et al., 2016). GNSS satellites operate at the L-band microwave frequency domain (between 1.2 GHz and 1.6 GHz). At these relatively low frequencies, the microwave signal is less perturbed by atmospheric effects and can better penetrate clouds and heavy rains than higher frequency signals. This ensures continuous operations, in all weather conditions, at either daytime or nighttime. The L-band signal emitted or reflected by terrestrial surfaces is related to surface parameters like surface soil moisture, roughness or vegetation characteristics. These properties have been exploited by e.g. the Soil Moisture and Ocean Salinity (SMOS) satellite and the Soil Moisture Active Passive (SMAP) missions (Kerr et al., 2001; Chan et al., 2016) for Earth surface remote sensing applications. While SMOS is a radiometer and measures the Earth surface microwave emission (passive microwaves), GNSS satellites emit a radar signal (active microwaves). Active microwaves can present improved temporal and spatial resolutions, but the signal may be more sensitive to the structure of the surface, such as soil roughness or vegetation effects than for passive microwaves (Wigneron et al., 1999; Njoku et al., 2002).

Existing geodetic-quality GNSS networks have the potential to provide a large number of *in situ* observations, depending on the receiver technology: (1) waveform acquisition with a specific receiver using two antennas (one zenith-oriented antenna and one surface-oriented antenna), called GNSS reflectometry (GNSS-R) technique (Zavarotny et al., 2014) or (2) GNSS signal strength represented by the Signal-to-Noise Ratio (SNR) acquired with a classical geodetic receiver using one antenna, called SNR GNSS interferometric reflectometry (GNSS-IR) technique (Larson, 2016). GNSS networks can be used to monitor small or large areas depending on the antenna height and satellite elevation (Roussel et al., 2014). Continuous monitoring of surface soil moisture can be made over a long period at spatial scales ranging from 100 m^2 (antenna height of about 2 m) to 8000 m^2 (antenna height of about 150 m) for classical geodetic receiver but can reach a few thousand square kilometers with waveform receivers embedded on satellites (e.g. TechDemoSat-1 mission, Foti et al. (2015)).

Using the SNR GNSS-IR technique, Larson et al. (2008) showed that SNR data obtained from existing networks of single ground-based geodetic antennas can be used to infer soil moisture. Other GNSS methods (besides reflectometry) can be used. For example, Koch et al. (2016) used three geodetic GNSS antennas (one was installed above the soil, the other two

were buried at a depth of 10 cm), to measure the GNSS signal strength attenuation and to retrieve soil moisture over bare soil.

~~For now, a~~A network called PBO H_2O based on single GNSS antennas at Plate Boundary Observatory (PBO) sites is currently used in western regions of the USA to monitor surface soil moisture (Larson et al., 2013; Chew et al., 2016) and snow depth (Larson and Nievinski, 2013; Boniface et al., 2015). It must be noted that most of the 161 GNSS stations of this network are located in mountainous areas or in areas of California characterized by a relatively arid climate. They are surrounded by sparse vegetation and are therefore not adapted to vegetation growth studies.

In the SNR GNSS-IR technique, the interference between the direct and the reflected signals is observed ~~in~~ through temporal variations of the SNR data (Bilich and Larson 2007; Zavorotny et al., 2010; Chew et al., 2014). Changes in geophysical or biophysical parameters affect the phase, amplitude and frequency of the SNR modulation pattern. The SNR is also influenced by surface roughness and by the position of the antenna with respect to the surface and to the satellite (Larson and Nievinski 2013; Chew et al., 2016). The SNR modulation primarily depends on:

- the relative height of the GNSS antenna above the reflecting surface (ground or vegetation surface),
- satellite elevation,
- the superposition of the direct signal and of the reflected signal, which varies along with changes in the satellite track positions,
- Right Hand Circular Polarization (RHCP) and Left Hand Circular Polarization (LHCP) gain pattern of the receiving antenna, (RHCP usually increases the SNR when the satellite elevation angle increases, LHCP is related to imperfections of the antenna and is greater than RHCP for the reflected signal);
- reflection coefficients for the reflecting surface, related to the water content and to the ground mineralogical content of the reflecting surface,
- surface topography and roughness and
- the satellite transmitted power.

A soil moisture retrieval algorithm from SNR data was derived by Chew et al. (2014) over bare soil. In subsequent modeling studies Chew et al. (2015) showed that the vegetation canopies affected the SNR modulation pattern. They showed that vegetation growth tended to trigger a decrease of the SNR amplitude. Because the vegetation effects tended to perturb the soil moisture retrieval, Chew et al. (2016) proposed an improved algorithm for soil moisture retrieval in vegetated environments, which used the amplitude decrease extent to decide when vegetation influence was too large. They used a model database for the SNR of L2C signal to remove most significant vegetation effects for the sites they considered in Western USA. Small et al. (2016) further compared different algorithms of GNSS-IR soil moisture retrieval in the presence of vegetation. Roussel et al. (2016) integrated both GPS and GLONASS SNR data to retrieve soil moisture over bare soil. Using data from a field study, Wan et al. (2015) showed that the amplitude of the SNR data presented a good linear relationship with the vegetation water content (VWC), but it was restricted to VWC values of less than ~1 kg m^{-2}. In addition

to the amplitude of the SNR data, it was also possible to infer VWC by the $MP1_{rms}$ index, which is a linear combination of L1 and L2 carrier phase data and L1 pseudorange data (Small et al., 2010), and by the NMRI (Normalized Microwave Reflection Index) which is ~~a normalization result based on~~derived from the $MP1_{rms}$ (Small et al., 2014; Larson and Small 2014).

In this study, the SNR GNSS-IR technique was used to analyze GNSS SNR data obtained~~,~~ with a single classical geodetic antenna receiver over an intensively cultivated wheat field in southwestern France. The data were used to retrieve either soil moisture or relative vegetation height during the growing period of the wheat crop. The method proposed by Chew et al. (2016) (hereafter referred to as CH16) was used to retrieve soil moisture. Moreover, we performed a wavelet analysis in order to extract the dominant period of the SNR ~~and further to retrieve vegetation height~~. We investigated to what extent vegetation height influenced the dominant period resulting from the wavelet analysis. The main justification for investigating the impact of vegetation height was that it impacted the relative antenna height (the distance from the antenna to the reflecting surface). Vegetation growth tended to decrease the relative antenna height and broke up the constant height assumption used in soil moisture retrieval algorithms. In this context, key objectives of this study were to (1) assess the soil moisture retrieval technique in either low or tall vegetation conditions, and (2) retrieve vegetation height along the wheat growth cycle.

2 Materials and methods

2.1. SNR data and pre-processing

The GNSS SNR data were acquired from an antenna at 2.51 m above the soil surface over an experimental field covered by rainfed winter wheat in Lamasquère, France (43°29'10"N, 1°13'57"E, see Fig. S1 in the Supplement). These GNSS data were collected by GET (Géosciences Environnement Toulouse) for a whole growing season, from January to July 2015. A Leica GR25 receiver equipped with an AS10 antenna was used and data were acquired at a sample frequency rate of 1 Hz. Only the S1C SNR signal strength on the civilian L1 C/A channel of the GPS constellation was used in this study because the used receiver could not track the L2C signal. The latter is only transmitted by the recent Block IIR-M ("Replenishment Modernized") and IIF ("Follow-on") GPS satellites. Vey et al. (2016) showed that soil moisture root mean square difference between L2C and L1 was 0.03 m^3m^{-3}. The quality of the more recently available L2C signal (used by PBO H_2O (CH16)) is higher than either L1 C/A or L2P from non-code tracking receivers. However, a number of studies (e.g. Vey et al., 2016) showed that the SNR of the L1 C/A signal can be used to provide reliable soil moisture estimates over sparse vegetation and bare soil surface, although it is less precise than the L2C signal. Although data from other constellations were also acquired (e.g., GLONASS, GALILEO), their orbital parameters such as satellite track positions or satellite altitude were not the same. In order to be consistent with the GPS-only studies of Larson et al. (2008), CH16, and Small et al. (2016), we only used GPS SNR data. For our site, four GPS satellites out of 32 were excluded from the analysis because their data were incomplete

(GPS03, 20, 26, these numbers corresponding to their Pseudo-Random Noise (PRN) numbers) or not received (GPS08). Finally, GPS SNR data were missing for only nine days: 8 and 9 February, 3 April and from 13 to 18 May 2015.

Following the method proposed by Larson et al. (2010), a low-order polynomial was fit to the SNR data, and the modulation pattern was then derived from the SNR by subtracting this polynomial from the SNR data. The logarithmic dB-Hz units were converted to a linear scale in V V^{-1} using the following conversion equation: $SNR_{linear} = 10^{\frac{SNR}{20}}$ (Vey et al., 2016). Figure 1a shows an example of the detrended multipath SNR data for the ascending track of GPS01 on 21 January 2015. The periodic signature of the multipath SNR data is visible. We only analyzed the modulation patterns in a valid segment for satellite configurations corresponding to low elevation angles, ranging from 5 to 20 degrees. This corresponded to a valid segment data recording of less than one hour (40 to 50 minutes). ~~Avoiding~~ We excluded very low elevation angles (less than 5 degrees) ~~limited~~ in order to avoid spurious effects from trees and artificial surfaces surrounding the field. ~~Avoiding high elevation angles (more than 20 degrees) limited the reduction of the multipath signal amplitude.~~ Because the SNR signal amplitude was much reduced and the wave pattern was not visible at high elevations for our field observations, we excluded elevation angles larger than 20 degrees.

2.2. Soil moisture and vegetation characteristics

The field campaign was ~~a~~ part of a coordinated effort led by CESBIO (Centre d'Etudes Spatiales de la BIOsphère) to monitor crops in southwestern France using both *in situ* and satellite Earth Observation data. Independent *in situ* observations of soil moisture and vegetation height were made together with model simulations of these quantities. Both observations and simulations were used to validate soil moisture and vegetation height retrievals.

Since the whole wheat growing cycle was ~~considered~~examined, both soil moisture and vegetation modulated the multipath SNR pattern. Soil roughness was considered as stable in time from sowing to harvest. Soil in the close vicinity of the antenna consisted of 18% of sand, 41% of clay, and 41% of silt. The row spacing of the wheat crop was 15 cm.

The wheat was sown during the autumn, on 1 October 2014 and was harvested from 26 to 30 June 2015. Volumetric soil moisture (VSM) was measured by FDR (Frequency Domain Reflectometry) ML2 Thetaprobes and was continuously monitored at a depth of 5 cm from 16 January to 10 March 2015 and from 30 March to 26 May 2015. Measurements of crop height were performed at seven dates during the plant growing cycle. The canopy height did not exceed 0.1 m at wintertime and rapidly increased at springtime: it reached 0.2 m on 10 March 2015 and 1 m on 29 May. It dropped to 0.39 m on 18 June because of a lodging event. The exact date of lodging could not be precisely determined. ~~but i~~It could be inferred ~~it~~ that lodging happened between 29 May and 18 June.

In addition to *in situ* observations, simulations of surface soil moisture (0-10 cm top soil layer), plant height and above-ground dry biomass were performed for this site by CNRM (Centre National de Recherches Météorologiques) using the ISBA (Interactions between Soil, Biosphere, and Atmosphere) land surface model within the SURFEX (version 8.0)

modeling platform (Masson et al., 2013). The ISBA configuration and the atmospheric analysis ~~we~~ used to force the model are described in Lafont et al. (2012). The C3 crop plant functioning type and a multilayer representation of the soil hydrology ~~were~~ are considered. The model soil depth is 12 meters, with 15 layers and the layer thickness ~~is not united~~increases from the top surface layer to the deepest layers (Decharme et al., 2011). These simulations were used as an independent benchmark for soil moisture and vegetation variables.

2.3. Multipath SNR characteristics

Due to the motion of the GPS satellites, the path delay between the direct and reflected signals causes an interference pattern in the signal power of SNR data. The distance from the antenna to the dominant reflecting surface directly affects the SNR frequency/period.

As noted by Georgiadou and Kleusberg (1988) and Bilich and Larson (2007), assuming the ground surface is horizontal, the additional distance (δ) travelled by a reflected signal relative to the direct signal is

$$\delta = 2h\sin(\theta) \tag{1}$$

where h is the relative antenna height, and θ is the satellite elevation angle. This path delay δ can also be expressed in terms of the multipath relative phase ψ :

$$\psi = 2\pi\frac{\delta}{\lambda} \tag{2}$$

where λ represents the L1 wavelength (0.1903 m).

Thus the multipath frequency (f) and period (T) can be written as:

$$\omega = 2\pi f = \frac{d\psi}{dt} = \frac{4\pi}{\lambda}h\cos(\theta)\frac{d\theta}{dt} \tag{3}$$

$$\frac{1}{T} = f = \frac{2h\cos(\theta)}{\lambda}\frac{d\theta}{dt} \tag{4}$$

This means that the relative antenna height (h) directly affects multipath frequency f and period T. Antennas far above the reflecting surface have higher multipath frequencies (smaller multipath periods) than antennas closer to the reflecting surface. Furthermore, satellite geometric information and motion substantially influences ~~the period (~~T~~) of the multipath SNR data~~ due to the $\cos(\theta)$ and $d\theta/dt$ terms in equation (4). When~~If~~ satellite passes reach high elevation angles ~~(e.g., GPS01 in Supplement Fig. S2),~~ $d\theta/dt$ becomes larger (Bilich and Larson, 2007). Conversely, satellites with ~~signals observed at~~passes presenting small maximum elevations ~~(e.g., GPS18 in Supplement Fig. S2) move more slowly (~~ present smaller $d\theta/dt$ ~~)~~ values than satellites ~~passing~~ orbiting overhead ~~(Bilich and Larson 2007)~~. Contrasting configurations are illustrated in the Supplement (Fig. S2). In order to limit the impact of these differences from satellite motion, only the full-track data with at least 40 degree maximum elevation angle were selected. Among the remaining tracks we ~~further~~ removed

the slowly moving tracks whose maximum $\cos\theta \cdot d\theta/dt$ was less than 9.5×10^{-5} rad s^{-1} (threshold value based on our field observations) of the valid segment (elevation angles ranging between 5 and 20 degrees). This specific data sorting was only made for vegetation height retrieval (Sect. 2.5). After this selection, the number of available satellite tracks was 37 per day.

Provided the reflecting surface is stable, the a priori antenna height can be used to estimate the SNR frequency. The SNR frequency is used to calculate the multipath SNR phase, and then the SNR phase is used to estimate VSM (Sect. 2.4). If the reflecting surface is changing in response to vegetation growth, relative vegetation height can be retrieved instead of VSM by directly estimating the dynamic SNR frequency/period with a wavelet analysis (Sect. 2.5).

2.4. Soil moisture retrieval

As the SNR frequency is known (Eq. (~~43~~)), it is possible to estimate the SNR amplitude and phase. Larson et al. (2008) and Larson et al. (2010) showed that phase varies linearly with VSM in m^{3}m^{-3} (R^2 = 0.76 to 0.90). Retrieving absolute VSM values in m^{3}m^{-3} is possible after a calibration phase. This result was used by Chew et al. (2014) to develop an algorithm to estimate surface soil moisture (top 5 cm) over bare ~~ground~~soil.

For bare soil, changes in surface soil moisture affect the signal penetration depth. The latter can be very small in wet conditions and tends to increase in dry conditions, up to a few centimeters (Chew et al., 2014; Roussel et al., 2016). This is a small change with respect to the antenna height (2.51 m in this study). Consequently, the relative antenna height (h) is considered as a constant (h_c = 2.51m) in this Section. Using sine of the elevation angle ($\sin(\theta)$) as the independent variable, the modulation frequency becomes proportional to h_c. Then the multipath SNR can be expressed as (Larson et al., 2008):

$$SNR_{mpi} = A\cos\left(\frac{4\pi h_c}{\lambda}\sin(\theta) + \varphi_{mpi}\right) \quad (5)$$

The least square estimation (LSE) method proposed by Larson et al. (2008) is used to estimate the multipath amplitude (A) and multipath phase (φ_{mpi}) from the multipath SNR data. Then, φ_{mpi} can be ~~further~~ used to estimate the soil moisture changes (CH16),

$$VSM_t = S \cdot \Delta\varphi_t + VSM_{resid} \quad (6)$$

Phase changes $\Delta\varphi_t = \varphi_t - \varphi_0$ are calculated with respect to φ_0, the reference phase. We used the method proposed by CH16 consisting in estimating φ_0 as the mean of the lowest 15% of the φ_{mpi} data for each track during the retrieval period. The same condition was used to estimate the VSM_{resid} residual soil moisture from the *in situ* VSM observations. The VSM_{resid} was taken as the minimum soil moisture observation, which presented a value of 0.252 m^{3}m^{-3} during the retrieval period. The S parameter (in m^{3}m^{-3}degree^{-1}) is the slope of the linear relationship between phase changes and soil moisture. For time

series with no significant vegetation effects, S = 0.0148 $m^3m^{-3}degree^{-1}$ for L2C signal (CH16). Following CH16, the median soil moisture estimate from all available satellite tracks (66 per day) that passed at different times during the day was used as the final soil moisture estimate.

We also used the *in situ* VSM_t, $\Delta\varphi_t$ and VSM_{resid} to fit a locally adjusted slope. ~~The minimum VSM had to be derived from the *in situ* observations during the experimental time period in order to determine the VSM_{resid} term in Eq. (6).~~ The retrieval of the S parameter requires at least one or two months of VSM *in situ* observations because soil moisture conditions ranging from dry to wet need to be sampled. However, if a scaled soil wetness index is used instead of soil moisture, no *in situ* VSM observations are needed.

Alternatively, the phase time series can be normalized for each satellite track, and using S is not needed. We considered the median value of the normalized phases from all available satellite tracks (66 per day) as the final scaled soil wetness index (φ_{index}) for each day:

$$\varphi_{index} = \frac{\varphi - \varphi_{\min}}{\varphi_{\max} - \varphi_{\min}} \tag{7}$$

VSM could then be estimated from φ_{index}:

$$VSM = VSM_{obs\_\min} + \varphi_{index} \cdot (VSM_{obs\_\max} - VSM_{obs\_\min}) \tag{8}$$

VSM_{obs_min} and VSM_{obs_max} are the minimum and maximum *in situ* VSM observations during the experimental time period, respectively.

CH16 defined the normalized amplitude (A_{norm}) as the ratio of amplitude to the average of the top 20 % amplitude values. The A_{norm} time series can be used to assess whether or not vegetation effects are significant. Values of A_{norm} above 0.78 (dimensionless) indicate that vegetation effects are small (CH16). In conditions of significant vegetation effects CH16 used an algorithm able to correct the phase for vegetation effects. This algorithm is based on an unpublished lookup table. Since we were not able to correct for vegetation effects, we retrieved surface soil moisture during a period with rather sparse vegetation, from 16 January to 5 March. During this time span, A_{norm} was above 0.78 as shown in Fig. 2 (black dots).

2.5. Vegetation height retrieval using a wavelet analysis

While vegetation grows, the vegetation surface gradually replaces the bare soil surface as the dominant reflecting surface. As a consequence, the height (h) of the antenna above the reflecting surface decreases. Equation (4) shows that changes in h impact ~~the multipath frequency f and consequently~~ T. This property allows the use of changes in T values to infer changes in h, and further estimate relative vegetation height. To retrieve relative vegetation height we propose a new approach based on

wavelet analysis. Wavelets have been used for many years in signal processing studies in geosciences (Ouillon et al., 1995; Darrozes et al., 1997; Gaillot et al., 1999), astrophysics (Escalera and MacGillivray, 1995), meteorology (e.g. Hagelberg and Helland, 1995; Torrence and Compo, 1998), hydrology (Labat, 2005) and in many other fields. The wavelet analysis is well suited for analyzing time series with non-stationary power and frequency changes across time as illustrated by Fig. 1. Our wavelet analysis methodology is based on the WaveletComp R-package (Roesch et al., 2014). To analyze the period structure, we used a well-known Morlet mother function~~-~~ which comes from a combination of a Gaussian function and a sinusoidal ~~one~~ function (Fig. S3 in the Supplement). Due to its shape, Morlet daughters allow detection of singularities in all scales/periods of the spectrum. Morlet wavelet is also well suited for environmental analysis (Grinsted et al., 2004). We calculate the Morlet wavelet transform of the multipath SNR and evaluate the power spectrum of the multipath SNR signal (see Eqs. S1-S4 in the Supplement).

Vegetation height can be retrieved using the dominant SNR period (T_d), which is the peak period of the average power spectrum derived from a wavelet analysis of SNR, from the multipath SNR segment at elevation angles from 5 to 20 degrees. After obtaining T_d time series, the relative antenna height (h) can be derived from Eq. (4) as:

$$h = \frac{\lambda}{2\cos\theta_{E9} \cdot \frac{d\theta_{E9}}{dt} \cdot T_d} \tag{9}$$

The T_d value is used to represent the multipath SNR data in order to estimate h. Also, changes in the elevation angle (θ) and in $d\theta/dt$ have to be accounted for. ~~This means that h is a variable depending on the elevation angle.~~ In this study, changes in h were surveyed across dates at an elevation angle of 9 degree (See Sect. 3.2).

Changes in relative antenna height (h) during vegetation growth are directly related to vegetation height increase:

$$\Delta H = h_0 - h \tag{10}$$

Similarly to the phase change estimates ($\Delta\varphi_t$ in Sect. 2.4), h_0 is the median value of the top 15% h data during the whole wheat growth cycle for each track.

The final retrieved vegetation height (H) is based on the mean relative antenna height change from all available satellite tracks (N = 37), plus one wavelength:

$$H = \frac{\sum_{N} \Delta H}{N} + \lambda \tag{11}$$

The minimum value of H is one wavelength. Therefore Eq. (11) can only be applied when the wheat height is higher than one wavelength (0.19 m for L1).

It must be noted that it is not necessary to retrieve soil moisture before retrieving vegetation height.

2.6. GDD (growing degree days) model

Because of the lack of *in situ* records of the field wheat growth stages, we built a reference GDD model based on the wheat growth stage dates observed at the same location in 2010 (Duveiller et al., 2011; Fieuzal et al., 2013, Betbeder et al., 2016). The GDD model is described in the Supplement (Eqs. S5-S6 and Fig. S4).

3. Results

3.1 Soil moisture retrieval

Figure 3 presents the surface soil moisture retrievals from 16 January to 5 March 2015, together with independent *in situ* VSM observations and ISBA simulations. The VSM retrievals are derived from GPS SNR observations using Eq. (6) in sparse vegetation conditions, when A_{norm} is above 0.78, with the a priori S value of 0.0148 $m^3m^{-3}degree^{-1}$ (Fig. 3a) and the adjusted local slope S = 0.0033 $m^3m^{-3}degree^{-1}$ (Fig. 3b). This adjusted S value is the mean of slope values obtained for satellite tracks whose phase presented a linear correlation with *in situ* soil moisture higher than 0.9. This occurred for the ascending tracks of GPS 13, 21, 24 and 30 and for the descending tracks of GPS 05, 09, 10, 15, and 23. Figure 3c shows the VSM retrievals from the scaled soil wetness index ~~based on the normalized multipath phase~~(Eq. (8)).

The GPS and ISBA scores are given in Table 1. The mean soil moisture values during the experimental period are 0.27, 0.28, 0.31, 0.26, and 0.28 m^3m^{-3} for *in situ* VSM measurements, ISBA simulations, GPS retrievals with S = 0.0148 $m^3m^{-3}degree^{-1}$, GPS retrievals with S = 0.0033 $m^3m^{-3}degree^{-1}$, and GPS retrievals from the scaled soil wetness index, respectively.

In Fig. 3, the sub-daily statistical distribution of the VSM retrievals is indicated by box plots. The range of daily standard deviation value of the various VSM estimates is shown in Table 2. The *in situ* VSM measurements present the smallest sub-daily variability, with a mean standard deviation value of 0.002 m^3m^{-3}. The largest variability is obtained for the GPS retrievals based on the a priori slope value S = 0.0148 $m^3m^{-3}degree^{-1}$, with a mean standard deviation value of 0.036 m^3m^{-3}. GPS retrievals based on the adjusted slope value S = 0.0033 $m^3m^{-3}degree^{-1}$ presents intermediate values (0.008 m^3m^{-3}), together with those based on the scaled soil wetness index (0.009 m^3m^{-3}) and with the ISBA simulations (0.005 m^3m^{-3}). Figure 3 shows that the sub-daily variability of GPS VSM retrievals tends to increase during the last 10 days of the retrieval period.

It must be noted that GPS data are missing on 8 and 9 February, and that the ISBA simulations indicate soil freezing (i.e. the presence of ice in the top soil layer) from 4 to 9 February. This period was excluded from the comparison. In the end, there were 47 valid observation days for the statistical analysis of the retrieved surface VSM, among which 43 days could be compared with model simulations.

The GPS VSM daily mean retrievals based on the CH16 method present a good agreement with both *in situ* observations and ISBA simulations: MAE (Mean Absolute Error) and RMSE (Root Mean Square Error) are lower than 0.05 m^3m^{-3}, and SDD

(Standard Deviation of Differences) does not exceed 0.04 m^3m^{-3} (Table 1). The errors are reduced by at least 50 % when the local adjusted slope is used. When the scaled soil wetness index is used, the errors are further reduced.

Figure 4a and 4b show the retrieved soil moisture as a function of the *in situ* observations for a priori and adjusted slopes (S = 0.0148 $m^3m^{-3}degree^{-1}$ and S = 0.0033 $m^3m^{-3}degree^{-1}$, respectively) from all available satellite tracks (66 per day), not only those tracks used for fitting the slope (see Supplement Fig. S5). The corresponding improvements in score values are given in Table 1: the MAE decreases from 0.036 to 0.011 m^3m^{-3}, the RMSE decreases from 0.046 to 0.014 m^3m^{-3}, the SDD decreases from 0.036 to 0.009 m^3m^{-3}. The retrievals based on the a priori slope markedly overestimate VSM in wet conditions. On the other hand, the retrievals based on the adjusted slope only slightly underestimate VSM. This shows that adjusting the slope is critical and has a major impact on the retrieval accuracy. Furthermore, Figure 4c gives the retrievals based on the scaled soil wetness index. Scores are further improved: the MAE decreases to 0.007 m^3m^{-3}, RMSE to 0.009 m^3m^{-3}, and SDD to 0.008 m^3m^{-3}.

We also compared the retrievals with the independent ISBA simulations. The ISBA model VSM simulations present a better agreement with the *in situ* VSM observations than the GPS retrievals, for all the scores, as shown by Table 1 (last column) and Fig. 3. In particular, R^2 = 0.88 for ISBA simulations, against R^2 = 0.74 for GPS retrievals. This shows that the ISBA simulations can be used as a reference to assess local GPS retrievals for this site. The statistical scores resulting from the comparison between the GPS retrievals and the simulations are similar to those based on *in situ* observations.

After 5 March, A_{norm} drops below 0.78 (Fig. 2), and the VSM retrievals are not valid. We made an attempt to retrieve VSM from 6 to 15 March. We obtained 10 VSM retrieved values and we compared them with ISBA VSM simulations, because *in situ* observations were lacking. The ~~retrievals looked sparser and the~~ R^2 score decreased from 0.63 before 6 March (Table 1) to only 0.21 from 6 to 15 March. This result confirms that the empirical A_{norm} threshold (0.78) is a good way to assess the VSM retrieval feasibility over vegetated areas. Additionally, we found that adjusting the A_{norm} threshold from 0.78 to 0.88 permitted making a distinction between harvest and post-harvest (after 30 June) A_{norm} values in Fig. 2. Four more days (2-5 March) are excluded. Figure 3 shows that the 25-75% percentile intervals for these days are larger, but the maximum retrieval differences for these days are acceptable, around 0.03 m^3m^{-3}.

3.2 Dominant SNR period analysis during the wheat growth cycle

Figure 1 shows an example of the multipath SNR data from the ascending track of GPS01 on 21 January 2015. Its average power spectrum (Fig. 1b) derived from a wavelet analysis is also shown, together with the power spectrum (Fig. 1c) for periods ranging from 128 to 1024 s. ~~From t~~The average power spectrum presents a single~~, there is only one~~ peak and the corresponding peak period is 362 s. The SNR data is reconstructed well ~~depending on this peak period~~ (red line in Fig. 1a), using this peak period~~which is a good fit to the SNR data~~. Both phases and amplitudes match very well. This shows that the peak period from the average power spectrum can be used to represent the multipath SNR data. Limiting elevation angle

values from 5 to 20 degrees (Sect. 2.1) ensures a relatively stable value of the peak period. The peak period is considered as the dominant period (T_d) of the multipath SNR data.

Additionally, the major part of the signal power is concentrated on elevation angles ranging from 7 to 11 degrees (see Fig. 1). A preliminary analysis for the entire wheat growing cycle showed that, more often than not, the best elevation angle corresponding to the peak power was around 9 degrees. In this study, elevation and its change rate at 9 degree are used to represent the SNR data for all available satellite tracks (37 per day). It must be noted that this reference elevation angle is specific to the gain pattern and height of the antenna encountered in this experiment. It could present different values in other antenna configurations.

During the wheat growth cycle, preliminary tests showed that the average power spectrum could present multiple peaks together with a reduced maximum average power. This made T_d unsuitable for the representation of the multipath SNR data. Under this situation the quality of the T_d value was considered as poor and the data were not used. An example of T_d time series is shown in Fig. 5 for GPS01 ascending tracks. Poor quality data (e.g. on 17-20 March, and 12-16 June) are indicated. We sorted out the data acquired in two situations: (1) track data presenting more than one peak in the highest 80% percentile of the power spectrum, (2) T_d value smaller by 10 seconds than the mean value of the lowest 10% of the dominant periods (e.g., T_d < 352 s for GPS01). This is further illustrated in Fig. 6, comparing a usable track and an unusable track. On 1 May, there is one peak in the average power spectrum (Fig. 6b), and the dominant period (456 s) obtained can be used to fit the SNR data in Fig. 6a. While on 15 June, there are two peaks in the average power spectrum as shown in Fig. 6d. Furthermore, the maximum average power is only 0.54 which is significantly smaller than the maximum average power of 1.0 observed on 1 May 2015 (Fig. 6b). In Fig. 6c, the SNR pattern is clearly noisier, with smaller amplitudes and a less clear pattern than in Figs. 1a and ~~/~~Fig. 6a. This data set is unusable. A possible cause is the more inhomogeneous reflecting surface after the lodging event. The probability distribution (grey bars) of bad quality tracks among all available 37 satellite tracks is shown in Fig. 2 on a daily basis from 16 January to 15 July 2015. Most unsuitable tracks are observed during two time periods: (1) at the beginning of spring, from 10 to 20 March, and (2) at the beginning of summer, from 12 to 26 June. The latter corresponded to lodging of vegetation, which occurred during a strong wind event and affected the reflecting surface height. The *in situ* observation of wheat height was only 39 cm on 18 June.

As shown in Sect. 2.4, vegetation effects on the SNR signal became significant after 5 March. After this date, A_{norm} (black dots in Fig. 2) decreased drastically, in relation to plant growth. After 10 March, wheat height exceeded one wavelength (> 0.19 m). In addition to lower A_{norm} values, an increasing number of unsuitable tracks was observed till 20 March, together with low values of the peak power (Fig. 5). During this time period, the vegetation gradually decreased the strength of the signal reflected from the soil surface and more signal was reflected by the vegetation. This triggered multiple peaks for some tracks. Such tracks were not used. When the vegetation surface completely replaced the soil surface as the dominant reflecting surface of the GNSS signal, a single peak period was observed again and its value increased in response to the rise of the reflecting surface. For example, T_d increased from 362 s (7 March) to 397 s (22 March) for GPS01 ascending tracks. Figure 5 shows that T_d is not sensitive to vegetation height when vegetation height is smaller than one wavelength.

Therefore, ~~we~~ it can be concluded that this relative vegetation height (at satellite elevation of 9 degrees) retrieval technique ~~was~~ does not work~~ing~~ for vegetation height below one λ (~ 0.19 m for L1) and when multiple peaks ~~were~~ are observed in the average power spectrum.

3.3 Vegetation height retrieval

Figure 7 shows the retrieved vegetation height from 16 January to 15 July 2015, together with seven *in situ* vegetation height measurements and daily vegetation height simulations by ISBA. Since the original H retrievals present a marked levelling effect, the moving average of the GPS height retrievals computed using a centred gliding window of 21 days is shown. The relative vegetation height retrievals are compared with ISBA height simulations and *in situ* height observations in Table 3. The differences between the seven *in situ* observations and the original H retrievals ~~were~~ are -8 cm, +4 cm, -5 cm, -10 cm, -6 cm, -2 cm and -2 cm. Most of them exhibit~~ed~~ a negative bias. In comparison with the errors between the *in situ* observations and the ISBA simulations (-5 cm, +6 cm, +10 cm, -15 cm, -3 cm, 0 cm and -61 cm), the GPS retrievals ~~were~~ are closer to the observations on 30 March and 24 April (the third and forth *in situ* observations). On 18 June, the last height *in situ* observation before harvest ~~was~~ is 39 cm, in relation to lodging. The GPS retrieval ~~was~~ is very close to this value with only -2 cm error. On the other hand, the ISBA simulation on 18 June ~~was~~ is still at 1 m with an error of -61 cm, because the wheat height was simulated without accounting for lodging. This result shows that the *in situ* GPS height retrievals are able to detect local changes in vegetation height. Figure 7 and the scores given in Table 4 show that the GPS retrievals are closer to the observed growing trend than the ISBA simulations. Additionally, the moving average height presents a much better fit to the *in situ* measurements than the raw GPS retrievals. We also compared the GPS retrievals with the ISBA model simulations. We obtained the following score values from 10 March to 11 June 2015: MAE = 8.9 cm, RMSE = 12.4 cm and R^2 = 0.89. Similar values were obtained for the comparison between the moving average height and ISBA simulations: MAE = 9.0 cm, RMSE = 11.6 cm and R^2 = 0.91.

3.4 Vegetation height vs. above-ground dry biomass

Figure 7 also shows that the retrieved vegetation height is related to the simulated above-ground dry biomass of the wheat (brown line). We found a linear relationship between the moving average height from GPS retrievals and the above-ground dry biomass simulated by the ISBA model from 10 March to 29 May 2015 (when the maximum vegetation height, 1 m, was measured), during the time period from tillering to flowering. The correlation coefficient between the moving average height and the above-ground dry biomass, with 81 observations, was 0.996.

A similar result was obtained using the *in situ* height and above-ground dry biomass measurements in Wigneron et al. (2002) over another wheat crop site (Triticum durum, cultivar prinqual) in spring 1993 (See Eqs. S7-S8 and Fig. S6 in the supplement).

4. Discussion

4.1. Can soil moisture be retrieved under significant vegetation effects?

Our results show that over a wheat field the vegetation gradually replaces the soil as the dominant reflecting surface when plant height becomes comparable to, or larger than one wavelength.

We tested the relationship between the multipath phase in Eq. (5) and soil moisture for the whole wheat growing cycle (Fig. 8). We found that when the vegetation effects are not significant (A_{norm} > 0.78), the multipath phase correlates well (R = 0.92, N = 47, for the GPS10 descending tracks) with the *in situ* soil moisture observations (Fig. 8a). During this time period, the variation of multipath phase is about 12 degrees, for *in situ* VSM values ranging from 0.25 m^3m^{-3} to 0.30 m^3m^{-3}. But when the vegetation effects are significant (A_{norm} < 0.78), the multipath phase (without or with unwrapping, Fig. 8b and 8c) is no longer linearly related to soil moisture. For example, when vegetation height starts exceedinged one wavelength, multipath phase rapidly decreased from 207 degrees to 43 degrees (between 10 and 20 March). Changes in multipath phase ~~were~~ are disconnected from ISBA VSM simulations. This is consistent with CH16, who showed that soil moisture cannot be retrieved unless vegetation effects are corrected for.

4.2. Why does the locally adjusted *S* parameter differ from CH16?

In our experiment, the possible VSM retrieval duration was less than two months, in relatively wet conditions and VSM varied little: 0.25 m^3m^{-3} < VSM < 0.30 m^3m^{-3}. This is probably not enough to represent the full yearly range of soil moisture. This might affect the representativeness of the *S* parameter (Sect. 2.4) we derived from our field observations. Furthermore, the different signal wavelength (L1 = 19.03 cm, L2 = 24.45 cm) and the different antenna gain pattern also affect the *S* parameter. Many local environment factors such as vegetation effects, precipitation, changes in soil roughness and soil composition, can perturb the GPS VSM estimates. All these factors contribute to changes in *S*, and further affect the retrieval accuracy and the sub-daily variability of VSM estimates. That is why we used a scaled soil wetness index based on the normalized multipath phase for each track, without a priori knowledge of *S* parameter. This approach also gives more accurate results.

4.3. Can vegetation water content be inferred from the wavelet analysis?

We found that VWC impacts the peak power but we were not able to retrieve VWC at this stage.

Figure 7 shows that the retrieved vegetation height is consistent with independent height measurements. However, vegetation height is not the only factor affecting the reflected GPS signal. Vegetation water content (VWC, in kg m^{-2}) may also play a role on the reflected GPS signal. *In situ* observations indicate that VWC increased together with H during the growing period, from March to mid-May. From mid-May to harvest, VWC tended to decrease but H also decreased in

relation to lodging. Can this specific behavior of VWC be detected from the results of the wavelet analysis? The latter provides three quantities: the dominant period (Sect. 2.5), A_{norm}, and the peak power.

The amplitude (A_{norm}) is related to some extent to VWC (see Sect. 1). However, A_{norm} is calculated assuming the relative antenna height is constant. Because the wheat height increased from 10 cm to 100 cm, the relative antenna height was reduced, and this assumption was not satisfied. This affected the estimates of the amplitude of the multipath SNR data, especially when the wheat was tall. Comparing Fig. 6a and Fig. 6c, it can be observed that the signal amplitude is larger on 1 May than that on 15 June. But A_{norm} (0.15) on 1 May is even smaller than the A_{norm} (0.33) on 15 June (Fig. 2). It is likely that A_{norm} was underestimated on 1 May. Therefore, it is difficult to unequivocally relate A_{norm} to vegetation characteristics, as illustrated in Fig. 2. However, the drop in A_{norm} observed at the beginning of June (Fig. 2) could be related to the drop in VWC.

From the wavelet analysis, we also obtained the peak power when we searched for the peak period from the average power spectrum. Peak power can represent changes in the multipath SNR strength. Figure 9 shows daily box plots of the peak power for all available satellite tracks from 16 January to 15 July 2015, together with the distribution of bad quality tracks (as in Fig. 2), and rainfall. There are two major possible causes for a sudden reduction of the strength of the ~~reflected~~ SNR signal: (1) the attenuation of the signal by the rain intercepted by vegetation or in the troposphere and (2) the occurrence of more than one dominant reflecting surface at different heights, and this two causes can occur at the same time.

Three events of rapid reduction of the peak power can be observed in Fig. 9a. These events are related to larger daily standard deviation (STD) values of vegetation height retrievals (see Fig. 9b). The last event in June could be related to lodging. However, whether maximum STD is an indicator of lodging or not is unclear. It seems that these events are not related to rainfall events, and that the attenuation by intercepted water content is not a major cause of peak power drops. On the other hand, the emergence of multiple peaks and of bad quality tracks is consistent with the rapid power reduction in March and June. Multiple peaks may indicate that the reflected signal originates from surfaces at different heights. A possible cause of multiple peaks is a more heterogeneous wheat canopy density during the first stage of the growing period and after lodging. In such sparse or mixed vegetation conditions, VWC is not uniformly distributed and the soil surface may significantly contribute to the SNR. In the middle of April, there is no such effect but STD score increases (Fig. 9b). It is interesting to note that the peak power drops in Fig. 9a correspond to rapid changes in the retrieved vegetation height in Fig. 9c at multiples of λ or 0.5λ. It must be noted that absolute daily changes in H (and h), of about 1.1 cm d^{-1} are fairly uniform throughout the growing period. Since h decreases when plants grow, relative changes in h tend to increase. According to Eq. (4), T behaves similarly. This means that the sensitivity of the retrieval method to changes in H is larger at the end of the growing period. This is probably why leveling is more pronounced between mid-March and mid-April than at the end of April (see Fig. 9c). Leveling is less noticeable in May.

4.4. Can unwrapped multipath phase be used to retrieve vegetation height?

Our results indicate that using the dominant period to retrieve vegetation height is more relevant than using the multipath phase.

The relationship between the multipath phase (Fig. 8) in Eq. (5) and vegetation height was investigated. Because changes in relative antenna height exceeded λ during vegetation growth, the multipath phase had to be unwrapped. When the vegetation height was smaller than λ (before 10 March), multipath phase (around 200 degrees) presented little changes (about 12 degrees). From 21 March to 18 April, multipath phase was much smaller (around 10 degrees) and relatively stable. On the other hand, the variability increased from 19 April to 11 June (Fig. 8c), and no relationship with plant growth could be found. It can be noted that multipath phase and dominant period are relatively stable when the vegetation height is smaller than λ. Both tend to aggregate at several value levels.

4.5. Can wheat phenological stages be inferred?

Figure 9 shows that the occurrence of multiple peaks together with a drop of the peak power can be used as an indicator of the start of the most active part of the growing season, and of the end of the senescence period preceding the harvest.

We applied the GDD model (see Sect. 2.6) to year 2015 and we obtained the following dates for tillering, flowering, and ripening: 12 March, 31 May, and 3 June, respectively (see Fig. S3 in the Supplement). The obtained tillering date (12 March) is close to the start date (10 March) of the multiple peaks (see Section 3.2). Tillering in wheat triggers nitrogen uptake and the accumulation of biomass (Gastal and Lemaire, 2002). This is consistent with the rapid changes in the indicators derived from the wavelet analysis: drop in A_{norm} values and high rate of multiple peaks (Fig. 2), rise in the retrieved H (Fig. 7), and drop in peak power (Fig. 9). For our site, the tillering date also corresponded to the period when H reached a value of about 0.2 m. This was the case in 2015 and also in 2010 at the same site (Betbeder et al., 2016).

Flowering and ripening did not trigger abrupt changes in the GPS retrievals. However, these stages corresponded to a change in H trend. This is illustrated in Supplement Fig. S7, which shows the difference between retrieved vegetation height at a given date and retrieved vegetation height 15 days before. Flowering and ripening occur towards the end of the growing period when the vegetation height is no longer increased compared with 15 days before but slightly declines due to wheat heads tipping down (Wigneron et al., 2002). In order to confirm these findings, it could be recommended to perform GNSS-IR measurements ~~further~~ over other wheat fields and other crops, together with phenological stage observations combined with in situ height measurements.

4.6 Potential future applicability and transferability of the retrieval method

In situ VSM observations are not widespread in France and *in situ* vegetation height observations are generally not available. Therefore, ISBA simulations are key for water resource monitoring at the country scale. It must be noted that the ISBA

model is forced by the SAFRAN atmospheric analysis (Durand et al., 1993; Durand et al., 1999) and that SAFRAN is able to integrate thousands of *in situ* raingage observations. ISBA is also able to simulate vegetation characteristics such as vegetation height, leaf area index and above-ground dry biomass. However, *in situ* VSM observations are needed to validate the model simulations (e.g. Albergel et al., 2010). From this point of view, the spatial resolution of GNSS retrievals is an asset. The area sampled by GNSS retrievals is much larger than what can be achieved using individual soil moisture probes and much smaller than pixel size of satellite-derived products. Longer continuous time periods of GNSS retrievals should be envisaged to serve as independent validation data sources in statistical methods such as Triple Collocation (Dorigo et al., 2010).

We successfully assessed the surface soil moisture retrieval technique over a wheat crop field, during the start of the growing period. However, the rather narrow range of surface soil moisture values during the corresponding experiment time period limited the representativeness of the obtained retrieval accuracy. Furthermore, our dataset did not include GNSS data and *in situ* VSM measurements for periods of bare soil. Longer periods presenting a bare soil surface should be investigated in ~~further~~ future studies. At the same time, more *in situ* vegetation measurements should be carried out ~~in further studies~~.

The retrieved vegetation height was based on the dominant period of the average power spectrum. The latter was derived from GPS multipath SNR data for elevation angles between 5 and 20 degrees. We only considered the dominant period variations, without accounting for instantaneous phase changes. The accuracy of the retrieved vegetation height could probably be improved considering changes in both period and phase of the multipath SNR oscillations.

In this study, only the SNR data of L1 C/A signal is used, SNR data from different wavelength (e.g., L1 C/A, L2C and L5) should also be compared or combined to survey canopy characteristics.

A linear relationship between wheat height and dry biomass was observed during the period from wheat tillering to ripening. Retrieving dry biomass is a motivation for further research because most current satellite vegetation products focus on retrieving vegetation indexes or leaf area index. The dry biomass is directly related to the wheat yield, and retrieving wheat height could have applications in crop monitoring. In this study, only wheat is considered. Other crops should be investigated in the future.

5. Conclusions

GNSS SNR data were obtained using the SNR GNSS-IR technique over an intensively cultivated wheat field in southwestern France. The data were used to retrieve either soil moisture or relative vegetation height during the growing period of wheat. Vegetation growth tended to decrease the relative antenna height and broke up the constant height assumption used in soil moisture retrieval algorithms. Soil moisture could not be retrieved after wheat tillering. A new algorithm based on a wavelet analysis was implemented and used to extract the dominant period of the SNR and ~~further~~ to retrieve vegetation height. The dominant period was derived from the peak period of the average power spectrum derived from a wavelet analysis of SNR. The method proposed by CH16 was used to retrieve soil moisture under sparse vegetation

conditions, before wheat tillering. Soil moisture was retrieved on a daily basis with a precision (SDD) of 0.008 m^3m^{-3}. Before tillering, only one stable peak was observed in the average power spectrum, because the soil surface was the dominant GNSS reflecting surface. During and after tillering (10-20 March), the reflected GNSS signal included contributions from both soil and vegetation. More than one peak was observed in the average power spectrum together with low values of peak power, showing that there were no clear dominant reflecting surface. Wheat growth gradually raised the reflecting surface of the GNSS signal, from the soil surface to the vegetation surface, which significantly modulated the dominant period of the multipath SNR data. In these conditions, vegetation effects could not be ignored and soil moisture could not be retrieved. The retrieved vegetation height was in good agreement with the *in situ* observations, and was consistent with a lodging event. However, the retrieved height consisted of several levels. Using a moving average on the retrieved height permitted a better match with the *in situ* height measurements: a precision of 3.8 cm could be achieved, against 5.5 cm for the original retrievals. Furthermore, several indicators derived from the wavelet analysis could be used to detect tillering. We also found that VWC impacts the peak power but the latter cannot be used to retrieve VWC at this stage.

“Use of reflected GNSS SNR data to retrieve either soil moisture or vegetation height over a wheat crop”
by Sibo Zhang et al.

Cover letter to the editor

8 August 2017

Dear Dr. Alberto Guadagnini,

The authors’ response to the comments of the two anonymous referees has been published on the HESS web site. The list of all relevant changes made in the manuscript can be found in the enclosed document.
All changes relative to the published HESS paper are detailed in the pdf of the new manuscript. They include all the response elements given by the authors in response to the reviewers’ comments (orange and blue for Reviewer 1 and 2, respectively). Other changes in the text are in red.

The title was changed in response to the comments of Reviewer 2.
Some parts of the paper were re-structured at the request of the reviewers. Former Sections 2 and 3 were merged in a new "Material and methods" Section. Former Section 3.3 was moved to the Supplement. The result Section was reorganised.
All the Figures were revised. In particular, former Figures 3 and 4 were merged. Former Figures S3, S4, S6, S9 and S10 are now embedded into the main text.

References

18 additional references were added (Albergel et al. 2010, Chan et al. 2016, Chew et al. 1997, Darrozes et al. 1997, Dorigo et al. 2010, Durand et al. 1993, 1999, Duveiller et al. 2011, Escalera et al;, 1995, Gaillot et al. 1999, Grinsted et al. 2004, Hagelberg et al. 1995, Koch et al. 2016, Labat 2005, Ouillon et al. 1995, Torrence and Compo 1998, Wigneron et al. 2002).

Yours sincerely,

Jean-Christophe Calvet, Sibo Zhang.

Zhang et al.: Use of GNSS SNR data to retrieve soil moisture and vegetation variables over a wheat crop, Hydrol. Earth Syst. Sci. Discuss., doi:10.5194/hess-2017-152, 2017.

RESPONSE TO REVIEWER #1

The authors thank anonymous reviewer 1 for his/her review of the manuscript and for the fruitful comments.

The revised text is shown in orange in the enclosed version of the manuscript.

1.1 [The study deals about soil moisture, vegetation height and phenological stages estimation by GNSS for a site in southern France and validation to in situ measurements and model simulations. The approach is sound, the manuscript well-written and adequate for the audience of HESS. Because of its high quality, just few attempts need to be made to improve the presentation of the study. E.g., a brief discussion how much in situ (soil moisture) data is necessary to retrieve soil moisture from GNSS signal could clarify the need for adequate calibration.]

Response 1.1:

Retrieving absolute VSM values in m^3m^{-3} is possible after a calibration phase. The minimum VSM has to be derived from the *in situ* observations during the experimental time period in order to determine the VSM_{resid} term in Eq. (6). Moreover, a locally adjusted value of the *S* parameter is needed. The retrieval of the *S* parameter requires at least one or two months of VSM *in situ* observations because soil moisture conditions ranging from dry to wet need to be sampled. However, if a scaled soil wetness index is used instead of soil moisture (see Response 1.17), no *in situ* VSM observations are needed. This aspect was clarified in the revised manuscript (P. 8, L. 3-7).

1.2 [During the investigation period little soil moisture variation has been recorded by in situ and GNSS sensors. The authors should discuss this low range and its relationship to the retrieval accuracy of 0.03 m^3m^{-3}.]

Response 1.2:

Yes, a short period of time is considered in this study. Vey et al. (2015) used the method from Chew et al. using field observations over a long period of time (2008-2014) for a site presenting a high percentage of bare soil. They obtained the following scores for GPS VSM retrievals: R^2 = 0.8, RMSE = 0.05 m^3m^{-3}. We successfully assessed this method for a wheat crop field. But the little soil moisture variation in the experiment time period limited the representativeness of the retrieval accuracy. Longer time periods should be investigated in further studies. We clarified this in the revised manuscript (P. 17, L. 9-11).

1.3 [Similarly, longer time periods should be envisaged for further studies, this delivers the basis for further statistical methods such as Triple Collocation. This would better identify the different uncertainties between the data sets. Especially with the very good results of ISBA simulations, one could question the need for (additional) GNSS measurements.]

Response 1.3:

Yes. In situ VSM observations are not widespread in France and the ISBA simulations are key for water resource monitoring at the country scale. It must be noted that the ISBA model is forced by the SAFRAN atmospheric analysis and that SAFRAN is able to integrate thousands of in situ raingage observations over France. However, in situ VSM observations are needed to validate land surface models and/or satellite-derived products (e.g. Albergel et al., 2010). From this point of view, the spatial resolution of GNSS retrievals is an asset. The area sampled by GNSS retrievals is much larger than what can be achieved using individual soil moisture probes and much smaller than pixel size of satellite-derived products. Longer time periods of GNSS retrievals should be envisaged to serve as independent validation data sources in statistical methods such as Triple Collocation (Dorigo et al., 2010). This aspect was clarified in the revised manuscript (P. 16, L. 29-30; P. 17, L. 1-8).

References:

Albergel, C., J.-C. Calvet, P. de Rosnay, G. Balsamo, W. Wagner, S. Hasenauer, V. Naemi, E. Martin, E. Bazile, F. Bouyssel, J.-F. Mahfouf, “Cross-evaluation of modelled and remotely sensed surface soil moisture with in situ data in southwestern France”, Hydrol. Earth Syst. Sci., 14, 2177–2191, 2010b.

Dorigo, W. A., Scipal, K., Parinussa, R. M., Liu, Y. Y., Wagner, W., de Jeu, R. A. M., and Naeimi, V.: Error characterisation of global active and passive microwave soil moisture datasets, Hydrol. Earth Syst. Sci., 14, 2605–2616, doi:10.5194/hess-14-2605-2010, 2010.

1.4 [Soil moisture retrieval results could better be discussed by including recent literature and comparing to other GNSS soil moisture retrieval methods.]

Response 1.4:

The method from Chew et al. is the latest proposed method, as far as we know. We will further increase the accuracy of our GNSS VSM retrievals using a scaled soil wetness index in the revised manuscript (see Response 1.17). This aspect was clarified in the revised manuscript (P. 8, L. 8-19; P. 10, L. 12-13 and 22; P. 11, L. 2 and 9-11; Table 1; Table 2; Fig. 3 and 4).

1.5 [The authors ask the question if phenological stages can be inferred from GNSS. The outcome and visibility of the paper could be increased by giving more specific information about different stages or managements, e.g. in form of an index or threshold for wheat as an important representative for all cereals.]

Response 1.5:

We found in our case study, that the tillering date (12 March) obtained from a GDD model is close to the start date (10 March) of a multiple peak period (see Section 5.5), when the vegetation height is about 20 cm, close to one wavelength. Flowering and ripening occur towards the end of the growing period when the vegetation height is no longer increased compared with 15 days before but slightly declines due to wheat heads tipping down. In order to confirm these findings, it could be recommended to perform GNSS-R measurements further over wheat fields and other crops, together with phenological stages observations. We clarified this in the revised manuscript (P. 16, L. 23-27).

1.6 [Specific comments: Abstract: More information about the retrieval method should be added.]

Response 1.6:

Soil moisture is retrieved from the multipath phase assuming the relative antenna height is constant, and the vegetation height is retrieved using the SNR's dominant period derived from a wavelet analysis. We rephrased the abstract accordingly (P. 1, L. 14-18).

1.7 [P. 2, L. 10f: Refer also to the other L-band satellite SMAP.]

Response 1.7:

Yes, we will cite the Soil Moisture Active Passive (SMAP) mission (Chan et al., 2016), in addition to SMOS. (P. 2, L. 15-16)

Reference:

Chan S. K., Bindlish, R., O'Neill, P. E., Njoku, E., Jackson, T., Colliander, A., Chen, F., Burgin, M., Dunbar, S., Piepmeier, J., Yueh, S., Entekhabi, D., Cosh, M. H., Caldwell, T., Walker, J., Wu, X., Berg, A., Rowlandson, T., Pacheco, A., McNairn, H., Thibeault, M., Martínez-Fernández, J., González-Zamora, A., Seyfried, M., Bosch, D., Starks, P., Goodrich, D., Prueger, J., Palecki, M., Small, E. E., Zreda, M., Calvet, J.-C., Crow, W., and Kerr, Y.: Assessment of the SMAP passive soil moisture product, IEEE Trans. Geosci. Remote Sens., 54 (8), 4994 - 5007, doi:10.1109/TGRS.2016.2561938, 2016.

1.8 [P. 3, L. 15: introduce L2C.]

Response 1.8:

The SNR of L2C signal is only transmitted by the recent Block IIR-M ("Replenishment Modernized") and IIF ("Follow-on") GPS satellites, which is with higher power and more precise than the signal L1 C/A. We introduced L2C in the revised manuscript (P. 4, L. 22-23).

1.9 [P. 3, L. 26: What characterizes the dominant period?]

Response 1.9:

The definition of the dominant period is: the peak period of the average power spectrum from the valid SNR segment data at elevation angles ranging from 5 to 20 degrees. We clarified this in the revised manuscript (P. 1, L. 17-18; P. 9, L. 10-11).

1.10 [P. 4, L. 10: Introduce PBO.]

Response 1.10:

PBO H_2O is an initiative to translate data from the Plate Boundary Observatory (PBO) sites of the GPS network in the western United States into environmental products (Larson, 2016). (P. 3, L. 3)

1.11 [P. 5, L. 15: Start the section with explaining the aim of the calculations.]

Response 1.11:

Due to the motion of the GPS satellites, the path delay δ between the direct and reflected signals cause an interference pattern in the signal power of SNR data. The SNR frequency/period is directly affected by the perpendicular distance from the antenna to the dominant reflecting surface. Provided the reflecting surface is stable, the a priori antenna height can be used to estimate the SNR frequency. The SNR frequency is used to calculate the multipath SNR phase. Then, the SNR phase is used to estimate VSM. If the reflecting surface is changing in response to vegetation growth, vegetation height can be retrieved instead of VSM by directly estimating the dynamic SNR frequency/period with a wavelet analysis. (P. 6, L. 6-8; P. 7, L. 3-6)

1.12 [P. 6, L.10: Again, explain in one or two sentences the general concept of soil moisture retrieval before starting the details of this section.]

Response 1.12:

As the SNR frequency is known (Eq. (3)), it is possible to estimate the SNR amplitude and phase. Larson et al. (2008) and Larson et al. (2010) showed that phase varies linearly with near-surface VSM (R^2 = 0.76 to 0.90). This result was used by Chew et al. (2014) to develop an algorithm to estimate surface soil moisture (top 5 cm) over bare ground. (P. 7, L. 8-11)

1.13 [P. 7, L. 9: A discussion about the reasons and needs for omitting a soil moisture retrieval under vegetation is necessary. Why were alternative methods not used?]

Response 1.13:

In conditions of significant vegetation effects, Chew et al. proposed an algorithm able to correct the phase for vegetation effects. Firstly, $A_{LSPnorm}$ and ΔH_{eff} are derived by a Lomb-Scargle Periodogram (LSP) method. Then the observed SNR metrics (A_{norm}, $A_{LSPnorm}$ and ΔH_{eff}) are smoothed using a low-pass filter (Savitzky-Golay filter or moving average filter). A

linear nearest neighbor search algorithm with A_{norm}, $A_{LSPnorm}$ and ΔH_{eff} is used to find the estimated phase (φ_{veg}) caused by vegetation in a modeled lookup table. The φ_{veg} values derived from the lookup table are then smoothed through time using the same filter. Then the expected phase changes (φ_{VSM}) due to soil moisture is equal to $\varphi_{VSM} = \Delta\varphi - \varphi_{veg}$, where $\Delta\varphi$ is the original observed phase change. This algorithm is based on the assumption that the total phase change is a linear combination of the phase change due to soil moisture and of the phase change due to vegetation. Another important difference for retrieving soil moisture with significant vegetation effects is that the slope (S) of the relationship between phase (φ_{VSM}) and soil moisture changes throughout the year. S is a function of time, which also needs to be searched for in the lookup table. Additionally, this algorithm is based on an unpublished lookup table for new L2C GPS signals. Since the receiver we used could not track L2C signals and since we could not access a relevant lookup table, we were not able to correct for vegetation effects and we retrieved surface soil moisture over a period with rather sparse vegetation, from 16 January to 5 March. (P. 14, L. 20-23)

1.14 [P. 10, L. 3: how independent are the in situ data when some have been used for calibration? This needs to be clarified.]

Response 1.14:

With the a priori S = 0.0148 $m^3m^{-3}degree^{-1}$, only the minimum soil moisture observation during the time period is used as the VSM_{resid}. We also used the *in situ* soil moisture observations and phases from SNR data to fit the local slope: S = 0.0033 $m^3m^{-3}degree^{-1}$. In this situation, only ISBA simulations can be considered as independent from the GNSS retrievals. This aspect was clarified in the revised manuscript (P. 8, L. 3-7).

1.15 [P. 10, L. 11ff: The reason for larger variability in GPS daily soil moisture estimates could be found in different locations observed. During satellite overpasses the observed location moves within the larger "footprint" of the GNSS system.]

Response 1.15:

Yes. Larger variability in GPS sub-daily VSM estimates might originate from the different locations observed. Many local environment factors such as vegetation effects, precipitation, changes in soil roughness and soil composition, can perturb the GPS VSM estimates. During satellite overpasses the observed location changes together with the size of the footprint (the First Fresnel Zone) of the GNSS system, in relation to the antenna height and elevation angle range. It might be another cause of the sub-daily variability of VSM estimates. Additionally, issues with the SNR data of the L1 C/A signal and the receiving antenna gain pattern may also affect the VSM estimates. (P. 14, L. 19-20; P. 1 in the supplement)

1.16 [P. 11, L. 12: What is the reason for using a curve smoothing procedure? What are the reasons for the leveling effect?]

Response 1.16:

The possible causes of the leveling effect are discussed in Section 5: (1) the occurrence of more than one dominant reflecting surface at different heights (Sect. 5.3) and (2) rapid phenological changes in the wheat canopy triggering a response of the H retrieval (Sect. 5.5). It must be noted that absolute daily changes in H (and h), of about 1.1 cm d^{-1} are fairly uniform throughout the growing period. Since h decreases when plants grow, relative changes in h tend to increase. According to Eq. 4, T behaves similarly. This means that the sensitivity of the retrieval method to changes in H is larger at the end of the growing period. This is probably why leveling is more pronounced between mid-March and mid-April than at the end of April (see Fig. 7). Leveling is less noticeable in May. (P. 15, L. 27-31)

1.17 [P. 12, L. 22ff: The authors could show the retrieval of a soil wetness index and relate it to in situ soil moisture by multiplying it to porosity (from in situ measurements or soil maps).]

Response 1.17:
(P. 8, L. 8-19; P. 10, L. 12-13 and 22; P. 11, L. 2 and 9-11; Table 1; Table 2; Fig. 3 and 4)
Yes. The phase time series can be normalized for each satellite track. Then the median value of the normalized phases from all available satellite tracks can be considered as the final soil wetness index (φ_{index}) for each day as shown in Fig. R1.1 (red line).

$$\varphi_{index} = \frac{\varphi - \varphi_{\min}}{\varphi_{\max} - \varphi_{\min}} \qquad \text{(R1.1)}$$

This soil wetness index time series is linearly related with in situ observations (R^2 = 0.74) and ISBA simulations (R^2 = 0.65). Moreover, VSM can be estimated from φ_{index}

$$VSM = VSM_{obs\_\min} + \varphi_{index} \cdot (VSM_{obs\_\max} - VSM_{obs\_\min}) \qquad \text{(R1.2)}$$

VSM_{obs_min} and VSM_{obs_max} are the minimum and maximum *in situ* VSM observations during the experimental time period, respectively. Figure R1.2 presents the estimated VSM from GPS soil wetness index (φ_{index}), together with *in situ* VSM observations and ISBA simulations. More related scores are shown in Table R1.1 and the scatter plot between GPS retrievals from φ_{index} and *in situ* observations are shown in Fig. R1.3. We will present these results in the revised manuscript.

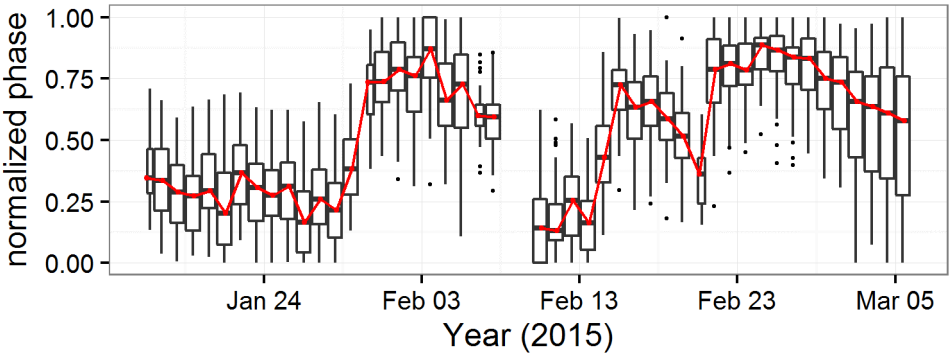

Fig. R1.1 - Median of the daily GPS normalized phases (soil wetness index, red line) and their daily statistical distribution (black box plots) for all available satellite tracks from 16 January to 5 March 2015.

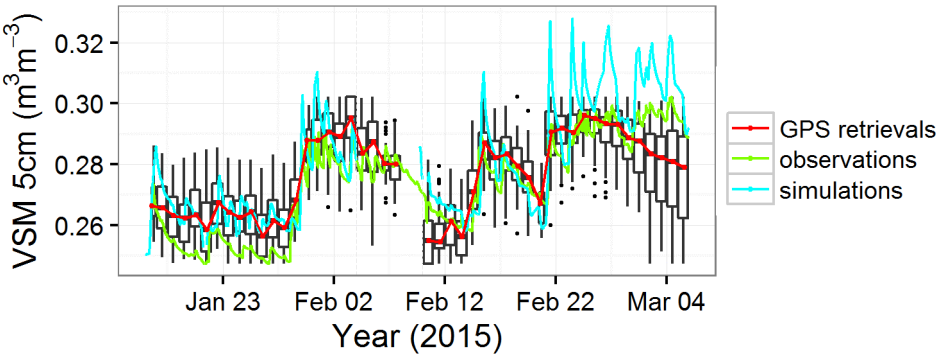

Fig. R1.2 - In situ daily mean surface volumetric soil moisture (VSM) observations at 5 cm depth (green line), ISBA daily mean simulations (blue line), median of the daily GPS retrievals with soil wetness index (red line) and their daily statistical distribution (black box plots) for all available satellite tracks from 16 January to 5 March 2015.

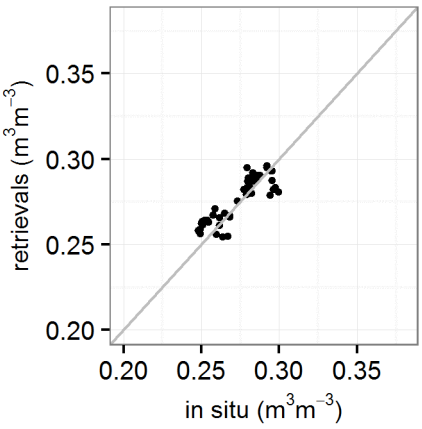

Fig. R1.3 - Scatter plot between GPS retrievals (Eq. (R1.1)) and *in situ* VSM observations (m^3m^{-3}) from 16 January to 5 March 2015.

Table R1.1 - Soil moisture scores from 16 January to 5 March 2015

	GPS vs. *in situ*	GPS vs. ISBA	GPS vs. *in situ*	GPS vs. ISBA	GPS (φ_{index}) vs. *in situ*	GPS (φ_{index}) vs. ISBA	ISBA vs. *in situ*
S ($m^3m^{-3}deg^{-1}$)	0.0148		0.0033		-	-	-
N	47	43	47	43	47	43	43
MAE (m^3m^{-3})	0.036	0.034	0.011	0.018	0.007	0.009	0.009
RMSE (m^3m^{-3})	0.046	0.041	0.014	0.022	0.009	0.012	0.010
SDD (m^3m^{-3})	0.036	0.037	0.009	0.012	0.008	0.011	0.006
Mean bias (m^3m^{-3})	0.029	0.019	-0.010	-0.018	0.003	-0.005	0.008
R^2	0.73	0.63	0.73	0.63	0.74	0.65	0.88

Zhang et al.: Use of GNSS SNR data to retrieve soil moisture and vegetation variables over a wheat crop, Hydrol. Earth Syst. Sci. Discuss., doi:10.5194/hess-2017-152, 2017.

RESPONSE TO REVIEWER #2

The authors thank anonymous reviewer 2 for his/her review of the manuscript and for the fruitful comments.

The revised text is shown in blue in the enclosed version of the manuscript.

2.1 [General comments
This paper presents a case study applying GNSS signals, which were reflected on the ground surface (soil, vegetation surface) to derive soil moisture and vegetation height data over a wheat crop field. The GPS antenna was installed at a height of 2.51 m. Soil moisture was retrieved as long as the vegetation height was lower than ~20 cm. However, with a further increase in plant height, it was not possible to retrieve soil moisture. Reaching a certain plant height, it was then possible to retrieve the vegetation height from the GNSS signals.
In general, the topic of this manuscript is interesting and worth to be published in HESS. The methods seem valid and transparent. However, before publishing, this manuscript has to undergo major revision as several points have to be clarified and described / discussed better / more clearly. The manuscript should undergo an English spell check. The following points should be improved in general:
- Please highlight in a more prominent way what is really new and what is the outcome and applicability of this approach.]

Response 2.1:

Yes. We revised the abstract and conclutions to highlight the new results presented in this study. (P. 1, L. 14-19; P. 17, L. 26-32; P. 18, L. 2-6 and 12)
In particular, the following information was given:

GNSS SNR data were obtained using the GNSS-IR technique over an intensively cultivated wheat field in southwestern France. The data were used to retrieve either soil moisture or vegetation height during the growing period of wheat. Vegetation growth tended to decrease the relative antenna height and broke up the constant height assumption used in soil moisture retrieval algorithms. Soil moisture could not be retrieved after wheat tillering. A new algorithm based on a wavelet analysis was implemented and used to extract the dominant period of the SNR and further to retrieve vegetation height.

Should a revised version of this paper be accepted in HESS, a copy editing work will be performed.

2.2 [- Please introduce and explain the so called ‘dominant period’ in more detail.]

Response 2.2:

A vegetation height retrieval algorithm is proposed using the dominant SNR period, which is the peak period in the average power spectrum derived from a wavelet analysis of SNR. We clarified this in the revised manuscript (P. 1, L. 17-18; P. 9, L. 10-11).

2.3 [- Please clarify that the GNSS retrieval of soil moisture and / or vegetation variables, actually only vegetation height, is only valid for different temporal stages. Especially, at the beginning it is unclear / confusing that soil moisture and vegetation height were retrieved at different time periods (before and after vegetation significant growth in March)].

Response 2.3:

Yes. We replaced "vegetation variables" or "vegetation characteristics" by "vegetation height". We mentioned in the Abstract that soil moisture and vegetation height were retrieved at different time periods (before and after vegetation significant growth in March). (P. 1, L. 18-19; P. 1, L. 12 and 29; P. 4, L. 6; P. 5, L. 17)

2.4 [- If the title contains ‘vegetation variables’ but only ‘vegetation height’ is retrieved, please change this in the title and at relevant parts of the manuscript.]

Response 2.4:

Yes. We modified the title as ‘Use of reflected GNSS SNR data to retrieve either soil moisture or vegetation height over a wheat crop’. We replaced "vegetation variables" or "vegetation characteristics" by "vegetation height" in the entire manuscript (P. 1, L. 1-2; P. 1, L. 12 and 29; P. 4, L. 6; P. 5, L. 17).

2.5 [- The structure of the paper is not always clear – especially the chapters ‘Method’, ‘Results’ and ‘Discussion’ should be structured better. Some results / discussions already appear in the methods part, some points of the discussion in the results part and some methods in the discussion part.]

Response 2.5:

Yes. We revised the manuscript accordingly. In particular, description of Fig. 1 was moved from Sections 2.1 and 3.2 to Section 4 (P. 11, L. 25-31; P. 12, L. 1-8). Description of Fig. 2 was moved from Sections 3.1 and 3.2 to Section 4 (P. 12, L. 21-25). Description of Figs. S3 and S4 was moved from Section 3.2 to Section 4 (P. 12, L. 9-21 and 26-34; P. 13, L. 1-3).

2.6 [- In some parts, the methods are explained very well, but in some parts they are presented too extensively. The manuscript should be more focused on your applied method and should be shortened as many aspects are already published in literature and don't have to be repeated in this manuscript.]

Response 2.6:

Yes. We improved the focus of Section 3. Note however that all readers of HESS are not familiar with GNSS reflectometry and that Eqs. 1-6 need to be presented. We moved Eqs. 10-12 in the manuscript to the revised supplement (Eqs. S9-S11).

2.7 [- Is it necessary to retrieve soil moisture before retrieving vegetation height? Please comment on this.]

Response 2.7:

No. It is not necessary to retrieve soil moisture before retrieving vegetation height. This was made clear in the revised manuscript (P. 9, L. 26).

2.8 [- Regarding the statistics, 7 or even only 5 (during the period you used to demonstrate vegetation height) in situ vegetation height samples are actually too low. Please comment at least that during further studies more in situ data should be carried out.]

Response 2.8:

Yes. The in situ vegetation height samples are few, but it must be noted that GNSS height retrievals are totally independent from the in situ measurements. We will make clear that in further studies, more in situ data enabling the characterization of vegetation would be needed. (P. 17, L. 13)

2.9 [- It is questionable if all information given in the supplement is needed. On the other hand, some figures (see specific comments below) would also be valuable within the manuscript itself and should be presented there.]

Response 2.9:

Yes. We adjusted this in the revised manuscript and supplement. Fig. S3 and Fig. S8 were combined together to get a new Fig. 6 in the revised manuscript. Fig. S4 and Fig. S6 were moved to the revised manuscript as Fig. 5 and Fig. 8, respectively. Fig. S7 replaced Fig. 2 in the revised manuscript. Fig. S9 was megred into Fig. 9 in the revised manuscript. Fig. S10 was omitted becasue it was similar as Fig. 8 in the revised manuscript.

2.10 [Specific comments
Page 1 – Title
Please clarify that the retrieval of soil moisture and vegetation variables are actually only valid for different temporal stages (before and after vegetation significant growth in March).

Moreover, it would be valuable to include that you use reflected GNSS signals in your approach as also other GNSS approaches exist on this topic.
Title suggestion: 'Use of reflected GNSS SNR data to retrieve either soil moisture or vegetation height, depending on the vegetation phase of a wheat crop field,']

Response 2.10:

Yes, we changed the title accordingly: 'Use of reflected GNSS SNR data to retrieve either soil moisture or vegetation height over a wheat crop' (P. 1, L. 1-2)

2.11 [Page 1 – Abstract
General: The absolute length of the abstract seems fine, however, the information given here should be compressed or information should be combined more functionally. Additionally, it should be added why this approach is generally useful (1 sentence) and what is missing so far regarding the state of art (1 sentence)]

Response 2.11:

Yes. Surface soil moisture can be retrieved based on the linear relationship between in situ soil moisture observations and SNR phases estimated by the Least Square Estimation method, assuming the relative antenna height is constant. However, it is found in this study that the vegetation growth breaks up the constant relative antenna height assumption, and modulates the SNR period. A vegetation height retrieval algorithm is proposed using the SNR dominant period, which is the peak period in the average power spectrum derived from a wavelet analysis of SNR.
We rephrased the abstract accordingly (P. 1, L. 14-19).

2.12 [p.1, l.15: '...numerical simulations of biomass...']

Response 2.12:

Yes. The sentence was modified (P. 1, L. 20-21) as:

"The retrievals are compared with two independent reference datasets: *in situ* observations of soil moisture and vegetation height, and numerical simulations of soil moisture, vegetation height and above-ground dry biomass from the ISBA (Interactions between Soil, Biosphere and Atmosphere) land surface model."

2.13 [p.1, l. 18: describe in few words the 'dominant period']

Response 2.13:

A vegetation height retrieval algorithm is proposed using the dominant SNR period, which is the peak period in the average power spectrum derived from a wavelet analysis of SNR. We clarified this in the revised manuscript (P. 1, L. 17-18).

2.14 [p.1, l. 18: '...SNR data, whereas changes in...']

Response 2.14:

Yes. The sentence was rephrased accordingly (P. 1, L. 23).

2.15 [p.1, l. 20: '...smaller than one wavelength (~19 cm).' This should also be changed in the entire manuscript.]

Response 2.15:

Yes. We corrected it (P. 1, L. 25).
"Surface volumetric soil moisture can be estimated (R^2 = 0.74, RMSE = 0.009 m^3m^{-3}) when the wheat is smaller than one wavelength (~ 19 cm)."

2.16 [p.1, l. 22: dry biomass?]

Response 2.16:

Yes. We corrected this (P. 1, L. 28 and 31).

2.17 [Page 1-3: 1. Introduction
General: The introduction is quite good, but it should be written more comprehensively, especially the parts where you describe already published techniques. However, the first part (p.1, l.27-p.2, l.2) where you introduce the necessity of this approach and the recent lack to monitor land surface variables at a local scale should be extended! Moreover, it should be written more clearly why GNSS reflectometry could be a solution.]

Response 2.17:

In situ VSM observations are not widespread in France and in situ vegetation height observations are generally not available. Therefore, ISBA (Interactions between Soil, Biosphere and Atmosphere) simulations are key for water resource monitoring at the country scale. It must be noted that the ISBA model is forced by the SAFRAN atmospheric analysis and that SAFRAN is able to integrate thousands of in situ raingage observations. ISBA is also able to simulate vegetation characteristics such as vegetation height, leaf area index, and above-ground dry biomass. However, in situ VSM observations are needed to validate land surface models and/or satellite-derived products (e.g. Albergel et al., 2010). From this point of view, the spatial resolution of GNSS retrievals is an asset. The area sampled by GNSS retrievals is much larger than what can be achieved using individual soil moisture probes and much smaller than pixel size of satellite-derived products. Longer time periods of GNSS retrievals should be envisaged to serve as independent validation data sources in statistical methods such as Triple Collocation (Dorigo et al., 2010).
We clarified it in the revised manuscript (P. 2, L. 6-7). We also discussed it in Sect. 4.6 (P. 16, L. 29-30; P. 17, L. 1-8).

References:

Albergel, C., J.-C. Calvet, P. de Rosnay, G. Balsamo, W. Wagner, S. Hasenauer, V. Naemi, E. Martin, E. Bazile, F. Bouyssel, J.-F. Mahfouf, “Cross-evaluation of modelled and remotely sensed surface soil moisture with in situ data in southwestern France”, Hydrol. Earth Syst. Sci., 14, 2177–2191, 2010b.

Dorigo, W. A., Scipal, K., Parinussa, R. M., Liu, Y. Y., Wagner, W., de Jeu, R. A. M., and Naeimi, V.: Error characterisation of global active and passive microwave soil moisture datasets, Hydrol. Earth Syst. Sci., 14, 2605–2616, doi:10.5194/hess-14-2605-2010, 2010.

2.18 [p.2, l.7: The frequency of GPS L1-band is 1.57542 GHz. Please write 1.6 GHz instead of 1.5 GHz.]

Response 2.18:

Yes. We corrected it (P. 2, L. 11).

"GNSS satellites operate at the L-band microwave frequency domain (between 1.2 GHz and 1.6 GHz). "

2.19 [p.2, l.10: ‘These properties have e.g. been...’]

Response 2.19:

Yes. We corrected it (P. 2, L. 15).

2.20 [p.2, l.10-15: As you generally mention L-band active and passive remote sensing techniques, also other GNSS methods (besides reflectometry) aiming to derive soil moisture or vegetation parameters should be mentioned (e.g. GNSS methods using signal attenuation).]

Response 2.20:

Yes. We cited a reference using GNSS signal strength attenuation.
Larson et al. (2008) showed that SNR data obtained from existing networks with single ground-based geodetic GNSS-IR antenna can be used to infer soil moisture. Other GNSS methods (besides reflectometry) can be used. For example, Koch et al. (2016) used three geodetic GNSS antennas (one was installed above the soil, the other two were buried at a depth of 10 cm), to measure the GNSS signal strength attenuation and to retrieve soil moisture over bare soil. (P. 2, L. 30-32; P. 3, L.1-2)

References:

Koch, F., Schlenz, F., Prasch, M., Appel, F., Ruf, T. and Mauser, W.: Soil moisture retrieval based on GPS signal strength attenuation, Water, 8(7), 276, 2016.

2.21 [p.2, l.17: please specify, how these two antennas are mounted?]

Response 2.21:

Yes. We clarified it in the revised manuscript (P. 2, L. 22-25).

"(1) waveform acquisition with a specific receiver using two antennas (one zenith-oriented antenna and one surface-oriented antenna), called GNSS reflectometry (GNSS-R) (Zavarotny et al., 2014) or (2) GNSS signal strength, Signal-to-Noise Ratio (SNR), acquisition with classical geodetic receiver using one antenna, called GNSS interferometric reflectometry (GNSS-IR) technique (Larson, 2016). "

2.22 [p.2, l.26: 'They are surrounded by sparse vegetation and are therefore not useful for vegetation studies.']

Response 2.22:

Yes. The sentence was modified accordingly (P. 3, L. 7).

2.23 [p.3, l.31/32: Better write 'lower and taller vegetation' as you are measuring the vegetation height and not their density.]

Response 2.23:

Yes. This sentence was rephrased accordingly (P. 4, L. 13).

2.24 [Page 4-5: 2. Data
General: Actually this section already belongs to the 'Method' section.
p.4, l.4: Fig. S1: This figure is not really valuable to show where the test field is situated (present either a picture of the GNSS antenna in the field or a map where the field is situated)]

Response 2.24:

Yes. We reorganized Sections 2 and 3 in a single "Materials and methods" Section.
We presented a picture of the GNSS antenna in the field (see Fig. S1 in the revised supplement).

2.25 [p.4, l.14: '..., four GPS satellites of in total 32...]

Response 2.25:

Yes. The sentence was modified (P. 4, L. 30).
For our site, four GPS satellites out of 32 were excluded from the analysis because their data were incomplete.

2.26 [p.4, l.18: refer to relevant figure]

Response 2.26:

Yes. We refered to Figure 1a here. Figure 1a shows an example of the multipath SNR data after detrending for the ascending track of GPS01 on 21 January 2015. The periodic signature of the multipath SNR data is visible. (P. 5, L. 5-7)

2.27 [p.4, l.1-2 and l.29: avoid repetitions]

Response 2.27:

Yes. The repeated sentence (P.4, L.29) was deleted (P. 5, L. 15 in the revised manuscript).

2.28 [p.4, l.1ff: add information on the soil type and texture; moreover, the row spacing of the wheat crop would be interesting.]

Response 2.28:

Yes. We added relevant the available information on soil and crop properties (P. 5, L. 20-21). Soil in the close vicinity of the antenna consisted of 18% of sand, 41% of clay, and 41% of silt. The row spacing of the wheat crop was 15 cm.

2.29 [p.4, l.30/31: which satellite observations are meant? GNSS satellites or EO satellites?]

Response 2.29:

EO satellites. The sentence was modified (P. 5, L. 16).

2.30 [p.5, l.2: 'soil moisture and vegetation height...']

Response 2.30:

Yes. The sentence was corrected ("height" was added) (P. 5, L. 17).

2.31 [p.5, l.5: Which soil moisture instruments did you use as reference, e.g. frequency domain probes?]

Response 2.31:

Yes, FDR ML2 Thetaprobes were used. We clarified it in the revised manuscript (P. 5, L. 23).

2.32 [p.5, l.8: add the vegetation height at the end of the season as well. Moreover, for each reference sample the measured height and the phenological status of the wheat crop would be interesting (e.g. listed in a table).]

Response 2.32:

Yes. We added information on the vegetation height and phenological status in the revised manuscript (P. 5, L. 26-28; Table 3).

2.33 [p.20, Fig. 1: Figure sub-captions (a-d) are not well structured; a legend in plot a) would be helpful (red and black line); please insert units if there are in y-axis of plot b) and plot d) and in the legend of plot c) (otherwise write []); the mentioned 128 to 1024 s are not shown in plot c –please mark or show tem additionally in a second x-axis; for more clarity in the manuscript, refer to Fig. 1a, 1b, 1c, 1d, not only to Fig. 1.]

Response 2.33:

Yes. We modified this figure (Fig. 1 in the revised manuscript). The units are $V^2V^{-2}s^{-1}$ for the y-axis of plot (b) and plot (d) and the legend of plot (c). y-axis of plot (c) ranges from 128 to 1024 s.

2.34 [Page 5-9: Methods
General: This chapter should be written more comprehensively and precisely, especially the parts of already known methods.
p.6, l.8ff: How many soil moisture and vegetation height results per day did you get out of the 37 available satellite tracks? As of Table 1 and Table 3 it seems that you got 1 results for each day. Please clarify (short) already at this point the temporal resolution and the daily composition of your retrieved results.]

Response 2.34:

Yes, there is one result for each day. The median soil moisture estimate from all available satellite tracks (66 per day) that passed at different times during the day was used as the final soil moisture estimate. The final retrieved vegetation height (*H*) was based on the mean height change from all available satellite tracks (37 per day), plus one wavelength. We clarified this in the revised manuscript (P. 7, L. 28; P. 8, L. 1-2).

2.35 [p.7, l.3: Is there any S-value specific for L1 already available in literature? Or is the mentioned and an adjusted S-value for the first time applied for L1-band signals? Then this should be introduced more prominently in the manuscript!]

Response 2.35:

In PBO H_2O network, only L2C is considered to retrieve soil moisture. There is no specific S parameter for L1. We adjusted S parameter to provide better results. Because the slope between in situ observations and SNR phase in our case is obviously different from the a priori S value, although the correlation is high. Moreover, it can be proposed to use a scaled wetness index to retrieve a scaled value of VSM. In this case, using the S parameter is not needed. For many applications, a scaled value of VSM is sufficient.

Additionally, Vey et al. (2015) used the method and S parameter value from Chew et al. with L1, L2P and L2C SNR data over a long period of time (2008-2014) for a site presenting a high percentage of bare soil. They compared VSM estimates from L1 data with VSM estimates from L2C data. They obtained the following VSM scores: RMSD was 0.03 m^3m^{-3}, and the regression slope was 1.03. We clarified this in the revised manuscript (P. 4, L. 23-24).

2.36 [p.7, l.5: It seems more logical to introduce the adjusted S-value in this chapter instead in the 'Results' chapter.]

Response 2.36:

Yes. We adjusted this in the revised manuscript (P. 8, L. 3-7).

2.37 [p.7, l.6ff: Perhaps it also makes sense to introduce your experimental A_norm threshold of 0.88 within this chapter. Moreover, Fig 2 should be combined with / replaced by Fig. S7.]

Response 2.37:

Yes. Fig. 2 was replaced by Fig. S7 in the revised manuscript; and Fig. S7 was removed from the revised supplement. We also introduced A_{norm} threshold of 0.88(P. 11, L. 20-24).

2.38 [p.7,12/13: are GNSS data available for periods of bare soil (e.g. before the wheat crops reached a vegetation height of 10 cm before January 16th) – this would be valuable to improve the final soil moisture estimate.]

Response 2.38:

We don't have GNSS data for periods of bare soil. The available data started being collected on 6 December 2014, and wheat had started growing (in situ height measurement was 10 cm on 17 December 2014). Because of discontinuities in the availability of both *in situ* soil moisture data and GNSS data before 16 January 2015, we started our analysis on 16 January 2015. Longer periods of time including bare soil situations should be investigated in further studies. (See Response 2.53) (P. 17, L. 11-13)

2.39 [p.7, l.21: 'see the Supplement' – which figure or part do you mean?]

Response 2.39:

We mean Eqs. S1-S4 in the Supplement. We clarified it in the revised manuscript (P. 9, L. 9).

2.40 [p. 8, l.9ff: 'One possible reason...' This part fits better to the 'Discussion' part.]

Response 2.40:

Yes. We modified this in the revised manuscript (P. 12, L. 26-34; P. 13, L. 1-3).

2.41 [p.9, l.8ff: In my opinion, the 'scores' don't have to be introduced with equations.]

Response 2.41:

We moved Section 3.3 to the revised Supplement (P. 9 in the revised supplement).

2.42 [p.21, Fig. 2: Should/could be combined with Fig. S7. Figure S3 and S4: Especially Fig. S4 is interesting. It should be demonstrated within the manuscript as it shows at which stages it is difficult to retrieve the results according to the dominant period.]

Response 2.42:

Yes. Fig. 2 was replaced by Fig. S7. Fig. S3 and Fig. S8 were combined as the new Fig. 6 in the revised manuscript (P. 15, L. 6-8). And we moved Fig. S4 from the supplement to the revised manuscript (Fig. 5; P. 12, L. 9-25).
After 10 March, wheat height exceeded one wavelength (> 0.19 m). In addition to lower A_{norm} values, an increasing number of unsuitable tracks was observed till 20 March, together with low values of peak power. The vegetation gradually decreased the strength of the signal reflected from the soil surface but increased the signal reflected from vegetation, causing more than one peak. The quality of such track data was considered too poor for retrieving biophysical variables. When the vegetation surface completely replaced the soil surface as the dominant reflecting surface of the GNSS signal, a single peak period was observed again and its value increased in response to the rise of the reflecting vegetation surface. We will revise the manuscript accordingly.

2.43 [Page 10-11: Results
p.10, l.3ff: Please insert also the mean soil moisture values of each method (for the entire observation period).]

Response 2.43:

Yes. The mean soil moisture values during the experimental period are 0.274 m^3m^{-3} for *in situ* VSM measurements, 0.281 m^3m^{-3} for ISBA simulations, 0.305 m^3m^{-3} for GPS retrievals with S=0.0148 $m^3m^{-3}degree^{-1}$, 0.264 m^3m^{-3} for GPS retrievals with S=0.0033 $m^3m^{-3}degree^{-1}$, and 0.276 m^3m^{-3} for GPS retrievals from the scaled soil wetness index. (P. 10, L. 14-16)

2.44 [p.10, l. 3-24 and p.23, Fig. 4: Is it generally possible to compare these three methods one by one? The model simulates the first 10 cm; the reference measurements record at a soil depth of 5 cm and the GPS technique observes the soil surface. Perhaps the results with a S-value of S=0.0148 are even more realistic!? Please state on this. The GPS retrieval seems to be slightly too low in this plot using a S-value of 0.0033; especially after soil freezing and at the end of the soil moisture retrieval period the correlation between GPS retrievals and observations / reference measurements is weaker.]

Response 2.44:
(P. 8, L. 8-19; P. 10, L. 12-13 and 22; P. 11, L. 2 and 9-11; Table 1 and 2; Fig. 3 and 4)
Yes. Chew et al. (2014) used an electrodynamic single-scattering forward model to test the empirical relationships observed in field data, showing that SNR phase is affected by soil moisture in the top 5 cm of the soil. Moreover, surface soil moisture (< 1 cm depth) exerts the strongest control. Validation VSM obervations over the top 6 cm were used in Small et al. (2016), using the same a priori S parameter value.
We checked that the top 1 cm VSM simulations by ISBA are very close to the simulations of the top 10 cm VSM. In order to keep the method as generic as possible, we didn't directly adjust the slope from the median phase value from all available satellites. This adjusted slope value is the mean of slope values obtained for satellite tracks whose phase presents a linear correlation with *in situ* soil moisture higher than 0.9. This is why VSM retrievals are slightly too low in Fig. 4. The scores confirmed the VSM retrievals with the adjusted S parameter are closer to the in situ observations at 5 cm. Furthermore, a scaled soil wetness index can be considered, instead of VSM in m^3m^{-3} (see response 2.35).
The detail method is described below:
The phase time series can be normalized for each satellite track. Then the median value of the normalized phases from all available satellite tracks can be considered as the final soil wetness index (φ_{index}) for each day as shown in Fig. R2.1 (red line):

$$\varphi_{index} = \frac{\varphi - \varphi_{\min}}{\varphi_{\max} - \varphi_{\min}} \qquad \text{(R2.1)}$$

This soil wetness index time series is linearly related with in situ observations (R^2 = 0.74) and ISBA simulations (R^2 = 0.65). Moreover, VSM can be estimated from φ_{index}

$$VSM = VSM_{obs\_\min} + \varphi_{index} \cdot (VSM_{obs\_\max} - VSM_{obs\_\min}) \qquad \text{(R2.2)}$$

VSM_{obs_min} and VSM_{obs_max} are the minimum and maximum *in situ* VSM observations during the experimental time period, respectively. Figure R2.2 presents the estimated VSM from GPS soil wetness index (φ_{index}), together with *in situ* VSM observations and ISBA simulations. More related scores are shown in Table R2.1 and the scatter plot between GPS retrievals from φ_{index} and *in situ* observations are shown in Fig. R2.3. We will present these results in the revised manuscript.

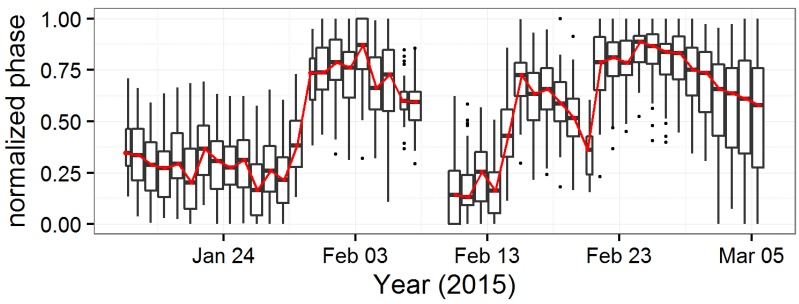

Figure R2.1 - Median of the daily GPS normalized phases (soil wetness index, red line) and their daily statistical distribution (black box plots) for all available satellite tracks from 16 January to 5 March 2015.

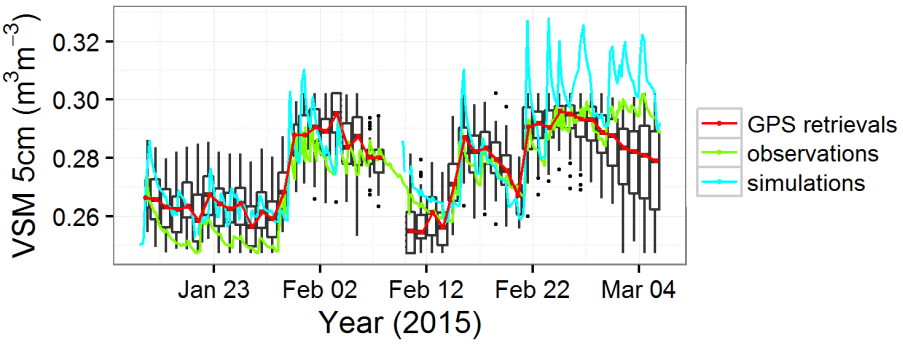

Figure R2.2 - In situ daily mean surface volumetric soil moisture (VSM) observations at 5 cm depth (green line), ISBA daily mean simulations (blue line), median of the daily GPS retrievals with soil wetness index (red line) and their daily statistical distribution (black box plots) for all available satellite tracks from 16 January to 5 March 2015.

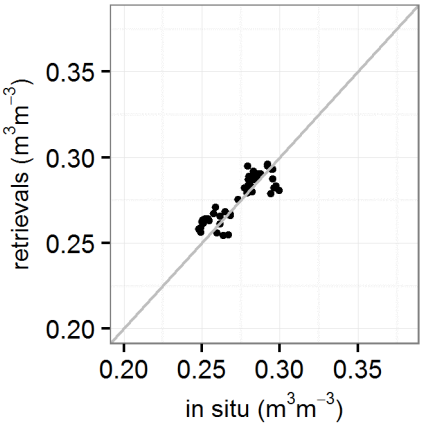

Figure R2.3 - Scatterplot between GPS retrievals (Eq. (R2.1)) and *in situ* VSM observations (m^3m^{-3}) from 16 January to 5 March 2015.

Table R2.1. Soil moisture scores from 16 January to 5 March 2015.

	GPS vs. *in situ*	GPS vs. ISBA	GPS vs. *in situ*	GPS vs. ISBA	GPS (φ_{index}) vs. *in situ*	GPS (φ_{index}) vs. ISBA	ISBA vs. *in situ*
S ($m^3m^{-3}deg^{-1}$)	0.0148		0.0033		-	-	-
N	47	43	47	43	47	43	43
MAE (m^3m^{-3})	0.036	0.034	0.011	0.018	0.007	0.009	0.009
RMSE (m^3m^{-3})	0.046	0.041	0.014	0.022	0.009	0.012	0.010
SDD (m^3m^{-3})	0.036	0.037	0.009	0.012	0.008	0.011	0.006

Mean bias (m^3m^{-3})	0.029	0.019	-0.010	-0.018	0.003	-0.005	0.008
R^2	0.73	0.63	0.73	0.63	0.74	0.65	0.88

2.45 [p.10, l. 14: 'a priori'

Response 2.45:

Yes. We corrected it (P. 10, L. 9).

2.46 [p.11, l.6: delete '(not shown)']

Response 2.46:

Yes. We corrected it (P. 11, L. 19).

2.47 [p.11, l.10ff: Please insert also the vegetation height determined either by GNSS or manually for each date, instead only listing the deviations.]

Response 2.47:

Yes. We added a table (Table 3) to include this information in the revised manuscript (P. 13, L. 7-8).

2.48 [p.11, l.12: why do you use a 21 gliding window approach? Is this really necessary? Perhaps the vegetation height levels in Figure 6 make sense (e.g. due to meteorological events and plant growth spurts)?]

Response 2.48:

The possible causes of the leveling effect are discussed in Section 5: (1) the occurrence of more than one dominant reflecting surface at different heights (Sect. 5.3) and (2) rapid phenological changes in the wheat canopy triggering a response of the H retrieval (Sect. 5.5). It must be noted that absolute daily changes in H (and h), of about 1.1 cm d^{-1} are fairly uniform throughout the growing period. Since h decreases when plants grow, relative changes in h tend to increase. According to Eq. 4, T behaves similarly. This means that the sensitivity of the retrieval method to changes in H is larger at the end of the growing period. This is probably why leveling is more pronounced between mid-March and mid-April than at the end of April (see Fig. 7). Leveling is less noticeable in May. A moving average permits smoothing the height retrievals, and presenting a better fit to the in situ observations. (P. 15, L. 27-31)

2.49 [p.11, l.26: Please state more on the overall possibility to compare dry biomass and vegetation height. Is this really possible? Are there some references available? Please state on this more detailed.]

Response 2.49:

We found a linear relationship between the moving average height from GPS retrievals and the above-ground dry biomass simulated by the ISBA model from 10 March to 29 May 2015 (when the maximum vegetation height, 1 m, was measured), during the time period from tillering to flowering. The correlation coefficient between the moving height and the dry biomass, with 81 observations, was 0.996.

$$dry\_mass = 1.05 \times moving\_height - 0.19 \quad \text{(R2.3)}$$

with with dry mass in kg m^{-2} and moving_height in meter.

A similar result was obtained by Wigneron et al. (2002) over another wheat crop site (Triticum durum, cultivar prinqual) in spring 1993. Although the sowing date (19 March) was late and the crop cycle was rather short, there was still a very good linear relationship between the in situ wheat height measurements and in situ dry biomass measurements from 20 April to 11 June 1993 (when the maximum vegetation height, 1 m, was measured). The correlation coefficient with 25 observations is 0.996.

$$dry\_mass = 1.11 \times height - 0.19 \quad \text{(R2.4)}$$

with dry mass in kg m^{-2} and height in meter.

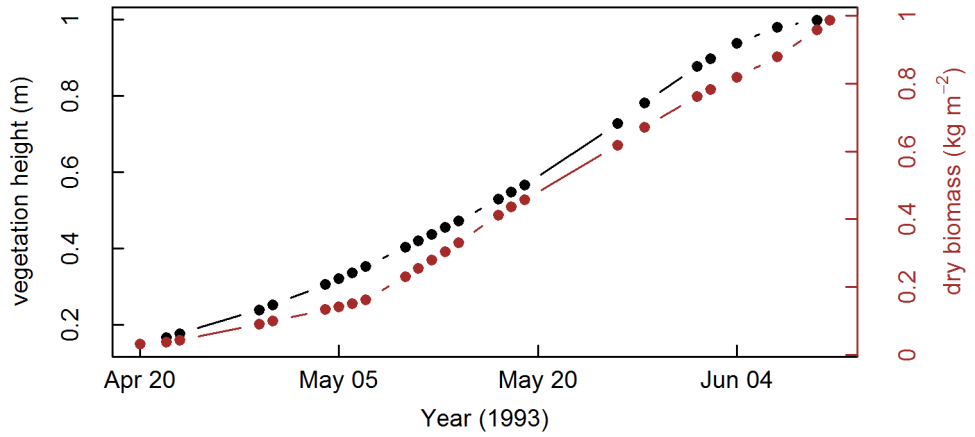

Figure R2.4 - In situ wheat canopy height measurements (25 black dots) and in situ wheat dry biomass measurements (brown dots) from 20 April to 11 June 1993 (adapted from Wigneron et al., 2002).

We clarified this in the revised manuscript (P. 13, L. 24-30) and supplement (P. 7).

Reference:

Wigneron, J.P., Chanzy, A., Calvet, J.C., Olioso, A. and Kerr, Y.: Modeling approaches to assimilating L band passive microwave observations over land surfaces. Journal of Geophysical Research: Atmospheres, 107(D14), 2002.

2.50 [p.22/23, Fig. 3/4: for better comparability, in both Figures the y-axis should have the same scale; They could also be combined in one figure with sub-figures a] and b].]

Response 2.50:

Yes. We modified the figures, and combined them in one figure. We also added the retrievals from scaled soil wetness index. On the other hand, using the same y-axis scale for all sub-figures is not possible, as some sub-figures become unreadable. (Fig. 3 in the revised manuscript)

2.51 [p.24, Fig. 5: How many dots are shown in this plot (N=47?)? Please add this information in the figure capture.]

Response 2.51:

Yes, there are 47 dots in Fig. 5. We clarified that (Fig. 4) in the revised manuscript.

2.52 [p.25, Fig 6: You don't have to repeat the legend in the figure column.]

Response 2.52:
OK. (Fig. 7 in the revised manuscript)

2.53 [Page 12-14: Discussion
General: The idea of asking questions is good. Please also insert a discussion section / further question on the potential future applicability and transferability (e.g. to other soils, other vegetation types, other GNSS signals etc.). What could be improved...]

Response 2.53:

Yes, we added another discussion subsection about the potential future applicability and transferability of the retrieval method. (Sect. 4.6: P. 16, L. 28-30; P. 17, L. 1-24)

We successfully assessed the surface soil moisture retrieval technique over a wheat crop field, during the start of the growing period. However, the rather narrow range of surface soil moisture values during the corresponding experiment time period limited the representativeness of the obtained retrieval accuracy. Furthermore, our dataset did not include GNSS data and in situ VSM measurements for periods of bare soil. Longer periods presenting a bare soil surface should be investigated in further studies. At the same time, more in situ vegetation measurements should be carried out for further studies.
The retrieved vegetation height was based on the dominant period of the average power spectrum. The latter was derived from GPS multipath SNR data for elevation angles between 5 and 20 degrees. We only considered the dominant period variations, without accounting for instantaneous phase changes. The accuracy of the retrieved vegetation height could probably be improved considering changes in both period and phase of the multipath SNR oscillations.
In this study, only the SNR data of L1 C/A signal is used, SNR data from different wavelength (e.g., L1 C/A, L2C and L5) should also be compared or combined to survey canopy characteristics.
A linear relationship between wheat height and above-ground dry biomass was observed during the period from wheat tillering to ripening. Retrieving dry biomass is a motivation for further research because most current satellite vegetation products focus on retrieving vegetation indexes or leaf area index. The dry biomass is directly related to the wheat yield, and retrieving wheat height could have applications in crop monitoring.
In this study, only wheat is considered. Other crops should be investigated in the future. Additionally, the algorithm we proposed might also be suitable to retrieve snow depth.

2.54 [p.12, l.3ff: As important findings (regarding the discussion) are shown in Fig. S6, this figure should also be shown in the manuscript (not only the supplement). Moreover, this issue should be discussed in more detail.]

Response 2.54:

Yes. We added Fig. S6 to the revised manuscript (Fig. 8) and adjusted its legend and description (P. 14, L. 6-12)

We tested the relationship between the multipath phase (φ_{mpi}) in Eq. (5) and soil moisture for the whole wheat growing cycle. We found that when the vegetation effects are not significant (A_{norm} > 0.78), φ_{mpi} correlates well (R = 0.92) with the *in situ* soil moisture observations (N = 47, Fig. R2.8a). During this time period, the variation of φ_{mpi} is only about 12 degrees in relation to the change of the in situ VSM between 0.25 m^3m^{-3} and 0.30 m^3m^{-3}. But when the vegetation effects are significant (A_{norm} < 0.78), φ_{mpi} (without or with unwrapping, Fig. R2.8b and R2.8c) is no longer linear related to soil moisture. For example, when vegetation height exceeded one wavelength, φ_{mpi} rapidly decreased from 207 degrees to 43 degrees (between 10 and 20 March). Changes in φ_{mpi} are disconnected from ISBA simulations. This is consistent with CH15, who showed that under this situation soil moisture cannot be retrieved unless vegetation effects are corrected for.

2.55 [p.12, l.9: Why did you increase this threshold exactly to the value 0.88? Is there any reason for this value?]

Response 2.55:

Adjusting the A_{norm} threshold from 0.78 to 0.88 permits making a distinction between harvest and post-harvest (after 30 June) A_{norm} values in Fig. S7. Fig. S7 replaced Fig. 2 in the revised manuscript. (P. 11, L. 20-24)

2.56 [p.12, l.26: Re-formulate your question: 'Can other vegetation characteristic besides vegetation height be inferred from the wavelet analysis?'. Or formulate two questions: 'Can vegetation height be inferred from...?' and 'Is it possible to additionally retrieve other vegetation characteristics from...?']

Response 2.56:

Yes. We modified it as 'Can vegetation water content be inferred from the wavelet analysis?' (P. 14, L. 24)

2.57 [p.12, l.27ff: The idea that you potentially also would like to retrieve the plant water content (or even other vegetation characteristics) should already be introduced earlier in the manuscript. Then an answer to this question would make more sense in the 'Discussion' part. Do you have reference data that show a decrease in plant water content?]

Response 2.57:

The VWC variable is already mentioned in the Introduction (P. 3, L. 19). The idea of retrieving VWC was expressed more clearly (P. 14, L. 25).
The conclusions of this paragraph are based on destructive gravimetric measurements (not shown).

2.58 [p.13, l.22: What do you mean with STD?]

Response 2.58:

Yes, we mean "daily standard deviation score". We clarified it (P. 15, L. 17-18 and 25).

2.59 [p.13, l.17: The rainfall/meteorological and logging events could additionally be shown in the figure, e.g., as a subplot.]

Response 2.59:

The exact day when the lodging event happened is unknown, we can only infer it happened between 29 May and 18 June. The height measurements on 29 May and 18 June are 100 cm and 39 cm, respectively. We added Fig. S9 into Fig. 7 for better comparing with rainfall data. However, whether maximum STD is an indicator of lodging or not is unclear. (P. 15, L. 19; Fig. 9 in the revised manuscript)

2.60 [p.14, l.2-8: This actually belongs to the 'Method' chapter. It is a further method to compare your retrievals to a reference.]

Response 2.60:

Yes. We introduced the GDD model in the ‘Method’ chapter. (Sect. 2.6: P. 10, L. 1-4)

2.61 [Page 14-15: Conclusions
General: Give also an outlook on potential applicability of this technique.]

Response 2.61:

We added a summary of the new Discussion section (See Response 2.53) (Sect. 4.6: P. 16, L. 28-30; P. 17, L. 1-24)

2.62 [p.14, l.19: Please specify – is this a new algorithm you developed or do you mean at this point the algorithm of CH15 and others you applied for the wheat crop test field?]

Response 2.62:

A new algorithm based on a wavelet analysis was implemented for retrieving vegetation height. We clarified it in the revised manuscript (P. 17, L. 29-31).

2.63 [p.15, l.2: L5 is introduced here for the first time. It could be mentioned already earlier (e.g., in the 'Discussion').]

Response 2.63:

Yes. We referred to L5 in the Discussion. (See Response 2.53) (P. 17, L. 18-19)

2.64 [Supplement
S p.1, Fig. S1: see comment above.]

Response 2.64:

Yes. We presented a picture of the GNSS antenna in the field. (See Response 2.24) (Fig. S1 in the revised supplement)

2.65 [S p.2, Fig. S2: Applying the same time scale in the x-axis of the two plots would be better for comparability or it would even be more helpful if both plots would be combined in one figure (e.g. with two different colours).]

Response 2.65:

Yes. We used the same time scale in the x-axis of the two plots (Fig. S2 in the revised supplement).

2.66 [S p.4, Fig. S3: a legend would be useful; it would be logical for comparison to combine Fig. S3 and Fig. S8]

Response 2.66:

Yes. We added a legend and combined Fig. S3 and Fig. S8 together to get a new Fig. 6 in the revised manuscript.

2.67 [S p.5, Fig. S4: see comment above; insert a legend and units if needed.]

Response 2.67:

Yes. We added units in this figure and moved it to the manuscript (Fig. 5 in the revised manuscript).

2.68 [S p.6, Fig. S5: see comment above; how many dots are shown in this plot (N=47?)? Please add this information in the figure capture.]

Response 2.68:

Yes, N=47, we clarified it in the figure capture (Fig. S5 in the revised supplement).

2.69 [S p.7, Fig. S6: please add the black dots also to the legend; regarding the blue line / dots: use either dots or lines for all of the three plots.]

Response 2.69:

Yes. We modified this figure and moved it to the revised manuscript (Fig. 8). (See Response 2.54).

2.70 [S p.8, Fig. S7: see comment above.]

Response 2.70:

Yes. Figure S7 replaced Fig. 2 in the revised manuscript.

2.71 [S p.9, Fig. S8: see comment above.]

Response 2.71:
Yes. We combined this figure with Fig. S3 to make a new figure in the reviesed manuscript (Fig. 6). (See Response 2.66)

2.72 [S p.9, Fig. S9: This information could visually be combined with Fig. 2 / Fig S8.]

Response 2.72:
We merged Fig. S9 into Fig. 9 in the revised manuscript for better comparing with rainfall data.

2.73 [S p. 11: Duveiller et al. 2011 should also be added to the references in the manuscript.]

Response 2.73:

We added this reference in the revised manuscript (P. 10, L. 3)

2.74 [S p. 12: Please clarify the figure capture. Was is actually meant with '...the value retrieved 15 days before, ...'? The dates of flowering and ripening should also occur in the figure or at least in the figure capture.]

Response 2.74:

Yes. We clarified the caption of Fig. S7 in the revised supplement and the corresponding sentence in the revised manuscript (P. 16, L. 22-23).
Figure S7 shows the diffrence between retrieved vegetation height at a given date and retrieved vegetation height 15 days before, from 31 January to 11 June 2015.

Use of reflected GNSS SNR data to retrieve either soil moisture or vegetation height over a wheat crop

Sibo Zhang[1,2], Nicolas Roussel[3], Karen Boniface[2,3,4,6], Minh Cuong Ha[3], Frédéric Frappart[3,5], José Darrozes[3], Frédéric Baup[4], and Jean-Christophe Calvet[1]

[1]CNRM – UMR3589 (Météo-France, CNRS), Toulouse, France

[2]Fondation STAE, Toulouse, France

[3]GET (UMR5563 CNRS/Université Paul Sabatier, UR254 IRD), Toulouse, France

[4]CESBIO, Université de Toulouse, CNES/CNRS/IRD/UPS, Toulouse, France

[5]LEGOS – UMR566 (CNES, CNRS, IRD, UPS), Toulouse, France

[6]now at Joint Research Centre / European Commission, Ispra, Italy

Correspondence to: Jean-Christophe Calvet (jean-christophe.calvet@meteo.fr)

Abstract. This work aims to estimate soil moisture and vegetation height from Global Navigation Satellite System (GNSS) Signal to Noise Ratio (SNR) data using direct and reflected signals by the land surface surrounding a ground-based antenna. Observations are collected over a rainfed wheat field in southwestern France. Surface soil moisture is retrieved based on SNR phases estimated by the Least Square Estimation method, assuming the relative antenna height is constant. It is found that vegetation growth breaks up the constant relative antenna height assumption. A vegetation height retrieval algorithm is proposed using the SNR dominant period (the peak period in the average power spectrum derived from a wavelet analysis of SNR). Soil moisture and vegetation height are retrieved at different time periods (before and after vegetation significant growth in March, respectively). The retrievals are compared with two independent reference datasets: *in situ* observations of soil moisture and vegetation height, and numerical simulations of soil moisture, vegetation height and above-ground dry biomass from the ISBA (Interactions between Soil, Biosphere and Atmosphere) land surface model. Results show that changes in soil moisture mainly affect the multipath phase of the SNR data (assuming the relative antenna height is constant) with little change in the dominant period of the SNR data, whereas changes in vegetation height are more likely to modulate the SNR dominant period. Surface volumetric soil moisture can be estimated (R^2 = 0.74, RMSE = 0.009 m^3m^{-3}) when the wheat is smaller than one wavelength (~ 19 cm). The quality of the estimates markedly decreases when the vegetation height increases. This is because the reflected GNSS signal is less affected by the soil. When vegetation replaces soil as the dominant reflecting surface, a wavelet analysis provides an accurate estimation of the wheat crop height (R^2 = 0.98, RMSE = 6.2 cm). The latter correlates with modeled above-ground dry biomass of the wheat from stem elongation to ripening. It is found that the vegetation height retrievals are sensitive to changes in plant height of at least one wavelength. A simple smoothing of the retrieved plant height allows an excellent matching to *in situ* observations, and to modeled above-ground dry biomass.

1 Introduction

In situ observations of soil moisture and vegetation variables are key to validate land surface models and satellite-derived products. Recent international initiatives, such as the International Soil Moisture Network (Dorigo et al., 2013) or the Committee on Earth Observation Satellites (CEOS) Land Product Validation group (Morisette et al., 2006) have improved the access to such observations. However, they remain very sparse and there is a need to develop new automatic techniques to monitor land surface variables at a local scale. Global Navigation Satellite System (GNSS) reflectometry could be a solution. A number of studies demonstrated that GNSS multipath signals can be used to retrieve various geophysical parameters of the surface surrounding a GNSS receiving antenna (Motte et al., 2016). Over land, variables such as soil moisture, snow depth and vegetation status can be observed (Larson et al., 2008; Small et al., 2010; Larson and Nievinski, 2013; Wan et al., 2015; Boniface et al., 2015; Larson, 2016; Roussel et al., 2016). GNSS satellites operate at the L-band microwave frequency domain (between 1.2 GHz and 1.6 GHz). At these relatively low frequencies, the microwave signal is less perturbed by atmospheric effects and can better penetrate clouds and heavy rains than higher frequency signals. This ensures continuous operations, in all weather conditions, at either daytime or nighttime. The L-band signal emitted or reflected by terrestrial surfaces is related to surface parameters like surface soil moisture, roughness or vegetation characteristics. These properties have been exploited by e.g. the Soil Moisture and Ocean Salinity (SMOS) satellite and the Soil Moisture Active Passive (SMAP) missions (Kerr et al., 2001; Chan et al., 2016) for Earth surface remote sensing applications. While SMOS is a radiometer and measures the Earth surface microwave emission (passive microwaves), GNSS satellites emit a radar signal (active microwaves). Active microwaves can present improved temporal and spatial resolutions, but the signal may be more sensitive to the structure of the surface, such as soil roughness or vegetation effects than for passive microwaves (Wigneron et al., 1999; Njoku et al., 2002).

Existing geodetic-quality GNSS networks have the potential to provide a large number of *in situ* observations, depending on the receiver technology: (1) waveform acquisition with a specific receiver using two antennas (one zenith-oriented antenna and one surface-oriented antenna), called GNSS reflectometry (GNSS-R) technique (Zavarotny et al., 2014) or (2) GNSS signal strength represented by the Signal-to-Noise Ratio (SNR) acquired with classical geodetic receiver using one antenna, called SNR GNSS interferometric reflectometry (GNSS-IR) technique (Larson, 2016). GNSS networks can be used to monitor small or large areas depending on the antenna height and satellite elevation (Roussel et al., 2014). Continuous monitoring of surface soil moisture can be made over a long period at spatial scales ranging from 100 m^2 (antenna height of about 2 m) to 8000 m^2 (antenna height of about 150 m) for classical geodetic receiver but can reach a few thousand square kilometers with waveform receivers embedded on satellites (e.g. TechDemoSat-1 mission, Foti et al. (2015)).

Using the SNR GNSS-IR technique, Larson et al. (2008) showed that SNR data obtained from existing networks of single ground-based geodetic antennas can be used to infer soil moisture. Other GNSS methods (besides reflectometry) can be used. For example, Koch et al. (2016) used three geodetic GNSS antennas (one was installed above the soil, the other two

were buried at a depth of 10 cm), to measure the GNSS signal strength attenuation and to retrieve soil moisture over bare soil.

For now, a network called PBO H_2O based on single GNSS antennas at Plate Boundary Observatory (PBO) sites is currently used in western regions of the USA to monitor surface soil moisture (Larson et al., 2013; Chew et al., 2016) and snow depth (Larson and Nievinski, 2013; Boniface et al., 2015). It must be noted that most of the 161 GNSS stations of this network are located in mountainous areas or in areas of California characterized by a relatively arid climate. They are surrounded by sparse vegetation and are therefore not adapted to vegetation growth studies.

In the SNR GNSS-IR technique, the interference between the direct and the reflected signals is observed in temporal variations of the SNR data (Bilich and Larson 2007; Zavorotny et al., 2010; Chew et al., 2014). Changes in geophysical or biophysical parameters affect the phase, amplitude and frequency of the SNR modulation pattern. The SNR is also influenced by surface roughness and by the position of the antenna with respect to the surface and to the satellite (Larson and Nievinski 2013; Chew et al., 2016). The SNR modulation primarily depends on:

- the relative height of the GNSS antenna above the reflecting surface (ground or vegetation surface),
- satellite elevation,
- the superposition of the direct signal and of the reflected signal, which varies along with changes in the satellite track positions,
- Right Hand Circular Polarization (RHCP) and Left Hand Circular Polarization (LHCP) gain pattern of the receiving antenna, (RHCP usually increases the SNR when the satellite elevation angle increases, LHCP is related to imperfections of the antenna and is greater than RHCP for the reflected signal);
- reflection coefficients for the reflecting surface, related to the water content and the ground mineralogical content of the reflecting surface,
- surface topography and roughness and
- the satellite transmitted power.

A soil moisture retrieval algorithm from SNR data was derived by Chew et al. (2014) over bare soil. In subsequent modeling studies Chew et al. (2015) showed that the vegetation canopies affected the SNR modulation pattern. They showed that vegetation growth tended to trigger a decrease of the SNR amplitude. Because the vegetation effects tended to perturb the soil moisture retrieval, Chew et al. (2016) proposed an improved algorithm for soil moisture retrieval in vegetated environments, which used the amplitude decrease extent to decide when vegetation influence was too large. They used a model database for the SNR of L2C signal to remove most significant vegetation effects for the sites they considered in Western USA. Small et al. (2016) further compared different algorithms of GNSS-IR soil moisture retrieval in the presence of vegetation. Roussel et al. (2016) integrated both GPS and GLONASS SNR data to retrieve soil moisture over bare soil. Using data from a field study, Wan et al. (2015) showed that the amplitude of the SNR data presented a good linear relationship with the vegetation water content (VWC), but it was restricted to VWC values of less than ~1 kg m^{-2}. In addition

to the amplitude of the SNR data, it was also possible to infer VWC by the $MP1_{rms}$ index, which is a linear combination of L1 and L2 carrier phase data and L1 pseudorange data (Small et al., 2010), and by the NMRI (Normalized Microwave Reflection Index) which is a normalization result based on the $MP1_{rms}$ (Small et al., 2014; Larson and Small 2014).

In this study, the SNR GNSS-IR technique was used to analyze GNSS SNR data obtained, with a single classical geodetic antenna receiver over an intensively cultivated wheat field in southwestern France. The data were used to retrieve either soil moisture or relative vegetation height during the growing period of the wheat crop. The method proposed by Chew et al. (2016) (hereafter referred to as CH16) was used to retrieve soil moisture. Moreover, we performed a wavelet analysis in order to extract the dominant period of the SNR and further to retrieve vegetation height. We investigated to what extent vegetation height influenced the dominant period resulting from the wavelet analysis. The main justification for investigating the impact of vegetation height was that it impacted the relative antenna height (the distance from the antenna to the reflecting surface). Vegetation growth tended to decrease the relative antenna height and broke up the constant height assumption used in soil moisture retrieval algorithms. In this context, key objectives of this study were to (1) assess the soil moisture retrieval technique in either low or tall vegetation conditions, and (2) retrieve vegetation height along the wheat growth cycle.

2 Materials and methods

2.1. SNR data and pre-processing

The GNSS SNR data were acquired from an antenna at 2.51 m above the soil surface over an experimental field covered by rainfed winter wheat in Lamasquère, France (43°29'10"N, 1°13'57"E, see Fig. S1 in the Supplement). These GNSS data were collected by GET (Géosciences Environnement Toulouse) for a whole growing season, from January to July 2015. A Leica GR25 receiver equipped with an AS10 antenna was used and data were acquired at a sample frequency rate of 1 Hz. Only the S1C SNR signal strength on the civilian L1 C/A channel of the GPS constellation was used in this study because the used receiver could not track the L2C signal. The latter is only transmitted by the recent Block IIR-M ("Replenishment Modernized") and IIF ("Follow-on") GPS satellites. Vey et al. (2016) showed that soil moisture root mean square difference between L2C and L1 was 0.03 m^3m^{-3}. The quality of the more recently available L2C signal (used by PBO H_2O (CH16)) is higher than either L1 C/A or L2P from non-code tracking receivers. However, a number of studies (e.g. Vey et al., 2016) showed that the SNR of the L1 C/A signal can be used to provide reliable soil moisture estimates over sparse vegetation and bare soil surface, although it is less precise than the L2C signal. Although data from other constellations were also acquired (e.g., GLONASS, GALILEO), their orbital parameters such as satellite track positions or satellite altitude were not the same. In order to be consistent with the GPS-only studies of Larson et al. (2008), CH16, and Small et al. (2016), we only used GPS SNR data. For our site, four GPS satellites out of 32 were excluded from the analysis because their data were incomplete

(GPS03, 20, 26, these numbers corresponding to their Pseudo-Random Noise (PRN) numbers) or not received (GPS08). Finally, GPS SNR data were missing for only nine days: 8 and 9 February, 3 April and from 13 to 18 May 2015.

Following the method proposed by Larson et al. (2010), a low-order polynomial was fit to the SNR data, and the modulation pattern was then derived from the SNR by subtracting this polynomial from the SNR data. The logarithmic dB-Hz units were converted to a linear scale in V V^{-1} using the following conversion equation: $SNR_{linear} = 10^{\frac{SNR}{20}}$ (Vey et al., 2016). Figure 1a shows an example of the detrended multipath SNR data for the ascending track of GPS01 on 21 January 2015. The periodic signature of the multipath SNR data is visible. We only analyzed the modulation patterns in a valid segment for satellite configurations corresponding to low elevation angles, ranging from 5 to 20 degrees. This corresponded to a valid segment data recording of less than one hour (40 to 50 minutes). Avoiding very low elevation angles (less than 5 degrees) limited spurious effects from trees and artificial surfaces surrounding the field. Avoiding high elevation angles (more than 20 degrees) limited the reduction of the multipath signal amplitude. Because the SNR signal amplitude was much reduced and the wave pattern was not visible at high elevations for our field observations, we excluded elevation angles larger than 20 degrees.

2.2. Soil moisture and vegetation characteristics

The field campaign was a part of a coordinated effort by CESBIO (Centre d'Etudes Spatiales de la BIOsphère) to monitor crops in southwestern France using both *in situ* and satellite Earth Observation data. Independent *in situ* observations of soil moisture and vegetation height were made together with model simulations of these quantities. Both observations and simulations were used to validate soil moisture and vegetation height retrievals.

Since the whole wheat growing cycle was considered, both soil moisture and vegetation modulated the multipath SNR pattern. Soil roughness was considered as stable in time from sowing to harvest. Soil in the close vicinity of the antenna consisted of 18% of sand, 41% of clay, and 41% of silt. The row spacing of the wheat crop was 15 cm.

The wheat was sown during the autumn, on 1 October 2014 and was harvested from 26 to 30 June 2015. Volumetric soil moisture (VSM) was measured by FDR (Frequency Domain Reflectometry) ML2 Thetaprobes and was continuously monitored at a depth of 5 cm from 16 January to 10 March 2015 and from 30 March to 26 May 2015. Measurements of crop height were performed at seven dates during the plant growing cycle. The canopy height did not exceed 0.1 m at wintertime and rapidly increased at springtime: it reached 0.2 m on 10 March 2015 and 1 m on 29 May. It dropped to 0.39 m on 18 June because of a lodging event. The exact date of lodging could not be precisely determined but it could be inferred it happened between 29 May and 18 June.

In addition to *in situ* observations, simulations of surface soil moisture (0-10 cm top soil layer), plant height and above-ground dry biomass were performed for this site by CNRM (Centre National de Recherches Météorologiques) using the ISBA (Interactions between Soil, Biosphere, and Atmosphere) land surface model within the SURFEX (version 8.0)

modeling platform (Masson et al., 2013). The ISBA configuration and the atmospheric analysis we used to force the model are described in Lafont et al. (2012). The C3 crop plant functioning type and a multilayer representation of the soil hydrology were considered. The model depth is 12 meters, with 15 layers and the layer thickness is not united (Decharme et al., 2011). These simulations were used as an independent benchmark for soil moisture and vegetation variables.

2.3. Multipath SNR characteristics

Due to the motion of the GPS satellites, the path delay between the direct and reflected signals causes an interference pattern in the signal power of SNR data. The distance from the antenna to the dominant reflecting surface directly affects the SNR frequency/period.

As noted by Georgiadou and Kleusberg (1988) and Bilich and Larson (2007), assuming the ground surface is horizontal, the additional distance (δ) travelled by a reflected signal relative to the direct signal is

$$\delta = 2h\sin(\theta) \tag{1}$$

where h is the relative antenna height, and θ is the satellite elevation angle. This path delay δ can also be expressed in terms of the multipath relative phase ψ :

$$\psi = 2\pi\frac{\delta}{\lambda} \tag{2}$$

where λ represents the L1 wavelength (0.1903 m).

Thus the multipath frequency (f) and period (T) can be written as:

$$\omega = 2\pi f = \frac{d\psi}{dt} = \frac{4\pi}{\lambda}h\cos(\theta)\frac{d\theta}{dt} \tag{3}$$

$$\frac{1}{T} = f = \frac{2h\cos(\theta)}{\lambda}\frac{d\theta}{dt} \tag{4}$$

This means that the relative antenna height (h) directly affects multipath frequency f and period T. Antennas far above the reflecting surface have higher multipath frequencies (smaller multipath periods) than antennas closer to the reflecting surface. Furthermore, satellite geometric information and motion substantially influences the period (T) of the multipath SNR data due to the $\cos(\theta)$ and $d\theta/dt$ terms in equation (4). If satellite passes reach high elevation angles (e.g., GPS01 in Supplement Fig. S2), $d\theta/dt$ becomes large. Conversely, satellites signals observed at small maximum elevations (e.g., GPS18 in Supplement Fig. S2) move more slowly (small $d\theta/dt$) than satellites passing overhead (Bilich and Larson 2007). In order to limit the impact of these differences from satellite motion, only the full-track data with at least 40 degree maximum elevation angle were selected. Among the remaining tracks we further removed the slowly moving tracks whose maximum $\cos\theta \cdot d\theta/dt$ was less than 9.5×10^{-5} rad s^{-1} (threshold value based on our field observations) of the valid

segment (elevation angles ranging between 5 and 20 degrees). This specific data sorting was only made for vegetation height retrieval (Sect. 2.5). After this selection, the number of available satellite tracks was 37 per day.

Provided the reflecting surface is stable, the a priori antenna height can be used to estimate the SNR frequency. The SNR frequency is used to calculate the multipath SNR phase, and then the SNR phase is used to estimate VSM (Sect. 2.4). If the reflecting surface is changing in response to vegetation growth, relative vegetation height can be retrieved instead of VSM by directly estimating the dynamic SNR frequency/period with a wavelet analysis (Sect. 2.5).

2.4. Soil moisture retrieval

As the SNR frequency is known (Eq. (3)), it is possible to estimate the SNR amplitude and phase. Larson et al. (2008) and Larson et al. (2010) showed that phase varies linearly with VSM in m^3m^{-3} (R^2 = 0.76 to 0.90). Retrieving absolute VSM values in m^3m^{-3} is possible after a calibration phase. This result was used by Chew et al. (2014) to develop an algorithm to estimate surface soil moisture (top 5 cm) over bare ground.

For bare soil, changes in surface soil moisture affect the signal penetration depth. The latter can be very small in wet conditions and tends to increase in dry conditions, up to a few centimeters (Chew et al., 2014; Roussel et al., 2016). This is a small change with respect to the antenna height (2.51 m in this study). Consequently, the relative antenna height (h) is considered as a constant (h_c = 2.51m) in this Section. Using sine of the elevation angle ($\sin(\theta)$) as the independent variable, the modulation frequency becomes proportional to h_c. Then the multipath SNR can be expressed as (Larson et al., 2008):

$$SNR_{mpi} = A\cos(\frac{4\pi h_c}{\lambda}\sin(\theta) + \varphi_{mpi}) \quad (5)$$

The least square estimation (LSE) method proposed by Larson et al. (2008) is used to estimate the multipath amplitude (A) and multipath phase (φ_{mpi}) from the multipath SNR data. Then, φ_{mpi} can be further used to estimate the soil moisture changes (CH16),

$$VSM_t = S \cdot \Delta\varphi_t + VSM_{resid} \quad (6)$$

Phase changes $\Delta\varphi_t = \varphi_t - \varphi_0$ are calculated with respect to φ_0, the reference phase. We used the method proposed by CH16 consisting in estimating φ_0 as the mean of the lowest 15% of the φ_{mpi} data for each track during the retrieval period. The same condition was used to estimate the VSM_{resid} residual soil moisture from the *in situ* VSM observations. The VSM_{resid} was taken as the minimum soil moisture observation, which presented a value of 0.252 m^3m^{-3} during the retrieval period. The S parameter (in $m^3m^{-3}degree^{-1}$) is the slope of the linear relationship between phase changes and soil moisture. For time series with no significant vegetation effects, S = 0.0148 $m^3m^{-3}degree^{-1}$ for L2C signal (CH16). Following CH16, the median

soil moisture estimate from all available satellite tracks (66 per day) that passed at different times during the day was used as the final soil moisture estimate.

We also used the *in situ* VSM_t, $\Delta\varphi_t$ and VSM_{resid} to fit a locally adjusted slope. The minimum VSM had to be derived from the *in situ* observations during the experimental time period in order to determine the VSM_{resid} term in Eq. (6). The retrieval of the *S* parameter requires at least one or two months of VSM *in situ* observations because soil moisture conditions ranging from dry to wet need to be sampled. However, if a scaled soil wetness index is used instead of soil moisture, no *in situ* VSM observations are needed.

Alternatively, the phase time series can be normalized for each satellite track, and using *S* is not needed. We considered the median value of the normalized phases from all available satellite tracks (66 per day) as the final scaled soil wetness index (φ_{index}) for each day:

$$\varphi_{index} = \frac{\varphi - \varphi_{\min}}{\varphi_{\max} - \varphi_{\min}} \tag{7}$$

VSM could then be estimated from φ_{index}:

$$VSM = VSM_{obs\_\min} + \varphi_{index} \cdot (VSM_{obs\_\max} - VSM_{obs\_\min}) \tag{8}$$

VSM_{obs_min} and VSM_{obs_max} are the minimum and maximum *in situ* VSM observations during the experimental time period, respectively.

CH16 defined the normalized amplitude (A_{norm}) as the ratio of amplitude to the average of the top 20 % amplitude values. The A_{norm} time series can be used to assess whether or not vegetation effects are significant. Values of A_{norm} above 0.78 (dimensionless) indicate that vegetation effects are small (CH16). In conditions of significant vegetation effects CH16 used an algorithm able to correct the phase for vegetation effects. This algorithm is based on an unpublished lookup table. Since we were not able to correct for vegetation effects, we retrieved surface soil moisture during a period with rather sparse vegetation, from 16 January to 5 March. During this time span, A_{norm} was above 0.78 as shown in Fig. 2 (black dots).

2.5. Vegetation height retrieval using a wavelet analysis

While vegetation grows, the vegetation surface gradually replaces the bare soil surface as the dominant reflecting surface. As a consequence, the height (*h*) of the antenna above the reflecting surface decreases. Equation (4) shows that changes in *h* impact the multipath frequency *f* and consequently *T*. This property allows the use of changes in *T* values to infer changes in *h*, and further estimate relative vegetation height. To retrieve relative vegetation height we propose a new approach based on wavelet analysis. Wavelets have been used for many years in signal processing studies in geosciences (Ouillon et al., 1995;

Darrozes et al., 1997; Gaillot et al., 1999), astrophysics (Escalera and MacGillivray, 1995), meteorology (e.g. Hagelberg and Helland, 1995; Torrence and Compo, 1998), hydrology (Labat, 2005) and in many other fields. The wavelet analysis is well suited for analyzing time series with non-stationary power and frequency changes across time as illustrated by Fig. 1. Our wavelet analysis methodology is based on the WaveletComp R-package (Roesch et al., 2014). To analyze the period structure, we used a well-known Morlet mother function which comes from a combination of a Gaussian function and a sinusoidal one (Fig. S3 in the Supplement). Due to its shape, Morlet daughters allow detection of singularities in all scales/periods of the spectrum. Morlet wavelet is also well suited for environmental analysis (Grinsted et al., 2004). We calculate the Morlet wavelet transform of the multipath SNR and evaluate the power spectrum of the multipath SNR signal (see Eqs. S1-S4 in the Supplement).

Vegetation height can be retrieved using the dominant SNR period (T_d), which is the peak period of the average power spectrum derived from a wavelet analysis of SNR, from the multipath SNR segment at elevation angles from 5 to 20 degrees. After obtaining T_d time series, the relative antenna height (h) can be derived from Eq. (4) as:

$$h = \frac{\lambda}{2\cos\theta_{E9} \cdot \frac{d\theta_{E9}}{dt} \cdot T_d} \tag{9}$$

The T_d value is used to represent the multipath SNR data in order to estimate h. Also, changes in the elevation angle (θ) and in $d\theta/dt$ have to be accounted for. This means that h is a variable depending on the elevation angle. In this study, changes in h were surveyed across dates at an elevation angle of 9 degree (See Sect. 3.2).

Changes in relative antenna height (h) are directly related to vegetation height increase:

$$\Delta H = h_0 - h \tag{10}$$

Similarly to the phase change estimates ($\Delta\varphi_t$ in Sect. 2.4), h_0 is the median value of the top 15% h data during the whole wheat growth cycle for each track.

The final retrieved vegetation height (H) is based on the mean relative antenna height change from all available satellite tracks (N = 37), plus one wavelength:

$$H = \frac{\sum_{N} \Delta H}{N} + \lambda \tag{11}$$

The minimum value of H is one wavelength. Therefore Eq. (11) can only be applied when the wheat height is higher than one wavelength (0.19 m for L1).

It must be noted that it is not necessary to retrieve soil moisture before retrieving vegetation height.

2.6. GDD (growing degree days) model

Because of the lack of *in situ* records of the field wheat growth stages, we built a reference GDD model based on the wheat growth stage dates observed at the same location in 2010 (Duveiller et al., 2011; Fieuzal et al., 2013, Betbeder et al., 2016). The GDD model is described in the Supplement (Eqs. S5-S6 and Fig. S4).

3. Results

3.1 Soil moisture retrieval

Figure 3 presents the surface soil moisture retrievals from 16 January to 5 March 2015, together with independent *in situ* VSM observations and ISBA simulations. The VSM retrievals are derived from GPS SNR observations using Eq. (6) in sparse vegetation conditions, when A_{norm} is above 0.78, with the a priori S value of 0.0148 $m^3m^{-3}degree^{-1}$ (Fig. 3a) and the adjusted local slope S = 0.0033 $m^3m^{-3}degree^{-1}$ (Fig. 3b). This adjusted S value is the mean of slope values obtained for satellite tracks whose phase presented a linear correlation with *in situ* soil moisture higher than 0.9. This occurred for the ascending tracks of GPS 13, 21, 24 and 30 and for the descending tracks of GPS 05, 09, 10, 15, and 23. Figure 3c shows the VSM retrievals from the scaled soil wetness index based on the normalized multipath phase.

The GPS and ISBA scores are given in Table 1. The mean soil moisture values during the experimental period are 0.27, 0.28, 0.31, 0.26, and 0.28 m^3m^{-3} for *in situ* VSM measurements, ISBA simulations, GPS retrievals with S = 0.0148 $m^3m^{-3}degree^{-1}$, GPS retrievals with S = 0.0033 $m^3m^{-3}degree^{-1}$, and GPS retrievals from the scaled soil wetness index, respectively.

In Fig. 3, the sub-daily statistical distribution of the VSM retrievals is indicated by box plots. The range of daily standard deviation value of the various VSM estimates is shown in Table 2. The *in situ* VSM measurements present the smallest sub-daily variability, with a mean standard deviation value of 0.002 m^3m^{-3}. The largest variability is obtained for the GPS retrievals based on the a priori slope value S = 0.0148 $m^3m^{-3}degree^{-1}$, with a mean standard deviation value of 0.036 m^3m^{-3}. GPS retrievals based on the adjusted slope value S = 0.0033 $m^3m^{-3}degree^{-1}$ presents intermediate values (0.008 m^3m^{-3}), together with those based on the scaled soil wetness index (0.009 m^3m^{-3}) and with the ISBA simulations (0.005 m^3m^{-3}). Figure 3 shows that the sub-daily variability of GPS VSM retrievals tends to increase during the last 10 days of the retrieval period.

It must be noted that GPS data are missing on 8 and 9 February, and that the ISBA simulations indicate soil freezing (i.e. the presence of ice in the top soil layer) from 4 to 9 February. This period was excluded from the comparison. In the end, there were 47 valid observation days for the statistical analysis of the retrieved surface VSM, among which 43 days could be compared with model simulations.

The GPS VSM daily mean retrievals based on the CH16 method present a good agreement with both *in situ* observations and ISBA simulations: MAE (Mean Absolute Error) and RMSE (Root Mean Square Error) are lower than 0.05 m^3m^{-3}, and SDD

(Standard Deviation of Differences) does not exceed 0.04 m^3m^{-3} (Table 1). The errors are reduced by at least 50 % when the local adjusted slope is used. When the scaled soil wetness index is used, the errors are further reduced.

Figure 4a and 4b show the retrieved soil moisture as a function of the *in situ* observations for a priori and adjusted slopes (S = 0.0148 $m^3m^{-3}degree^{-1}$ and S = 0.0033 $m^3m^{-3}degree^{-1}$, respectively) from all available satellite tracks (66 per day), not only those tracks used for fitting the slope (see Supplement Fig. S5). The corresponding improvements in score values are given in Table 1: the MAE decreases from 0.036 to 0.011 m^3m^{-3}, the RMSE decreases from 0.046 to 0.014 m^3m^{-3}, the SDD decreases from 0.036 to 0.009 m^3m^{-3}. The retrievals based on the a priori slope markedly overestimate VSM in wet conditions. On the other hand, the retrievals based on the adjusted slope only slightly underestimate VSM. This shows that adjusting the slope is critical and has a major impact on the retrieval accuracy. Furthermore, Figure 4c gives the retrievals based on the scaled soil wetness index. Scores are further improved: the MAE decreases to 0.007 m^3m^{-3}, RMSE to 0.009 m^3m^{-3}, and SDD to 0.008 m^3m^{-3}.

We also compared the retrievals with the independent ISBA simulations. The ISBA model VSM simulations present a better agreement with the *in situ* VSM observations than the GPS retrievals, for all the scores, as shown by Table 1 (last column) and Fig. 3. In particular, R^2 = 0.88 for ISBA simulations, against R^2 = 0.74 for GPS retrievals. This shows that the ISBA simulations can be used as a reference to assess local GPS retrievals. The statistical scores resulting from the comparison between the GPS retrievals and the simulations are similar to those based on *in situ* observations.

After 5 March, A_{norm} drops below 0.78 (Fig. 2), and the VSM retrievals are not valid. We made an attempt to retrieve VSM from 6 to 15 March. We obtained 10 VSM retrieved values and we compared them with ISBA VSM simulations, because *in situ* observations were lacking. The retrievals looked sparser and the R^2 score decreased from 0.63 before 6 March (Table 1) to only 0.21 from 6 to 15 March. This result confirms that the empirical A_{norm} threshold (0.78) is a good way to assess the VSM retrieval feasibility over vegetated areas. Additionally, we found that adjusting the A_{norm} threshold from 0.78 to 0.88 permitted making a distinction between harvest and post-harvest (after 30 June) A_{norm} values in Fig. 2. Four more days (2-5 March) are excluded. Figure 3 shows that the 25-75% percentile intervals for these days are larger, but the maximum retrieval differences for these days are acceptable, around 0.03 m^3m^{-3}.

3.2 Dominant SNR period analysis during the wheat growth cycle

Figure 1 shows an example of the multipath SNR data from the ascending track of GPS01 on 21 January 2015. Its average power spectrum (Fig. 1b) derived from a wavelet analysis is also shown, together with the power spectrum (Fig. 1c) for periods ranging from 128 to 1024 s. From the average power spectrum, there is only one peak and the corresponding peak period is 362 s. The SNR data is reconstructed depending on this peak period (red line in Fig. 1a), which is a good fit to the SNR data. Both phases and amplitudes match very well. This shows that the peak period from the average power spectrum can be used to represent the multipath SNR data. Limiting elevation angle values from 5 to 20 degrees (Sect. 2.1) ensures a

relatively stable value of the peak period. The peak period is considered as the dominant period (T_d) of the multipath SNR data.

Additionally, the major part of the signal power is concentrated on elevation angles ranging from 7 to 11 degrees (see Fig. 1). A preliminary analysis for the entire wheat growing cycle showed that, more often than not, the best elevation angle corresponding to the peak power was around 9 degrees. In this study, elevation and its change rate at 9 degree are used to represent the SNR data for all available satellite tracks (37 per day). It must be noted that this reference elevation angle is specific to the gain pattern and height of the antenna encountered in this experiment. It could present different values in other antenna configurations.

During the wheat growth cycle, preliminary tests showed that the average power spectrum could present multiple peaks together with a reduced maximum average power. This made T_d unsuitable for the representation of the multipath SNR data. Under this situation the quality of the T_d value was considered as poor and the data were not used. An example of T_d time series is shown in Fig. 5 for GPS01 ascending tracks. Poor quality data (e.g. on 17-20 March, and 12-16 June) are indicated. We sorted out the data acquired in two situations: (1) track data presenting more than one peak in the highest 80% percentile of the power spectrum, (2) T_d value smaller by 10 seconds than the mean value of the lowest 10% of the dominant periods (e.g., T_d < 352 s for GPS01). This is further illustrated in Fig. 6, comparing a usable track and an unusable track. On 1 May, there is one peak in the average power spectrum (Fig. 6b), and the dominant period (456 s) obtained can be used to fit the SNR data in Fig. 6a. While on 15 June, there are two peaks in the average power spectrum as shown in Fig. 6d. Furthermore, the maximum average power is only 0.54 which is significantly smaller than the maximum average power of 1.0 observed on 1 May 2015 (Fig. 6b). In Fig. 6c, the SNR pattern is clearly noisier, with smaller amplitudes and less clear pattern than in Fig. 1a/Fig. 6a. This data set is unusable. A possible cause is the more inhomogeneous reflecting surface after the lodging event. The probability distribution (grey bars) of bad quality tracks among all available 37 satellite tracks is shown in Fig. 2 on a daily basis from 16 January to 15 July 2015. Most unsuitable tracks are observed during two time periods: (1) at the beginning of spring, from 10 to 20 March, and (2) at the beginning of summer, from 12 to 26 June. The latter corresponded to lodging of vegetation, which occurred during a strong wind event and affected the reflecting surface height. The *in situ* observation of wheat height was only 39 cm on 18 June.

As shown in Sect. 2.4, vegetation effects on the SNR signal became significant after 5 March. After this date, A_{norm} (black dots in Fig. 2) decreased drastically, in relation to plant growth. After 10 March, wheat height exceeded one wavelength (> 0.19 m). In addition to lower A_{norm} values, an increasing number of unsuitable tracks was observed till 20 March, together with low values of the peak power (Fig. 5). During this time period, the vegetation gradually decreased the strength of the signal reflected from the soil surface and more signal was reflected by the vegetation. This triggered multiple peaks for some tracks. Such tracks were not used. When the vegetation surface completely replaced the soil surface as the dominant reflecting surface of the GNSS signal, a single peak period was observed again and its value increased in response to the rise of the reflecting surface. For example, T_d increased from 362 s (7 March) to 397 s (22 March) for GPS01 ascending tracks. Figure 5 shows that T_d is not sensitive to vegetation height when vegetation height is smaller than one wavelength.

Therefore, we concluded that this relative vegetation height (at satellite elevation of 9 degrees) retrieval technique was not working for vegetation height below one λ (~ 0.19 m for L1) and when multiple peaks were observed in the average power spectrum.

3.3 Vegetation height retrieval

Figure 7 shows the retrieved vegetation height from 16 January to 15 July 2015, together with seven *in situ* vegetation height measurements and daily vegetation height simulations by ISBA. Since the original H retrievals present a marked levelling effect, the moving average of the GPS height retrievals computed using a centred gliding window of 21 days is shown. The relative vegetation height retrievals are compared with ISBA height simulations and *in situ* height observations in Table 3. The differences between the seven *in situ* observations and the original H retrievals were -8 cm, +4 cm, -5 cm, -10 cm, -6 cm, -2 cm and -2 cm. Most of them exhibited a negative bias. In comparison with the errors between the *in situ* observations and the ISBA simulations (-5 cm, +6 cm, +10 cm, -15 cm, -3 cm, 0 cm and -61 cm), the GPS retrievals were closer to the observations on 30 March and 24 April (the third and forth *in situ* observations). On 18 June, the last height *in situ* observation before harvest was 39 cm in relation to lodging. The GPS retrieval was very close to this value with only -2 cm error. On the other hand, the ISBA simulation on 18 June was still at 1 m with an error of -61 cm, because the wheat height was simulated without accounting for lodging. This result shows that the *in situ* GPS height retrievals are able to detect local changes in vegetation height. Figure 7 and the scores given in Table 4 show that the GPS retrievals are closer to the observed growing trend than the ISBA simulations. Additionally, the moving average height presents a much better fit to the *in situ* measurements than the raw GPS retrievals. We also compared the GPS retrievals with the ISBA model simulations. We obtained the following score values from 10 March to 11 June 2015: MAE = 8.9 cm, RMSE = 12.4 cm and R^2 = 0.89. Similar values were obtained for the comparison between the moving average height and ISBA simulations: MAE = 9.0 cm, RMSE = 11.6 cm and R^2 = 0.91.

3.4 Vegetation height vs. above-ground dry biomass

Figure 7 also shows that the retrieved vegetation height is related to the simulated above-ground dry biomass of the wheat (brown line). We found a linear relationship between the moving average height from GPS retrievals and the above-ground dry biomass simulated by the ISBA model from 10 March to 29 May 2015 (when the maximum vegetation height, 1 m, was measured), during the time period from tillering to flowering. The correlation coefficient between the moving average height and the above-ground dry biomass, with 81 observations, was 0.996.

A similar result was obtained using the *in situ* height and above-ground dry biomass measurements in Wigneron et al. (2002) over another wheat crop site (Triticum durum, cultivar prinqual) in spring 1993 (See Eqs. S7-S8 and Fig. S6 in the supplement).

4. Discussion

4.1. Can soil moisture be retrieved under significant vegetation effects?

Our results show that over a wheat field the vegetation gradually replaces the soil as the dominant reflecting surface when plant height becomes comparable to, or larger than one wavelength.

We tested the relationship between the multipath phase in Eq. (5) and soil moisture for the whole wheat growing cycle (Fig. 8). We found that when the vegetation effects are not significant (A_{norm} > 0.78), the multipath phase correlates well (R = 0.92, N = 47, for the GPS10 descending tracks) with the *in situ* soil moisture observations (Fig. 8a). During this time period, the variation of multipath phase is about 12 degrees, for *in situ* VSM values ranging from 0.25 m^3m^{-3} to 0.30 m^3m^{-3}. But when the vegetation effects are significant (A_{norm} < 0.78), the multipath phase (without or with unwrapping, Fig. 8b and 8c) is no longer linearly related to soil moisture. For example, when vegetation height exceeded one wavelength, multipath phase rapidly decreased from 207 degrees to 43 degrees (between 10 and 20 March). Changes in multipath phase were disconnected from ISBA VSM simulations. This is consistent with CH16, who showed that soil moisture cannot be retrieved unless vegetation effects are corrected for.

4.2. Why does the locally adjusted *S* parameter differ from CH16?

In our experiment, the possible VSM retrieval duration was less than two months, in relatively wet conditions and VSM varied little: 0.25 m^3m^{-3} < VSM < 0.30 m^3m^{-3}. This is probably not enough to represent the full yearly range of soil moisture. This might affect the representativeness of the *S* parameter (Sect. 2.4) we derived from our field observations. Furthermore, the different signal wavelength (L1 = 19.03 cm, L2 = 24.45 cm) and the different antenna gain pattern also affect the *S* parameter. Many local environment factors such as vegetation effects, precipitation, changes in soil roughness and soil composition, can perturb the GPS VSM estimates. All these factors contribute to changes in *S*, and further affect the retrieval accuracy and the sub-daily variability of VSM estimates. That is why we used a scaled soil wetness index based on the normalized multipath phase for each track, without a priori knowledge of *S* parameter. This approach also gives more accurate results.

4.3. Can vegetation water content be inferred from the wavelet analysis?

We found that VWC impacts the peak power but we were not able to retrieve VWC at this stage.

Figure 7 shows that the retrieved vegetation height is consistent with independent height measurements. However, vegetation height is not the only factor affecting the reflected GPS signal. Vegetation water content (VWC, in kg m^{-2}) may also play a role on the reflected GPS signal. *In situ* observations indicate that VWC increased together with H during the growing period, from March to mid-May. From mid-May to harvest, VWC tended to decrease but H also decreased in

relation to lodging. Can this specific behavior of VWC be detected from the results of the wavelet analysis? The latter provides three quantities: the dominant period (Sect. 2.5), A_{norm}, and the peak power.

The amplitude (A_{norm}) is related to some extent to VWC (see Sect. 1). However, A_{norm} is calculated assuming the relative antenna height is constant. Because the wheat height increased from 10 cm to 100 cm, the relative antenna height was reduced, and this assumption was not satisfied. This affected the estimates of the amplitude of the multipath SNR data, especially when the wheat was tall. Comparing Fig. 6a and Fig. 6c, it can be observed that the signal amplitude is larger on 1 May than that on 15 June. But A_{norm} (0.15) on 1 May is even smaller than the A_{norm} (0.33) on 15 June (Fig. 2). It is likely that A_{norm} was underestimated on 1 May. Therefore, it is difficult to unequivocally relate A_{norm} to vegetation characteristics, as illustrated in Fig. 2. However, the drop in A_{norm} observed at the beginning of June (Fig. 2) could be related to the drop in VWC.

From the wavelet analysis, we also obtained the peak power when we searched for the peak period from the average power spectrum. Peak power can represent changes in the multipath SNR strength. Figure 9 shows daily box plots of the peak power for all available satellite tracks from 16 January to 15 July 2015, together with the distribution of bad quality tracks (as in Fig. 2), and rainfall. There are two major possible causes for a sudden reduction of the strength of the reflected SNR signal: (1) the attenuation of the signal by the rain intercepted by vegetation or in the troposphere and (2) the occurrence of more than one dominant reflecting surface at different heights, and this two causes can occur at the same time.

Three events of rapid reduction of the peak power can be observed in Fig. 9a. These events are related to larger daily standard deviation (STD) values of vegetation height retrievals (see Fig. 9b). The last event in June could be related to lodging. However, whether maximum STD is an indicator of lodging or not is unclear. It seems that these events are not related to rainfall events, and that the attenuation by intercepted water content is not a major cause of peak power drops. On the other hand, the emergence of multiple peaks and of bad quality tracks is consistent with the rapid power reduction in March and June. Multiple peaks may indicate that the reflected signal originates from surfaces at different heights. A possible cause of multiple peaks is a more heterogeneous wheat canopy density during the first stage of the growing period and after lodging. In such sparse or mixed vegetation conditions, VWC is not uniformly distributed and the soil surface may significantly contribute to the SNR. In the middle of April, there is no such effect but STD score increases (Fig. 9b). It is interesting to note that the peak power drops in Fig. 9a correspond to rapid changes in the retrieved vegetation height in Fig. 9c at multiples of λ or 0.5λ. It must be noted that absolute daily changes in H (and h), of about 1.1 cm d^{-1} are fairly uniform throughout the growing period. Since h decreases when plants grow, relative changes in h tend to increase. According to Eq. (4), T behaves similarly. This means that the sensitivity of the retrieval method to changes in H is larger at the end of the growing period. This is probably why leveling is more pronounced between mid-March and mid-April than at the end of April (see Fig. 9c). Leveling is less noticeable in May.

4.4. Can unwrapped multipath phase be used to retrieve vegetation height?

Our results indicate that using the dominant period to retrieve vegetation height is more relevant than using the multipath phase.

The relationship between the multipath phase (Fig. 8) in Eq. (5) and vegetation height was investigated. Because changes in relative antenna height exceeded λ during vegetation growth, the multipath phase had to be unwrapped. When the vegetation height was smaller than λ (before 10 March), multipath phase (around 200 degrees) presented little changes (about 12 degrees). From 21 March to 18 April, multipath phase was much smaller (around 10 degrees) and relatively stable. On the other hand, the variability increased from 19 April to 11 June (Fig. 8c), and no relationship with plant growth could be found. It can be noted that multipath phase and dominant period are relatively stable when the vegetation height is smaller than λ. Both tend to aggregate at several value levels.

4.5. Can wheat phenological stages be inferred?

Figure 9 shows that the occurrence of multiple peaks together with a drop of the peak power can be used as an indicator of the start of the most active part of the growing season, and of the end of the senescence period preceding the harvest.

We applied the GDD model (see Sect. 2.6) to year 2015 and we obtained the following dates for tillering, flowering, and ripening: 12 March, 31 May, and 3 June, respectively (see Fig. S3 in the Supplement). The obtained tillering date (12 March) is close to the start date (10 March) of the multiple peaks (see Section 3.2). Tillering in wheat triggers nitrogen uptake and the accumulation of biomass (Gastal and Lemaire, 2002). This is consistent with the rapid changes in the indicators derived from the wavelet analysis: drop in A_{norm} values and high rate of multiple peaks (Fig. 2), rise in the retrieved H (Fig. 7), and drop in peak power (Fig. 9). For our site, the tillering date also corresponded to the period when H reached a value of about 0.2 m. This was the case in 2015 and also in 2010 at the same site (Betbeder et al., 2016).

Flowering and ripening did not trigger abrupt changes in the GPS retrievals. However, these stages corresponded to a change in H trend. This is illustrated in Supplement Fig. S7, which shows the difference between retrieved vegetation height at a given date and retrieved vegetation height 15 days before. Flowering and ripening occur towards the end of the growing period when the vegetation height is no longer increased compared with 15 days before but slightly declines due to wheat heads tipping down (Wigneron et al., 2002). In order to confirm these findings, it could be recommended to perform GNSS-IR measurements further over other wheat fields and other crops, together with phenological stage observations combined with in situ height measurements.

4.6 Potential future applicability and transferability of the retrieval method

In situ VSM observations are not widespread in France and *in situ* vegetation height observations are generally not available. Therefore, ISBA simulations are key for water resource monitoring at the country scale. It must be noted that the ISBA

model is forced by the SAFRAN atmospheric analysis (Durand et al., 1993; Durand et al., 1999) and that SAFRAN is able to integrate thousands of *in situ* raingage observations. ISBA is also able to simulate vegetation characteristics such as vegetation height, leaf area index and above-ground dry biomass. However, *in situ* VSM observations are needed to validate the model simulations (e.g. Albergel et al., 2010). From this point of view, the spatial resolution of GNSS retrievals is an asset. The area sampled by GNSS retrievals is much larger than what can be achieved using individual soil moisture probes and much smaller than pixel size of satellite-derived products. Longer continuous time periods of GNSS retrievals should be envisaged to serve as independent validation data sources in statistical methods such as Triple Collocation (Dorigo et al., 2010).

We successfully assessed the surface soil moisture retrieval technique over a wheat crop field, during the start of the growing period. However, the rather narrow range of surface soil moisture values during the corresponding experiment time period limited the representativeness of the obtained retrieval accuracy. Furthermore, our dataset did not include GNSS data and *in situ* VSM measurements for periods of bare soil. Longer periods presenting a bare soil surface should be investigated in further studies. At the same time, more *in situ* vegetation measurements should be carried out in further studies.

The retrieved vegetation height was based on the dominant period of the average power spectrum. The latter was derived from GPS multipath SNR data for elevation angles between 5 and 20 degrees. We only considered the dominant period variations, without accounting for instantaneous phase changes. The accuracy of the retrieved vegetation height could probably be improved considering changes in both period and phase of the multipath SNR oscillations.

In this study, only the SNR data of L1 C/A signal is used, SNR data from different wavelength (e.g., L1 C/A, L2C and L5) should also be compared or combined to survey canopy characteristics.

A linear relationship between wheat height and dry biomass was observed during the period from wheat tillering to ripening. Retrieving dry biomass is a motivation for further research because most current satellite vegetation products focus on retrieving vegetation indexes or leaf area index. The dry biomass is directly related to the wheat yield, and retrieving wheat height could have applications in crop monitoring. In this study, only wheat is considered. Other crops should be investigated in the future.

5. Conclusions

GNSS SNR data were obtained using the SNR GNSS-IR technique over an intensively cultivated wheat field in southwestern France. The data were used to retrieve either soil moisture or relative vegetation height during the growing period of wheat. Vegetation growth tended to decrease the relative antenna height and broke up the constant height assumption used in soil moisture retrieval algorithms. Soil moisture could not be retrieved after wheat tillering. A new algorithm based on a wavelet analysis was implemented and used to extract the dominant period of the SNR and further to retrieve vegetation height. The dominant period was derived from the peak period of the average power spectrum derived from a wavelet analysis of SNR. The method proposed by CH16 was used to retrieve soil moisture under sparse vegetation

conditions, before wheat tillering. Soil moisture was retrieved on a daily basis with a precision (SDD) of 0.008 m^3m^{-3}. Before tillering, only one stable peak was observed in the average power spectrum, because the soil surface was the dominant GNSS reflecting surface. During and after tillering (10-20 March), the reflected GNSS signal included contributions from both soil and vegetation. More than one peak was observed in the average power spectrum together with low values of peak power, showing that there were no clear dominant reflecting surface. Wheat growth gradually raised the reflecting surface of the GNSS signal, from the soil surface to the vegetation surface, which significantly modulated the dominant period of the multipath SNR data. In these conditions, vegetation effects could not be ignored and soil moisture could not be retrieved. The retrieved vegetation height was in good agreement with the *in situ* observations, and was consistent with a lodging event. However, the retrieved height consisted of several levels. Using a moving average on the retrieved height permitted a better match with the *in situ* height measurements: a precision of 3.8 cm could be achieved, against 5.5 cm for the original retrievals. Furthermore, several indicators derived from the wavelet analysis could be used to detect tillering. We also found that VWC impacts the peak power but the latter cannot be used to retrieve VWC at this stage.

Acknowledgments. The work of Sibo Zhang and Karen Boniface was supported by the STAE (Sciences et Technologies pour l'Aéronautique et l'Espace) foundation, in the framework of the PRISM (Potentialités de la Réflectométrie GNSS In-Situ et Mobile) project. Authors would also thanks the farmer, Mr Blanquet, for his time and the person who helped for collecting ground data.

References

Albergel, C., Calvet, J.C., De Rosnay, P., Balsamo, G., Wagner, W., Hasenauer, S., Naeimi, V., Martin, E., Bazile, E., Bouyssel, F. and Mahfouf, J.F.: Cross-evaluation of modelled and remotely sensed surface soil moisture with *in situ* data in southwestern France, Hydrol. Earth Syst. Sci., 14(11), 2177–2191, doi:10.5194/hess-14-2177-2010, 2010.

Betbeder, J., Fieuzal, R., Philippets, Y., Ferro-Famil, L., and Baup, F.: Contribution of multitemporal polarimetric synthetic aperture radar data for monitoring winter wheat and rapeseed crops, J. Appl. Remote Sens., 10(2), 026020, doi:10.1117/1.JRS.10.026020, 2016.

Bilich, A., and Larson, K. M.: Mapping the GPS multipath environment using the signal-to-noise ratio (SNR), Radio Science, 42(6), RS6003, doi:10.1029/2007RS003652, 2007.

Boniface, K., Braun, J. J., McCreight, J.L., and Nievinski, F.G.: Comparison of snow data assimilation system with GPS reflectometry snow depth in the western United States, Hydrological Processes, 29 (10), 2425-2437, doi:10.1002/hyp.10346, 2015.

Chan S. K., Bindlish, R., O'Neill, P. E., Njoku, E., Jackson, T., Colliander, A., Chen, F., Burgin, M., Dunbar, S., Piepmeier, J., Yueh, S., Entekhabi, D., Cosh, M. H., Caldwell, T., Walker, J., Wu, X., Berg, A., Rowlandson, T., Pacheco, A., McNairn, H., Thibeault, M., Martínez-Fernández, J., González-Zamora, A., Seyfried, M., Bosch, D., Starks, P., Goodrich, D., Prueger, J., Palecki, M., Small, E. E., Zreda, M., Calvet, J.-C., Crow, W., and Kerr, Y.: Assessment of the SMAP passive soil moisture product, IEEE Trans. Geosci. Remote Sens., 54 (8), 4994 - 5007, doi:10.1109/TGRS.2016.2561938, 2016.

Chew, C. C., Small, E. E., Larson, K. M., and Zavorotny, V. U.: Effects of near-surface soil moisture on GPS SNR data: development of a retrieval algorithm for soil moisture, IEEE Transactions on Geoscience and Remote Sensing, 52(1), 537-543, doi:10.1109/TGRS.2013.2242332, 2014.

Chew, C. C., Small, E. E., Larson, K. M., and Zavorotny, V. U.: Vegetation sensing using GPS-interferometric reflectometry: theoretical effects of canopy parameters on signal-to-noise ratio data, IEEE Transactions on Geoscience and Remote Sensing, 53(5), 2755-2764, doi:10.1109/TGRS.2014.2364513, 2015.

Chew, C., Small, E. E., and Larson, K. M.: An algorithm for soil moisture estimation using GPS-interferometric reflectometry for bare and vegetated soil, GPS Solutions, 20(3), 525-537, doi:10.1007/s10291-015-0462-4, 2016.

Darrozes, J., Gaillot, P., De Saint-Blanquat, M., and Bouchez, J.L.: Software for multi-scale image analysis: The normalized optimized Anisotropic Wavelet Coefficient method, Computers & Geosciences, 23(8), 889-895, doi:10.1016/S0098-3004(97)00063-0, 1997.

Decharme, B., Boone, A., Delire, C., and Noilhan, J.: Local evaluation of the Interaction between Soil Biosphere Atmosphere soil multilayer diffusion scheme using four pedotransfer functions, J. Geophys. Res., 116, D20126, doi:10.1029/2011JD016002, 2011.

Dorigo, W. A., Scipal, K., Parinussa, R. M., Liu, Y. Y., Wagner, W., de Jeu, R. A. M., and Naeimi, V.: Error characterisation of global active and passive microwave soil moisture datasets, Hydrol. Earth Syst. Sci., 14(12), 2605–2616, doi:10.5194/hess-14-2605-2010, 2010.

Dorigo, W.A., Xaver, A., Vreugdenhil, M., Gruber, A., Hegyiová, A., Sanchis-Dufau, A.D., Zamojski, D., Cordes, C, Wagner, W, and Drusch, M.: Global automated quality control of *in situ* soil moisture data from the International Soil Moisture Network, Vadose Zone Journal, 12(3), doi:10.2136/vzj2012.0097, 2013.

Durand, Y., Brun, E., Merindol, L., Guyomarc'h, G., Lesaffre, B., and Martin, E.: A meteorological estimation of relevant parameters for snow models, Ann. Geophys., 18(1), 65–71, doi:10.1017/S0260305500011277, 1993.

Durand, Y., Giraud, G., Brun, E., Merindol, L., and Martin, E.: A computer-based system simulating snow-pack structures as a tool for regional avalanche forecasting, Ann. Glaciol., 45(151), 469–484, doi:10.1017/S0022143000001337, 1999.

Duveiller, G., Weiss, M., Baret, F., and Defourny, P.: Retrieving wheat green area index during the growing season from optical time series measurements based on neural network radiative transfer inversion, Remote Sensing of Environment, 115(3), 887-896, doi:10.1016/j.rse.2010.11.016, 2011.

Escalera, E., and MacGillivray, H.T.: Topology in galaxy distributions: method for a multi-scale analysis. A use of the wavelet transform, Astronomy and Astrophysics, 298, 1-21, 1995.

Fieuzal, R., Baup, F., and Marais-Sicre, C.: Monitoring wheat and rapeseed by using synchronous optical and radar satellite data—From temporal signatures to crop parameters estimation, Advances in Remote Sensing, 2(2), 33222, doi:10.4236/ars.2013.22020, 2013.

Foti, G., Gommenginger, C., Jales, P., Unwin, M., Shaw, A., Robertson, C., and Rosello, J.: Spaceborne GNSS reflectometry for ocean winds: First results from the UK TechDemoSat-1 mission, Geophysical Research Letters, 42(13), 5435-5441, doi:10.1002/2015GL064204, 2015.

Gaillot, P., Darrozes, J. and Bouchez, J.L.: Wavelet transform: a future of rock fabric analysis?, Journal of Structural Geology, 21(11), 1615-1621, doi:10.1016/S0191-8141(99)00073-5, 1999.

Gastal, F., and Lemaire, G.: N uptake and distribution in crops: an agronomical and ecophysiological perspective, J. Exp. Bot., 53(370), 789-799, doi:10.1093/jexbot/53.370.789, 2002.

Georgiadou, Y.,and Kleusberg, A.: On carrier signal multipath effects in relative GPS positioning, Manuscripta geodaetica, 13(3), 172-179, 1988.

Grinsted, A., Moore, J.C., and Jevrejeva, S.: Application of the cross wavelet transform and wavelet coherence to geophysical time series, Nonlinear processes in geophysics, 11(5/6), 561-566, 2004.

Hagelberg, C. and Helland, J.: Thin-line detection in meteorological radar images using wavelet transforms, Journal of Atmospheric and Oceanic Technology, 12(3), 633-642, doi:10.1175/1520-0426, 1995.

Kerr, Y., Waldteufel, P., Wigneron, J., Martinuzzi, J., Font, J., and Berger, M.: Soil moisture retrieval from space: The Soil Moisture and Ocean Salinity (SMOS) mission, IEEE T. Geosci. Remote, 39(8), 1729–1735, doi:10.1109/36.942551, 2001.

Koch, F., Schlenz, F., Prasch, M., Appel, F., Ruf, T. and Mauser, W.: Soil Moisture Retrieval Based on GPS Signal Strength Attenuation, Water, 8(7), 276, doi:10.3390/w8070276, 2016.

Labat, D.: Recent advances in wavelet analyses: Part 1. A review of concepts, Journal of Hydrology, 314(1), 275-288, 2005.

Lafont, S., Zhao, Y., Calvet, J.-C., Peylin, P., Ciais, P., Maignan, F., and Weiss, M.: Modelling LAI, surface water and carbon fluxes at high-resolution over France: comparison of ISBA-A-gs and ORCHIDEE, Biogeosciences, 9(1), 439–456, doi:10.5194/bg-9-439-2012, 2012.

Larson, K. M., Small, E. E., Gutmann, E. D., Bilich, A. L., Braun, J. J., and Zavorotny, V. U.: Use of GPS receivers as a soil moisture network for water cycle studies, Geophysical Research Letters, 35(24), doi:10.1029/2008GL036013, 2008.

Larson, K. M., Braun, J. J., Small, E. E., Zavorotny, V. U., Gutmann, E. D., and Bilich, A. L.: GPS multipath and its relation to near-surface soil moisture content, IEEE Journal of Selected Topics in Applied Earth Observations and Remote Sensing, 3(1), 91-99, doi:10.1109/JSTARS.2009.2033612, 2010.

Larson, K. M., and Nievinski, F. G.: GPS snow sensing: results from the EarthScope Plate Boundary Observatory, GPS solutions, 17(1), 41-52, doi:10.1007/s10291-012-0259-7, 2013.

Larson, K. M., Small, E. E., Chew, C. C., Nievinski, F. G., Pratt, J., McCreight, J. L., Braun, J., Boniface, K., and Evans, S. G.: PBO H2O: Plate Boundary Observatory Studies of the Water Cycle, American Geophysical Union, Fall Meeting, San Francisco, 9-13 December, 2013.

Larson, K. M., and Small, E. E.: Normalized microwave reflection index: A vegetation measurement derived from GPS networks, IEEE Journal of Selected Topics in Applied Earth Observations and Remote Sensing, 7(5), 1501-1511, doi:10.1109/JSTARS.2014.2300116, 2014.

Larson, K. M.: GPS interferometric reflectometry: applications to surface soil moisture, snow depth, and vegetation water content in the western United States, Wiley Interdisciplinary Reviews: Water, 3(6), 775-787, doi:10.1002/wat2.1167, 2016.

Masson, V., Le Moigne, P., Martin, E., Faroux, S., Alias, A., Alkama, R., Belamari, S., Barbu, A., Boone, A., Bouyssel, F., Brousseau, P., Brun, E., Calvet, J.-C., Carrer, D., Decharme, B., Delire, C., Donier, S., Essaouini, K., Gibelin, A.-L., Giordani, H., Habets, F., Jidane, M., Kerdraon, G., Kourzeneva, E., Lafaysse, M., Lafont, S., Lebeaupin Brossier, C., Lemonsu, A., Mahfouf, J.-F., Marguinaud, P., Mokhtari, M., Morin, S., Pigeon, G., Salgado, R., Seity, Y., Taillefer, F., Tanguy, G., Tulet, P., Vincendon, B., Vionnet, V., and Voldoire, A.: The SURFEXv7.2 land and ocean surface platform

for coupled or offline simulation of earth surface variables and fluxes, Geosci. Model Dev., 6, 929–960, doi:10.5194/gmd-6-929-2013, 2013.

Morisette, J.T., Baret, F., Privette, J.L., Myneni, R.B., Nickeson, J.E., Garrigues, S., Shabanov, N., Weiss, M., Fernandes, R., Leblanc, S., Kalacska, M., Sánchez-Azofeifa, G.A., Chubey, M., Rivard, B., Stenberg, P., Rautiainen, M., Voipio, P., Manninen, T., Pilant, A.N., Lewis, T.E., Iiames, J.S., Colombo, R., Meroni, M., Busetto, L., Cohen, W., Turner, D.P., Warner, E.D., Petersen, G.W., Seufert, G., and Cook, R.: Validation of global moderate-resolution LAI products: A framework proposed within the CEOS land product validation subgroup, IEEE Transactions on Geoscience and Remote Sensing, 44(7), 1804–1817, 2006.

Motte, E., Egido, A., Roussel, N., Boniface, K., Frappart, F., Baghdadi, N., and Zribi, M.: Applications of GNSS-R in continental hydrology, Land Surface Remote Sensing in Continental Hydrology, Amsterdam, The Netherlands: Elsevier, 281-321, doi:10.1016/B978-1-78548-104-8.50009-7, 2016.

Njoku, E.G., Wilson, W.J., Yueh, S.H., Dinardo, S.J., Li, F.K., Jackson, T.J., Lakshmi, V. and Bolten, J.: Observations of soil moisture using a passive and active low-frequency microwave airborne sensor during SGP99, IEEE Transactions on Geoscience and Remote Sensing, 40(12), 2659-2673, doi:10.1109/TGRS.2002.807008, 2002.

Ouillon, G., Sornette, D. and Castaing, C.: Organisation of joints and faults from 1-cm to 100-km scales revealed by optimized anisotropic wavelet coefficient method and multifractal analysis, Nonlinear Processes in Geophysics, 2(3/4), 158-177, 1995.

Roesch, A., Schmidbauer, H., and Roesch, M. A.: Package 'WaveletComp', 2014.

Roussel, N., Frappart, F., Ramillien, G., Darrozes, J., Desjardins, C., Gegout, P., Pérosanz, F., and Biancale, R.: Simulations of direct and reflected wave trajectories for ground-based GNSS-R experiments, Geoscientific Model Development, 7, 2261-2279, doi:10.5194/gmd-7-2261-2014, 2014.

Roussel, N., Frappart, F., Ramillien, G., Darrozes, J., Baup, F., Lestarquit, L., and Ha, M. C.: Detection of Soil Moisture Variations Using GPS and GLONASS SNR Data for Elevation Angles Ranging From 2° to 70°, IEEE Journal of Selected Topics in Applied Earth Observations and Remote Sensing, 9(10), 4781-4794, doi:10.1109/JSTARS.2016.2537847, 2016.

Small, E. E., Larson, K. M., and Braun, J. J.: Sensing vegetation growth with reflected GPS signals, Geophysical Research Letters, 37(12), L12401, doi:10.1029/2010GL042951, 2010.

Small, E. E., Larson, K. M., and Smith, W. K.: Normalized microwave reflection index: validation of vegetation water content estimates from Montana grasslands, IEEE Journal of Selected Topics in Applied Earth Observations and Remote Sensing, 7(5), 1512-1521, doi:10.1109/JSTARS.2014.2320597, 2014.

Small, E. E., Larson, K. M., Chew, C. C., Dong, J., and Ochsner, T. E.: Validation of GPS-IR soil moisture retrievals: Comparison of different algorithms to remove vegetation effects, IEEE Journal of Selected Topics in Applied Earth Observations and Remote Sensing, 9(10), 4759-4770, doi:10.1109/JSTARS.2015.2504527, 2016.

Torrence, C. and Compo, G.P.: A practical guide to wavelet analysis, Bulletin of the American Meteorological society, 79(1), 61-78, doi:10.1175/1520-0477, 1998.

Vey, S., Güntner, A., Wickert, J., Blume, T., and Ramatschi, M.: Long-term soil moisture dynamics derived from GNSS interferometric reflectometry: A case study for Sutherland, South Africa, GPS Solutions, 20(4), 641-654, doi:10.1007/s10291-015-0474-0, 2016.

Wan, W., Larson, K. M., Small, E. E., Chew, C. C., and Braun, J. J.: Using geodetic GPS receivers to measure vegetation water content, GPS Solutions, 19(2), 237-248, doi:10.1007/s10291-014-0383-7, 2015.

Wigneron, J.P., Ferrazzoli, P., Olioso, A., Bertuzzi, P. and Chanzy, A.: A simple approach to monitor crop biomass from C-band radar data, Remote Sens. Environ., 69(2), 179-188, doi:10.1016/S0034-4257(99)00011-5, 1999.

Wigneron, J.P., Chanzy, A., Calvet, J.C., Olioso, A. and Kerr, Y.: Modeling approaches to assimilating L band passive microwave observations over land surfaces, Journal of Geophysical Research: Atmospheres, 107(D14), doi:10.1029/2001JD000958, 2002.

Zavorotny, V. U., Larson, K. M., Braun, J. J., Small, E. E., Gutmann, E. D., and Bilich, A. L.: A physical model for GPS multipath caused by land reflections: Toward bare soil moisture retrievals, IEEE Journal of Selected Topics in Applied Earth Observations and Remote Sensing, 3(1), 100-110, doi:10.1109/JSTARS.2009.2033608, 2010.

Zavorotny, V. U., Gleason, S., Cardellach, E., and Camps, A.: Tutorial on remote sensing using GNSS bistatic radar of opportunity, IEEE Geoscience and Remote Sensing Magazine, 2(4), 8-45, doi:10.1109/MGRS.2014.2374220, 2014.

Table 1. Soil moisture scores from 16 January to 5 March 2015.

	GPS vs. *in situ*	GPS vs. ISBA	GPS vs. *in situ*	GPS vs. ISBA	GPS (φ_{index}) vs. *in situ*	GPS (φ_{index}) vs. ISBA	ISBA vs. *in situ*
S ($m^3m^{-3}deg^{-1}$)	0.0148		0.0033		-	-	-
N	47	43	47	43	47	43	43
MAE (m^3m^{-3})	0.036	0.034	0.011	0.018	0.007	0.009	0.009
RMSE (m^3m^{-3})	0.046	0.041	0.014	0.022	0.009	0.012	0.010
SDD (m^3m^{-3})	0.036	0.037	0.009	0.012	0.008	0.011	0.006
Mean bias (m^3m^{-3})	0.029	0.019	-0.010	-0.018	0.003	-0.005	0.008
R^2	0.73	0.63	0.73	0.63	0.74	0.65	0.88

Table 2. Sub-daily variability (standard deviation, in m^3m^{-3}) of VSM estimates.

	Minimum	Maximum	Average value
In situ observations	0.000	0.009	0.002
ISBA simulations	0.000	0.021	0.005
GPS retrievals with S = 0.0148 $m^3m^{-3}deg^{-1}$	0.012	0.090	0.036
GPS retrievals with S = 0.0033 $m^3m^{-3}deg^{-1}$	0.003	0.020	0.008
GPS retrievals from scaled soil wetness indexes	0.005	0.017	0.009

Table 3. Vegetation height retrievals from GPS and simulations from ISBA, and their relative deviations for each *in situ* height observation. The phenological statuses are derived from the GDD model.

Dates (Year 2015)	Phenological status	*in situ* height (cm)	GPS height (cm)	ISBA height (cm)	*in situ* - GPS (cm)	*in situ* - ISBA (cm)
20 January	-	10	18.4	15.4	-8.4	-5.4
10 March	-	20	15.7	14.5	4.3	5.5
12 March	Tillering	-	15.5	15.6	-	-
30 March	-	35	40.4	24.6	-5.4	10.4
24 April	-	55	65.3	70.0	-10.3	-15.0
19 May	-	97	102.9	100.0	-5.9	-3.0
29 May	-	100	101.7	100.0	-1.7	0.0
31 May	Flowering	-	102.4	100.0	-	-
3 June	Ripening	-	101.9	100.0	-	-
18 June	-	39	40.5	100.0	-1.5	-61.0

Table 4. Vegetation height scores from 10 March to 11 June 2015.

	GPS vs. *in situ*	Moving average (21 days) GPS vs. *in situ*	GPS vs. ISBA	Moving average (21 days) GPS vs. ISBA	ISBA vs. *in situ*
N	5	5	87	94	5
MAE (cm)	5.5	3.7	8.9	9.0	6.8
RMSE (cm)	6.2	5.0	12.4	11.6	8.6
SDD (cm)	5.5	3.8	12.5	11.6	9.6
Mean bias (cm)	3.8	3.7	-0.6	-0.8	0.4
R^2	0.98	0.99	0.89	0.91	0.95

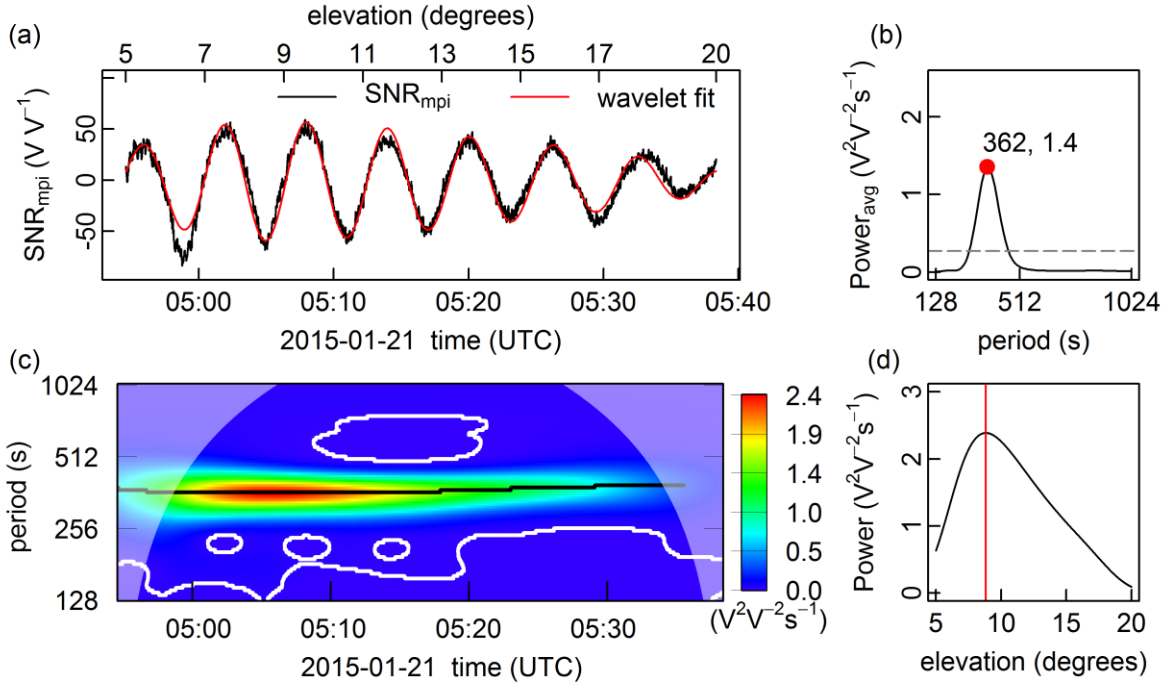

Figure 1. Example of a usable GPS01 ascending track SNR data set from 04:50 UTC to 05:38 UTC on 21 January 2015: (a) Multipath SNR data (in V V^{-1}), (b) average power spectrum with its maximum value (red dot), and (c) power spectrum for periods from 128 to 1024 s. The red line in (a) is the reconstructed SNR data by the daughter wavelet corresponding to the peak period (362 s) indicated in (b). The power at the peak period across elevation angles (d) presents a maximum value at an elevation angle of about 9 degrees.

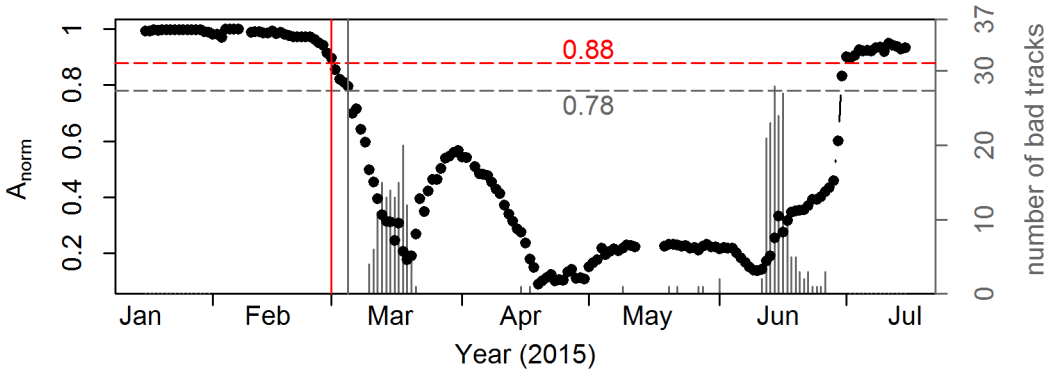

Figure 2. Normalized amplitude (A_{norm}) time series (black dots) and probability distribution (grey bars) of low quality tracks among all available satellite tracks on a daily basis from 16 January to 15 July 2015. The empirical A_{norm} threshold (0.78) is shown by the grey dashed line, and the soil moisture can be retrieved from 16 January to 5 March 2015 depending on it. Our field intuitive estimated A_{norm} threshold (0.88) depending on the A_{norm} in post-harvest (after 30 June) is shown by the red dashed line, and it indicates the soil moisture can be retrieved from 16 January to 1 March 2015.

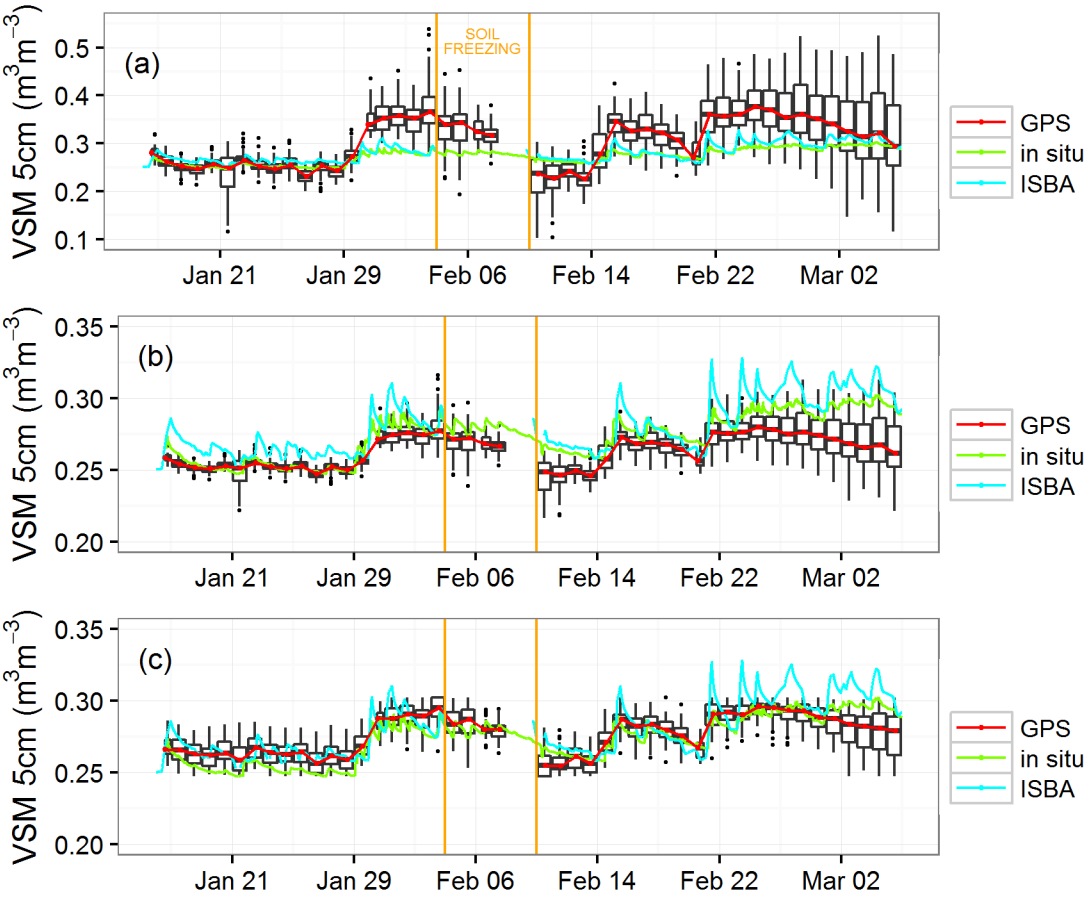

Figure 3. ***In situ*** **surface volumetric soil moisture (VSM) observations at 5 cm depth (green line), ISBA simulations (blue line), median of the daily GPS retrievals (a) with the a priori slope (*S* = 0.0148 $m^3m^{-3}degree^{-1}$) (red line), (b) with a locally adjusted slope (*S* = 0.0033 $m^3m^{-3}degree^{-1}$) (red line) and (c) from scaled soil wetness index (red line), and their daily statistical distribution (black box plots) for all available satellite tracks from 16 January to 5 March 2015. Boxes: 25-75% percentiles; bars: maximum (minimum) values below (above) 1.5 IQR (Inter Quartile Range, corresponding to the 25-75% percentile interval); dots: data outside the 1.5 IQR interval. The ISBA simulations indicate soil freezing (i.e. the presence of ice in the top soil layer) from 4 to 9 February.**

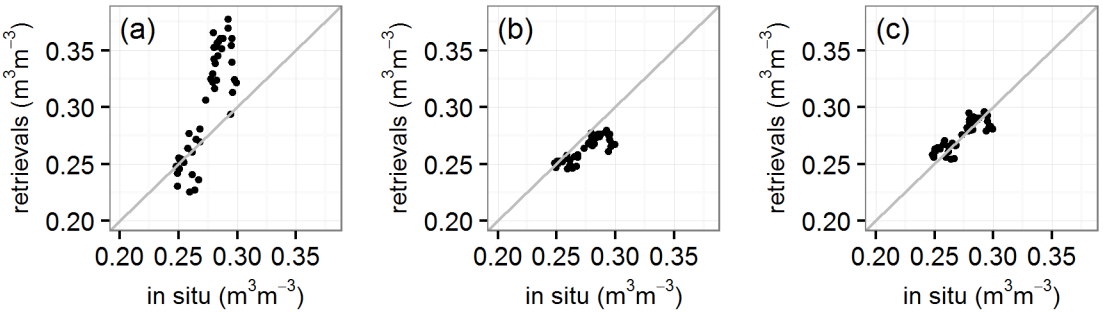

Figure 4. VSM GPS retrievals (N = 47) versus daily mean *in situ* VSM observations (m^3m^{-3}) at 5 cm from 16 January to 5 March 2015, (a) with the a priori slope S = 0.0148 $m^3m^{-3}degree^{-1}$, VSM = 0.0148Δφ + 0.252, (b) with the locally adjusted slope S = 0.0033 $m^3m^{-3}degree^{-1}$, VSM = 0.0033Δφ + 0.252, and (c) from scaled soil wetness indexes, VSM = 0.055φ_{index} + 0.247. More scores can be referred from Table 1.

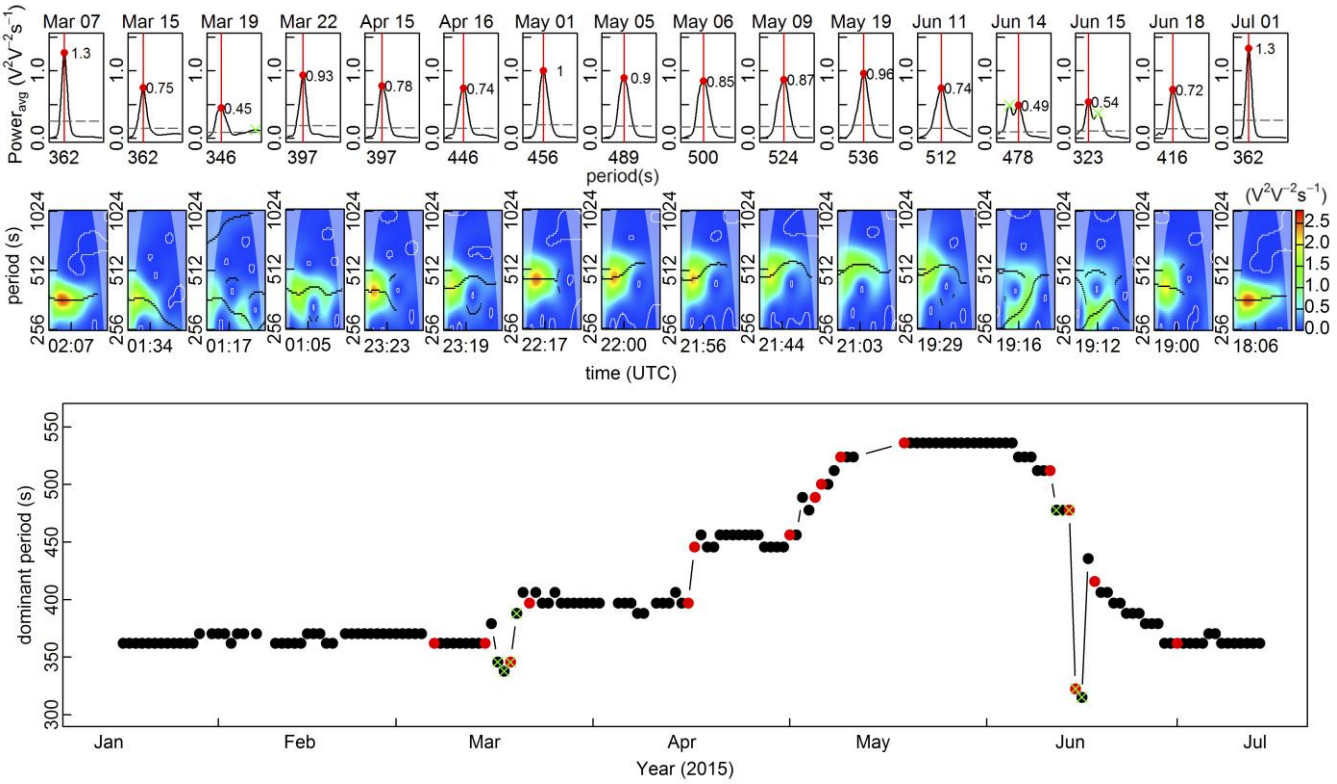

Figure 5. SNR dominant period (T_d) time series (black dots in the bottom sub-figure) derived from the GPS01 ascending tracks, with the green crosses indicate more than one peak are recognized as bad quality data, from 16 January to 15 July 2015. And (top) the average power spectrums with their maximum values (red dots), and (middle) power spectrums on the selected days (red dots in the bottom sub-figure) are also shown.

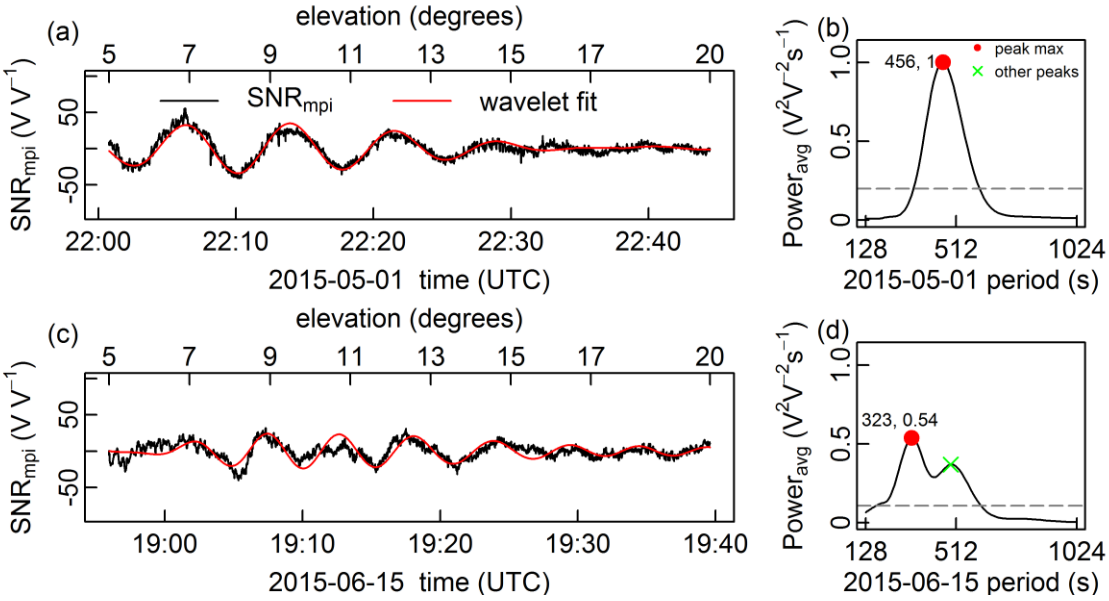

Figure 6. Examples of (a) usable and (c) unusable track data sets from the ascending tracks of GPS01 on1 May 2015 and 15 June 2015, respectively: (a, c) multipath SNR data, and (b, d) average power spectrums. The red lines in (a, c) are the reconstructed SNR data by the daughter wavelet corresponding to the maximum peak periods in (b, d), respectively. The green cross in (d) shows there is more than one peak in this track data, indicating bad quality, unusable data.

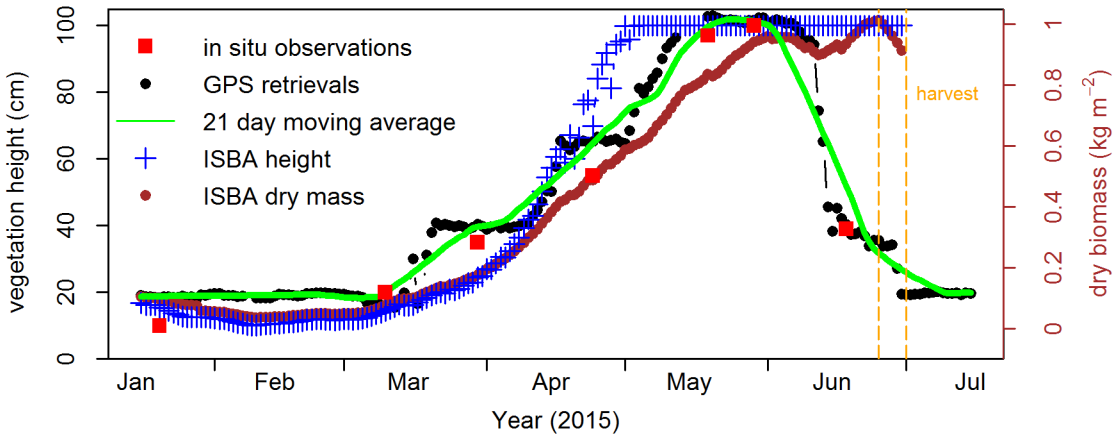

Figure 7. Wheat canopy height from 16 January to 15 July 2015 derived from GPS SNR data (black dots), from *in situ* observations (red squares), and from ISBA simulations (blue crosses). The green line represents the moving average of the GPS retrievals, computed using a centred gliding window of 21 days. Wheat above-ground dry biomass simulated by the ISBA model is indicated by brown dots.

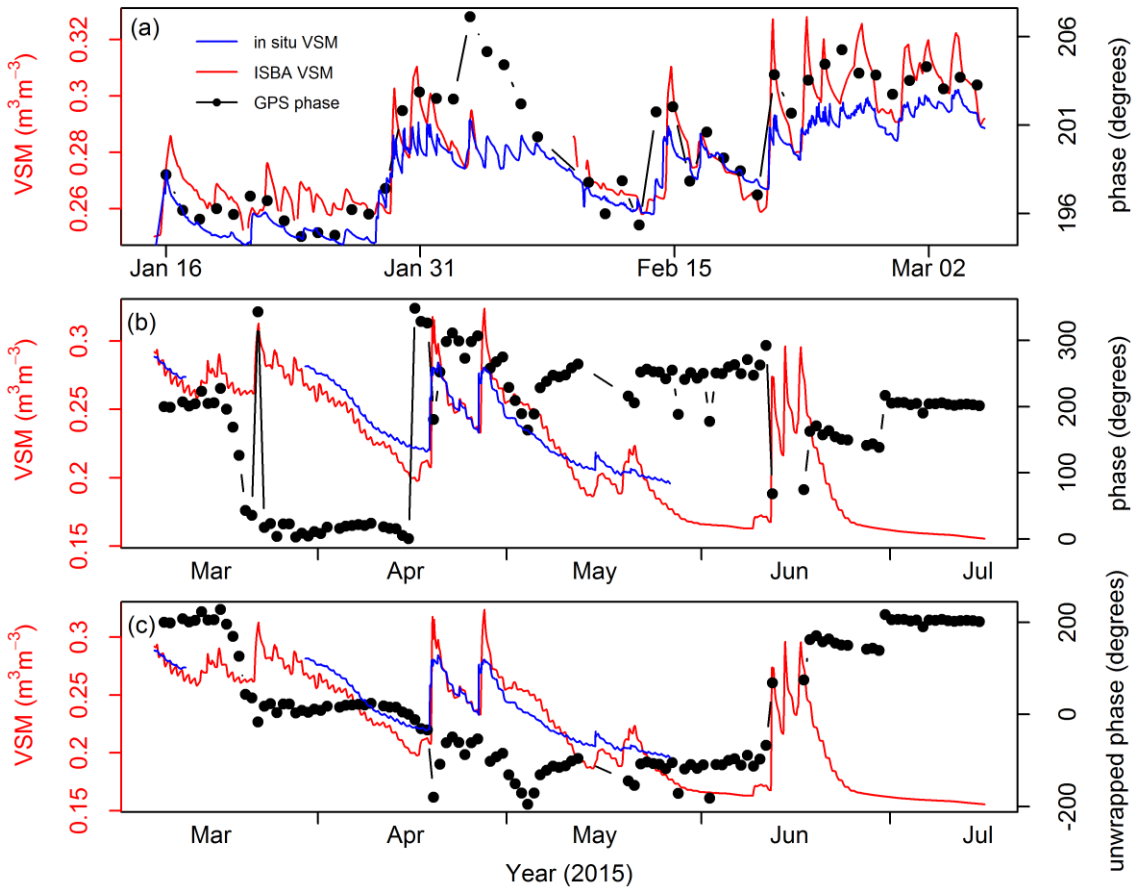

Figure 8. Example of a track data set (descending tracks from GPS10): (a) from 16 January to 5 March, with no significant vegetation effects; (b) and (c) from 6 March to 15 July, with significant vegetation effects. In (a) and (b), multipath phases (black dots) are compared with *in situ* VSM measurements at 5 cm (blue line) and ISBA simulations (red line). In (c), unwrapped multipath phases (black dots) are used to compare with *in situ* and simulated VSM.

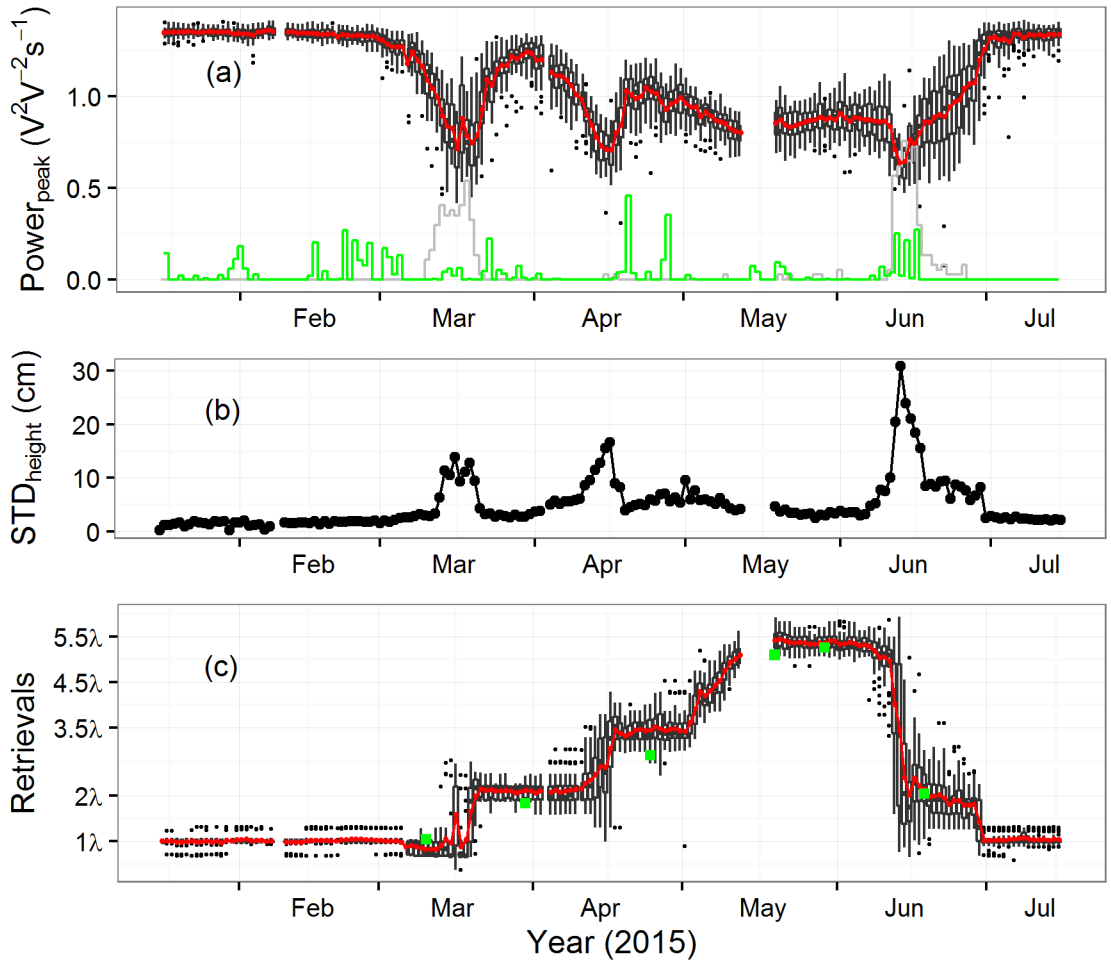

Figure 9. The box plots of (a) the peak power from a wavelet analysis, (b) standard deviation (STD) score of the retrieved vegetation height and (c) the retrieved vegetation height (rescaled in λ units) for all available satellite tracks from 16 January to 15 July 2015. The mean value of the peak power in (a) and of the retrievals in (c) are shown by red lines. In (a), the grey line shows the statistical distribution of bad quality tracks (the number of the bad quality tracks can be obtained multiplying by 37), the green line represents the rainfall (daily precipitation in mm d^{-1} can be obtained multiplying by 50). In (c), the rescaled *in situ* observations are shown by green squares.

Supplement of

Use of reflected GNSS SNR data to retrieve either soil moisture or vegetation height over a wheat crop

S. Zhang et al.

Correspondence to: J.-C. Calvet (jean-christophe.calvet@meteo.fr)

Locations of the GPS specular reflection points and first Fresnel zones

Larger variability in GPS sub-daily VSM estimates might originate from the different locations observed. Many local environment factors such as vegetation effects, precipitation, changes in soil roughness and soil composition, can perturb the GPS VSM estimates. During satellite overpasses the observed location changes together with the size of the footprint (the First Fresnel Zone, FFZ) of the GNSS system, in relation to the antenna height and elevation angle range. It might be another cause of the sub-daily variability of VSM estimates. Additionally, issues with the SNR data of the L1 C/A signal and the receiving antenna gain pattern may also affect the VSM estimates. The experiment site of the GPS receiving antenna, and the corresponding specular points and FFZ areas at 5 degrees and at 20 degrees of satellite elevation angles (outer circle and inner circle, respectively) are shown in Fig. S1.

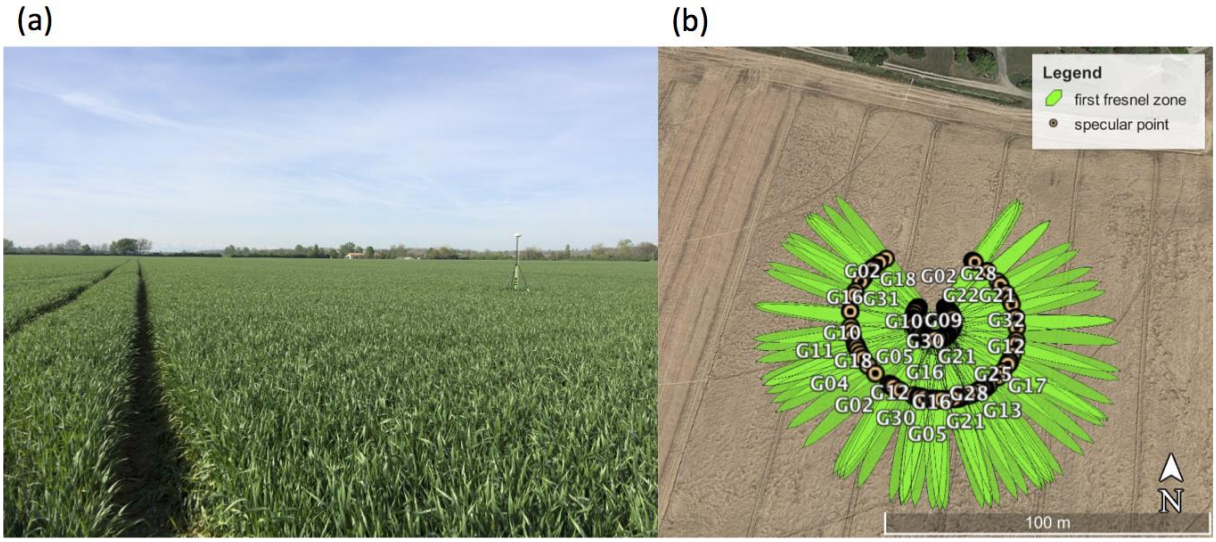

Figure S1 - (a) Antenna of the GNSS site at 2.51 m above the soil surface over an experimental field covered by rainfed winter wheat in Lamasquère, France (43°29'10"N, 1°13'57"E) on 24 April 2015. (b) Locations of the GPS specular reflection points and first Fresnel zones (FFZ). This simulation is done on 21 January 2015 for satellite elevation angles ranging from 5 to 20 degrees (outer circle and inner circle, respectively).

SNR data

At the Lamasquère site, data from GPS satellites should in theory be received twice per day. However, in practice, some of the satellites were only received once per day.
Figure S2 shows two typical satellite SNR time series for one day (21 January 2015). For GPS01 (top figure), only one ascending track (from low elevation to high elevation) and one descending track (from high elevation to low elevation) were recorded. For GPS18 (bottom figure), there were two ascending tracks and two descending tracks. The observation area (i.e. the reflecting surface) for the ascending track differed from the area seen by the descending track. Thus, we separated the ascending data from data of the descending satellite tracks. For GPS01, we obtained two time series (ascending and descending), and for GPS18 we obtained four time series. Furthermore, GPS01 reached high elevation angles (its maximum elevation angle was about 77°), making its elevation angle change faster than that of GPS18 (its maximum elevation angles were about 45° and 29°). Because these differences in maximum satellite elevation angle and elevation angle change rate substantially affected the period of the SNR data, we only used the satellite tracks with at least 40° maximum elevation for retrieving vegetation height. In the case of Fig. S2, this means that we only used the GPS01 track and the morning GPS18 track. The evening GPS18 track was discarded. Then, within selected tracks, only a valid segment SNR data for elevation angles between 5° and 20° were used.

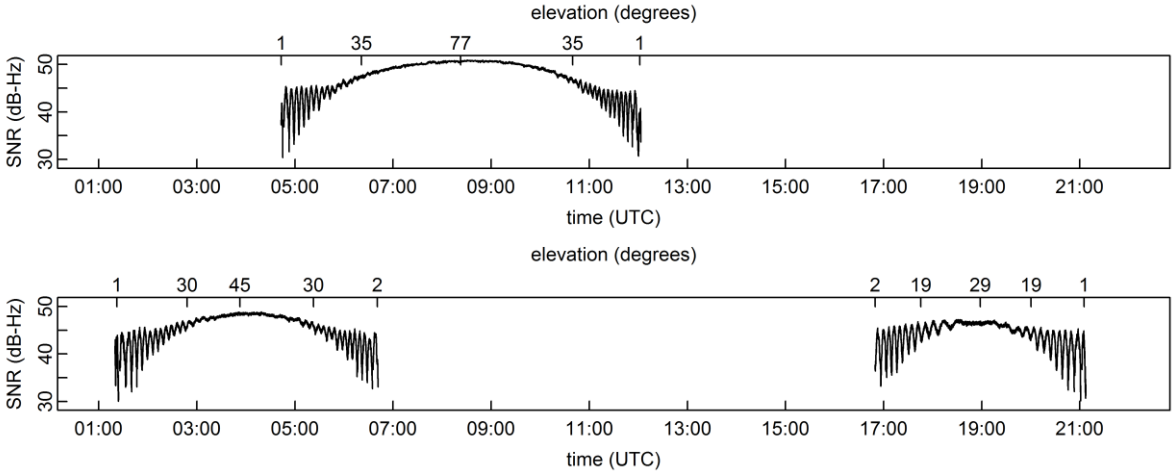

Figure S2 - Recorded S1C SNR data at Lamasquère for (top) GPS01 and (bottom) GPS18, on 21 January 2015.

Wavelet Analysis

The WaveletComp R package analyzes the period structure using the "mother" Morlet wavelet (Fig. S3):

$$\psi(t) = \pi^{-1/4} e^{i\omega t} e^{-t^2/2} \quad \text{(S1)}$$

The angular frequency ω is set to 6, as recommended by Torrence and Compo (1998). The Morlet wavelet transform of the multipath SNR time series (SNR_{mpi}) is defined as the convolution of the series with a set of "wavelet daughters" generated by the mother wavelet by translation in time by τ and scaling by s:

$$Wave(\tau, s) = \sum_t SNR_{mpi} \frac{1}{\sqrt{s}} \psi^*\left(\frac{t-\tau}{s}\right) \quad \text{(S2)}$$

where (*) denotes the complex conjugate. The localized estimates of the particular daughter wavelet in the time domain is determined by the localizing time parameter τ being shifted by a time increment of dt depending on the sampling interval. The wavelet transform is computed for a wavelet scale (s) set of interest, which is a fractional power of 2,

$$s_j = s_{\min} 2^{jdj},\ j = 0,1,\ldots,J \quad \text{(S3)}$$

The minimum (maximum) scale is fixed via the choice of the minimum (maximum) period interest depending on the possible relative antenna height change through the conversion factor $6/(2\pi)$. In this study they were set as 128 s and 1024 s, respectively. The wavelet transform can be separated into real part and imaginary part, thus providing information on both local amplitude and instantaneous phase of any periodic process across time. The local power of any periodic component of the time series under investigation is

$$Power(\tau, s) = \frac{1}{s} |Wave(\tau, s)|^2 \quad \text{(S4)}$$

Known as the wavelet power spectrum.

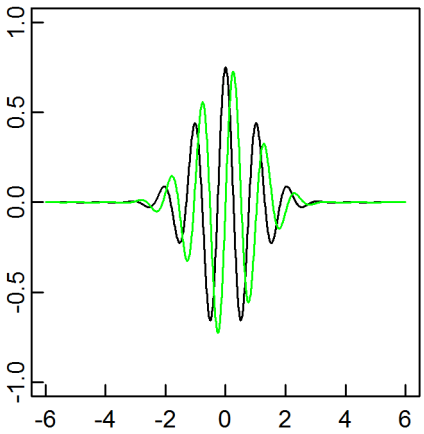

Figure S3- The Morlet mother wavelet, real part (black line) and imaginary part (green line)

References

Torrence, C., and Compo, G. P.: A practical guide to wavelet analysis, *Bulletin of the American Meteorological Society*, 79(1), 61-78, 1998.

Roesch, A., Schmidbauer, H., and Roesch, M. A.,: 'WaveletComp' package, 2014.

GDD (growing degree days) model

Temperatures at 2 meter from a large scale simulations made over France with a spatial resolution of 8 km by 8 km were extracted in order to build the growing degree days (GDD) model for Lamasquère site. The reference data was between year 2009 and 2010, it was sown on 1 October 2009, and the tillering, flowering and ripening were on 26 March, 9 June and 12 June 2010, respectively. T_{GDD} is calculated as the accumulation of daily mean temperatures (T_{mean}), T_{mean} is calculated in the following way:

$$T_{mean} = \frac{T_{\max} + T_{\min}}{2} - T_{base} \quad \text{(S5)}$$

based on the daily minimum (T_{min}) and maximum (T_{max}) temperatures. T_{mean} is further forced to range between 0°C and 35°C. The base temperature (T_{base}) used here for winter wheat is 0°C and the starting date for the accumulated temperature is from 1 October 2009, the accumulated temperature (T_{GDD}) is calculated as

$$T_{GDD} = \sum T_{mean} \quad \text{(S6)}$$

This GDD model was applied to year 2015 for our study (Fig. S4), according to the T_{GDD} in the GDD model, we obtained the following dates for tillering, flowering, and ripening: 12 March, 31 May, and 3 June 2015, respectively.

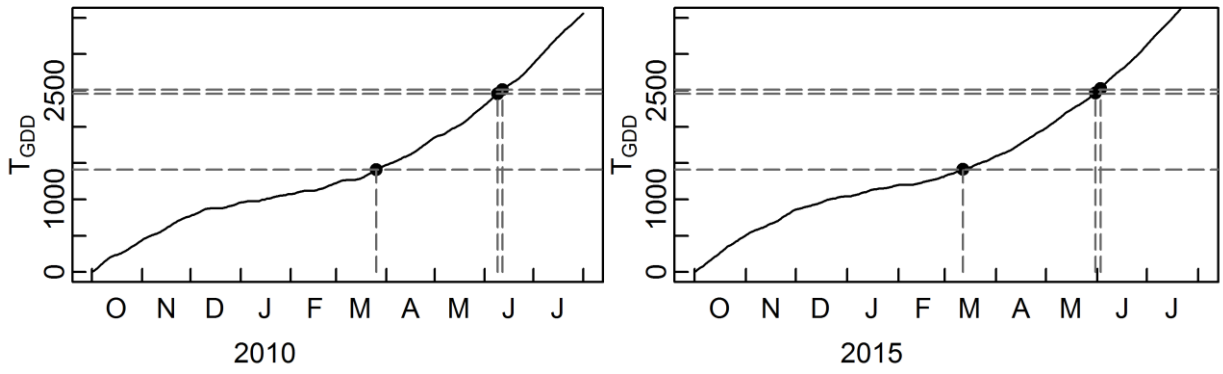

Figure S4 - (left) The growing degree days (GDD) model build in 2010 for winter wheat at Lamasquère and (right) GDD model build in 2015 at the same site. According to the T_{GDD} (°C) on the tillering, flowering and ripening in 2010, the corresponding phenological stage dates in 2015 are estimated.

References

Betbeder, J., Fieuzal, R., Philippets, Y., Ferro-Famil, L., and Baup, F.: Contribution of multitemporal polarimetric synthetic aperture radar data for monitoring winter wheat and rapeseed crops, J. Appl. Remote Sens. 10(2), 026020, doi: 10.1117/1.JRS.10.026020, 2016.

Duveiller, G., Weiss, M., Baret, F., and Defourny, P.: Retrieving wheat green area index during the growing season from optical time series measurements based on neural network radiative transfer inversion, Remote Sensing of Environment, 115(3), 887-896, 2011.

From phase to volumetric soil moisture

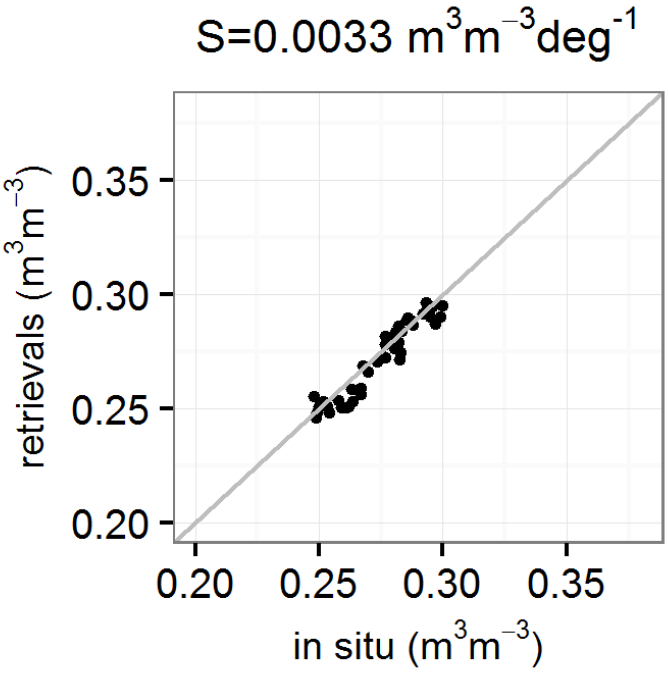

Figure S5 - Volumetric soil moisture (VSM) GPS retrievals (N = 47) versus in situ VSM observations (m^3m^{-3}) from 16 January to 5 March 2015, with fitted slope = 0.0033 $m^3m^{-3}deg^1$ for satellite tracks whose phase presents a linear correlation with in situ soil moisture higher than 0.9. This occurred for the ascending tracks of GPS 13, 21, 24, 30 and for the descending tracks of GPS 05, 09, 10, 15, and 23.

Linear relationship between vegetation height and above-ground dry biomass

We found a good linear relationship between the moving average height from GPS retrievals and the above-ground dry biomass simulated by the ISBA model from 10 March to 29 May 2015 (when the maximum vegetation height, 1 m, was measured), during the time period from tillering to flowering. The correlation coefficient between the moving average height and the above-ground dry biomass, with 81 observations, was 0.996.

$$biomass_{dry} = 1.05 \times height_{moving\_avg} - 0.19 \quad \text{(S7)}$$

with $biomass_{dry}$ (the above-ground dry biomass simulations) in kg m^{-2} and $height_{moving\_avg}$ (the moving average height from GPS retrievals) in meter.
A similar result was obtained by Wigneron et al. (2002) over another wheat crop site (Triticum durum, cultivar prinqual) in spring 1993 (Fig. S6). Although the sowing date (19 March) was late and the crop cycle was rather short, there was still a very good linear relationship between the in situ wheat height measurements and in situ dry biomass measurements from 20 April to 11 June 1993 (when the maximum vegetation height, 1 m, was measured). The correlation coefficient with 25 observations was 0.996.

$$biomass_{dry} = 1.11 \times height - 0.19 \quad \text{(S8)}$$

with $biomass_{dry}$ (in situ above-ground dry biomass measurements) in kg m^{-2} and height (in situ measurements) in meter.

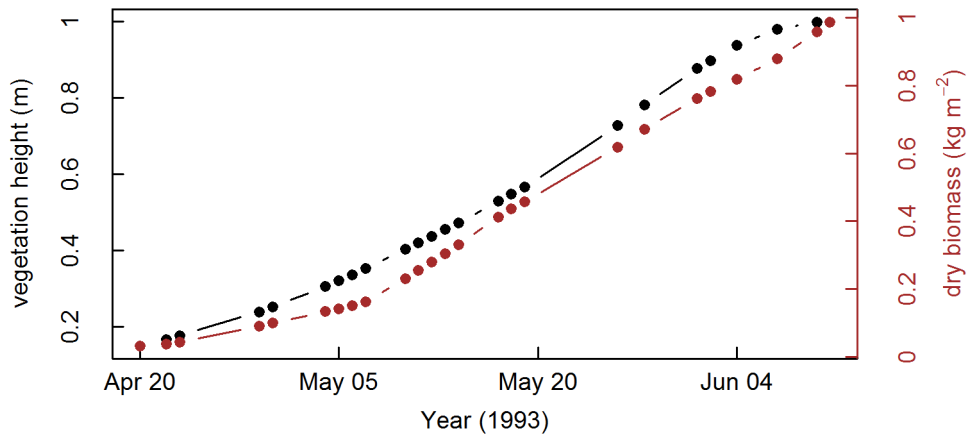

Figure S6 - In situ wheat canopy height measurements (25 black dots) and in situ wheat above-ground dry biomass measurements (brown dots) from 20 April to 11 June 1993 (adapted from Wigneron et al., 2002).

Reference:
Wigneron, J.P., Chanzy, A., Calvet, J.C., Olioso, A. and Kerr, Y.: Modeling approaches to assimilating L band passive microwave observations over land surfaces, Journal of Geophysical Research: Atmospheres, 107(D14), 2002.

GPS retrieved vegetation height difference

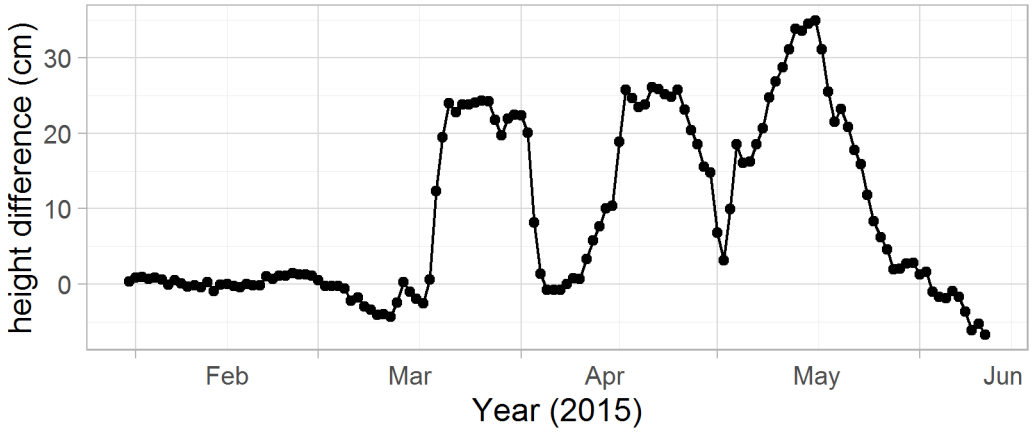

Figure S7 - The difference between retrieved vegetation height at a given date and retrieved vegetation height 15 days before, from 31 January to 11 June 2015.

Scores

The mean absolute error (MAE) is a quantity used to measure how close retrievals are to the observations, MAE is given by

$$MAE = \frac{1}{n}\sum_{i=1}^{n}\left|VSM_i^{OBS} - VSM_i^{GPS}\right| \quad \text{(S9)}$$

VSM^{OBS} represents the *in situ* VSM observations, VSM^{GPS} represents the retrieved soil moisture by GPS data, n is the valid number of data.

The root mean square error (RMSE) represents the sample standard deviation of the differences between retrieved values and observed values:

$$RMSE = \sqrt{\frac{\sum_{i=1}^{n}\left(VSM_i^{OBS} - VSM_i^{GPS}\right)^2}{n}} \quad \text{(S10)}$$

The standard deviation of the difference between observations and retrievals (SDD) is

$$SDD = \sqrt{\frac{\sum_{i=1}^{n}(x_i - \bar{x})^2}{n}} \quad \text{(S11)}$$

$x_i = VSM_i^{GPS} - VSM_i^{OBS}$, $\bar{x}$ is the mean value of x.

The fraction of explained variance is represented by the squared Pearson correlation coefficient, R^2.